DOE STI Product/ Final Report Number 3

Electrochemical Investigation of Novel Electrolytes for Ambient Temperature Sodium Batteries

Final report for the Period 01-AUG-2002 to 31-JAN-2006
Summary of Full Report

Ketack Kim, Christopher M. Lang, Kevin Doyle, and Paul A. Kohl
(Jack Winnick, Consultant)

PREPARED FOR THE UNITED STATES
DEPARTMENT OF ENERGY
ARGONNE, IL

Work performed Under Contract No. DE-FG02-02ER15328

Table of Contents

Summary of Full Report

Introduction

The need for low-cost, high-energy density, durable, secondary batteries continues to rise with the demands of the electronics and automobile industries. A room-temperature version of the (high-temperature) 'Zebra Cell' may provide an interesting technology for portable electronics and transportation. Sodium-based batteries have received attention as an alternative to the lithium-based batteries due to several factors including the absence of dendrite formation during sodium deposition and the abundance of sodium.

This work focused on (i) the development of room-temperature ionic liquids (IL) for use in electrochemical devices, including batteries, (ii) development and evaluation of secondary sodium batteries using room-temperature ILs, and (iii) advancing the fundamental understanding of the electrochemical processes involving ILs and battery technology. Several objectives were accomplished during this program.

New ionic liquids have been synthesized and investigated for the purpose of optimizing the following properties: low-cost (simple and high yield synthetic route), safe, low operating temperature, low viscosity, high stability (especially to reduction), and excellent battery performance. In this study, non-imidazolium ionic liquids were investigated because of their low cost and structural versatility. Quaternary ammonium salts (Quats) are less harmful and easier to make than other ILs.

The chloroaluminate ILs of the following seven Quats have been synthesized and investigated.

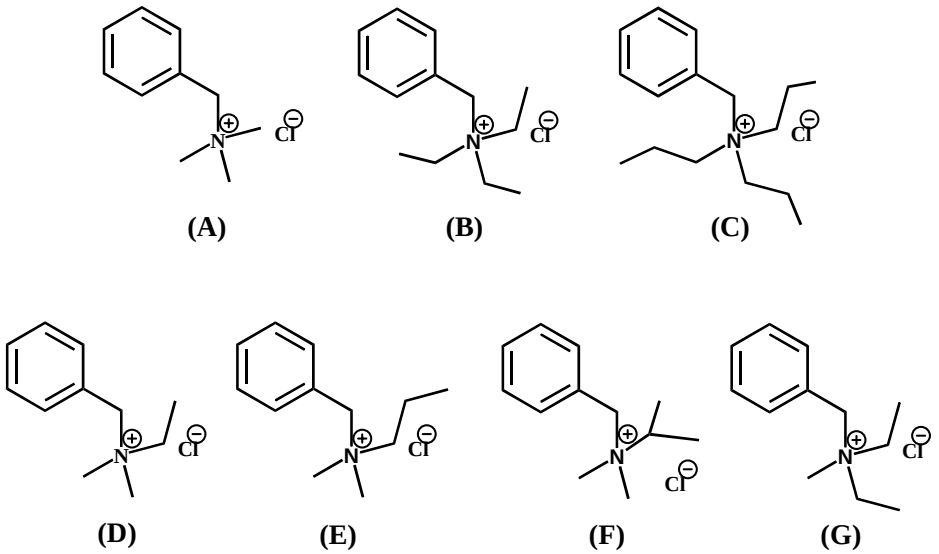

Figure 1 Quaternary ammonium salts (Quats): (A) Benzyltrimethylammonium chloride (BTMACl); (B) Benzyltriethylammonium chloride (BTEACl); (C) Benzyltributylammonium chloride (BTBACl); (D) Benzylethyldimethylammonium chloride (BEDMACl); (E) Benzyldimethylpropylammonium chloride (BDMPACl); (F) Benzyldimethylisopropylammonium chloride (BDMIPACl); (G) Benzyldiethylmethylammonium chloride (BDEMACl).

Based on systematic studies with these and previous ILs, it has been shown that the melting points and other physical properties are highly dependent on two critical properties: asymmetry and molecular weight. The optimum IL needs to as asymmetric as possible, and low molecular weight.

The electrochemical stability of the cation in acetonitrile has also been investigated. For select cations, these results were then compared to those obtained from the IL. In a neutral IL, sodium plating or IL reduction limits the negative potential. The stability of the cation (and resulting IL potential window) was found to be dependent on the ability of the quaternary ammonium constituents to act as leaving groups.

A plausible mechanism for the role of the ‘acid additives’, which catalytically enable the deposition of sodium metal from the ILs, has been found and described for the first time. It has been widely known for over 12 years that sodium can be

electrodeposited from ILs. Previously, there have been several guesses as to the role of the catalyst, however, no 'acceptable' mechanism has been found. In this work, we provide experimental evidence supporting the catalytic mechanism. Previously, reports have focused on the electrochemical stability of the organic cation and formation of a surface insulation layer.

In this work, we show that although the neutral ILs contain sodium ions (via NaCl neutralization), the sodium is effectively ion-paired and not available for deposition. The detailed conductivity studies have shown that sodium ions do not contribute to IL conductivity, and the addition of sodium tetrachloroaluminate decreases the conductivity. The addition of trace amounts of (normally) non-ionizing catalysts dramatically improves the conductivity by acting as a Lewis acid toward the chloride base in the IL. This understanding allowed us to identify five new molecules that can be used as 'additives'.

The ILs synthesized here and those made elsewhere were used in the evaluation of the battery half-cells. The ILs were neutralized with a two-fold excess of NaCl to provide the widest potential window and to provide a supply of sodium ions for the anode couple (sodium metal/sodium ion). The best coulombic efficiency with the benzyldimethylethylammonium chloroaluminate IL was 92.4 % at 50ºC and the lowest self-discharge current was 3.96 $\mu A/cm^2$ at 25ºC. This result is a substantial improvement over previous work. The IL made from benzyltriethylammonium chloroaluminate also had a coulombic efficiency over 91%. The self-discharge current for a sodium electrode in this ionic liquid was 18 $\mu A/cm^2$.

Finally, preliminary investigations of Li-Na alloys have been carried out in the IL. The deposition of a Li-Na alloy could prevent dendritic growth allowing for the use of a

metallic anode. Such an anode could have a charge density ten times greater than that found in the current lithium intercalation anodes while allowing for the use of currently available lithium cathodes.

A summary of the results is presented below and a detailed description is presented in the full report.

Summary of Results

In chapter 1, quaternary ammonium salts have been studied as ionic liquids for electrochemical applications, including sodium batteries. Mixtures of benzyltrialkylammonium chlorides with chloroaluminate formed ionic liquids near room temperature. The maximum coulombic efficiency for the reduction and re-oxidation of sodium ions with benzyltriethylammonium chloride ionic liquid was over 91%. The self-discharge current for a sodium electrode in this ionic liquid was 32.7 and 18 $\mu A/cm^2$ by chronopotentiometry at tungsten electrodes at 6.37 and 2.55 mA/cm^2, respectively. These are comparable to values in 1-methyl-3-propylimidazolium chloride melt. Issues with coulombic efficiencies and the self-discharge currents are discussed.

In chapter 2, benzyl-substituted quaternary ammonium ions were used to form room-temperature ionic liquids with chloroaluminate ions. Asymmetric benzyl-substituted ammonium chlorides were mixed with $AlCl_3$ to form acidic room-temperature ionic liquids. The asymmetric ammonium structures significantly lowered the melting point of the ionic liquid. It is shown that the melting point and viscosity are a function of the symmetry of the quaternary ammonium ion and its molecular weight. Asymmetry

and low molecular weight favor lower viscosity and melting point, and higher conductivity.

These liquids were neutralized with NaCl and tested as electrolytes for sodium batteries in chapter 3. The neutralized ionic liquid of benzyldimethylethylammonium chloride has a low self-discharge current (3.96 $\mu A/cm^2$) at room temperature on a platinum electrode substrate. The best coulombic efficiency with this IL was 92.4 % at 50ºC.

Ionic liquids are an ionically conductive medium that can provide a wide potential window for the study of electrochemical processes. In chapter 4, we observed that the degree of ionization of the ions depends on the charge density of the ions with significant ion pairing possible. Previously, it was shown that sodium ions can only be reduced to sodium metal if an acidic additive (e.g. $SOCl_2$) is added to the liquid. It is shown here that the additive increases the degree of dissociation of the Na^+ from its counter ion in the liquid, making it available for electrodeposition. The observed increase in ionic conductivity provided by the $SOCl_2$ supports this proposed mechanism. It is believed that the additive coordinates with chloride in the liquid, to provide greater freedom for the Na^+ ion. In addition, conditions were found for the reduction of sodium ions to sodium metal without the use of an additive.

In chapter 5, the electrochemical stability of ten organic cations, which can be used in ionic liquids (IL), was investigated as solutes in acetonitrile (ACN). Figure 2 shows the structures of the ten cations investigated. The stability of three of the salts, $BenMe_2EtNCl$ (salt III), 1-butyl-2-methyl pyrrolidium chloride (salt VI), and its

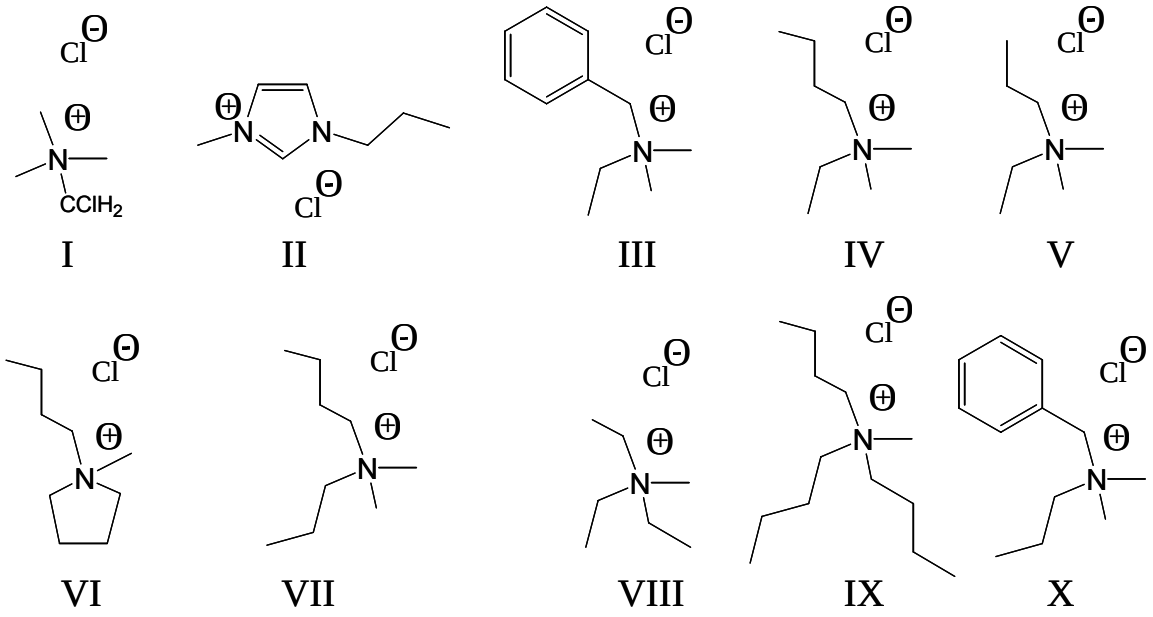

Figure 2 I: $Me_3MeClNCl$; II: 1-methyl-3-propylimidazolium chloride; III: benzylethyldimethylammonium chloride; IV: butylethyldimethylammonium chloride; V: ethyldimethylpropylammonium chloride; VI: butylmethylpyrrolidinium chloride; VII: butyldimethylpropylammonium chloride; VIII triethylmethylammonium chloride; IX tributylmethylammonium chloride; X benzyldimethylpropylammonium chloride.

structural isomer, $BuMe_2ProNCl$ (salt VII) were also compared in chloroaluminate ILs. The chloroaluminate ILs of salts VI and VII are investigated for the first time. The NaCl neutralized ILs of VI and VII have melting points of 43.2 and 3.7°C, respectively. The benzyl substituted cation, salt III, was more easily reduced in ACN or as the neutral, chloroaluminate IL, than the alkyl substituted cation, salt VII, due to the better leaving ability of the benzyl group. Mass spectroscopy measurements before and after electrolysis on the benzyl-substituted solutions confirmed that reduction involves the loss of an alkyl group. In ACN, salt VI was found to be the most difficult to reduce (1 mA/cm^2 at -2.09 V) due to its cyclic structure. However, in the chloroaluminate IL, the pyrrolidinium cation was more easily reduced than salt III or its isomer, salt VII, resulting in an insoluble black deposit. This is consistent with the mass spectrometry data, which did not show formation of low molecular weight products, as in the reduction of salts III

and VII. The IL of salt VII was the most stable in the presence of sodium. Sodium ions could be reduced and reoxidized with a maximum coulombic efficiency of 94.1% versus 87.2% for salt VI. Reduction of the pyrrolidinium cation produces insoluble products, most likely through opening of the cyclic ring, and an inferior medium for sodium ion reduction compared to the benzyl and butyl-substituted cations, even though reduction of the cation occurs at a more negative potential in acetonitrile.

In chapter 6, the deposition of Li-Na alloys from an ionic liquid medium has been demonstrated and evaluated with respect to dendrite growth, oxidation potential, and stability. Dendrite-free growth was observed at all current densities (ranging from 1 mA/cm^2 to 10 mA/cm^2). The maximum coulombic efficiency for the re-oxidation of the Li-Na alloy was found to be 91%. The conductivity of the ionic liquid medium containing the alloy salts was 364 $\mu S/cm^2$ to 466 $\mu S/cm^2$.

The ability of five different compounds to facilitate reduction of sodium from a chloroaluminate IL was investigated in chapter 7. PCl_6^- and 18-Crown-6 act to disrupt the Na^+ and $AlCl_4^-$ ion pairs producing reducible sodium ions. The addition of the small chlorinated compounds, CH_2Cl_2, $CDCl_3$ or CCl_4, resulted in the efficient reduction and reoxidation of sodium. It is believed that the electronegative chlorine atoms are oriented near the positive sodium cation, weakening its attraction to $AlCl_4^-$. For the five compounds tested, the highest coulombic efficiencies were measured after the addition of $CDCl_3$ (90.5%) and CCl_4 (88.2%). The addition of $CDCl_3$ was found to substantially increase the conductivity of the IL.

List of Figures

Figure III-2.2 Structural comparison of Quats and their MPs. Quats are: BTMACl, BTEACl and BDMEACl.

Figure III-2.3 DSC curves for two acidic melts. The curve shows glass transition (T_g), crystallization (T_c), and melting point (T_m).

Figure III-2.4 Cyclic voltammetry of the neutral Quat A ionic liquid. Working electrodes are platinum, gold and tungsten electrodes, 1 mm diameter discs. The scan rate was 100 mV/sec.

Figure III-3.1 Quats with a benzyl substituent. Quat A: BEDMACl; Quat B: BDMPACl; Quat C: BDMIPACl; Quat D: BDEMACl.

Figure III-3.2 Conductivity vs. temperature with the acidic melts (N= 0.55).

Figure III-3.3 Conductivity vs. temperature with the neutal melts.

Figure III-4.1 Conductivity versus $AlCl_4^-$ mole fraction for a mixture of 55% $AlCl_3$ and 45% BDMEACl at 27ºC.

Figure III-4.2 Conductivity versus temperature for: (A) Mixture of 53% $AlCl_3$ and 47% BDMEACl; (B) Mixture of 53% $AlCl_3$, 43.3% BDMEACl, and 3.7% NaCl.; (C) Mixture of 51% $AlCl_3$ and 49% BDMEACl; (D) Mixture of 51% $AlCl_3$, 35.3% BDMEACl, and 13.7% NaCl.

Figure III-4.3 Conductivity versus mole % $NaAlCl_4$ for an initial mixture of 53% $AlCl_3$ and 47% BDMEACl at 27°C.

Figure III-4.4 Conductivity at 30°C versus weight % $SOCl_2$ for an initial mixture of 50% $AlCl_3$, 40.9% BDMEACl, and 9.1% NaCl.

Figure III-4.5 CV scan at 27°C for a mixture of 55% AlCl3 and 45% BDMEACl neutralized with 100% excess NaCl and 0.18 mole % $SOCl_2$ added.

Scheme III-4.1 Interaction between additives and $NaAlCl_4$ ion.

Figure III-5.1 I: $Me_3MeClNCl$; II: 1-methyl-3-propylimidazolium chloride; III: benzylethyldimethylammonium chloride; IV: butylethyldimethylammonium chloride; V: ethyldimethylpropylammonium chloride; VI: butylmethylpyrrolidinium chloride; VII: butyldimethylpropylammonium chloride; VIII triethylmethylammonium chloride; IX tributylmethylammonium chloride; X benzyldimethylpropylammonium chloride.

Figure III-5.2 CV scans for 0.1M solutions of salts I, II and III in acetonitrile.

Figure III-5.3 CV scans for 0.1M solutions of salts III, IV and V in acetonitrile.

Figure III-5.4 CV scans for 0.1M solutions of salts III, V and VI in acetonitrile.

Figure III-5.5 Mass spectroscopy results for 0.1M acetonitrile solution of salt III before and after 12.5% reduction.

Figure III-5.6 Mass spectroscopy results for 0.1M acetonitrile solution of salt VI before and after 10% reduction.

Figure III-5.7 Mass spectroscopy results for 0.1M acetonitrile solution of salt VII before and after 20% reduction.

Figure III-5.8 CV scans with 100% excess sodium and: (A) N=0.55 Mixture of Salt III; (B) N=0.55 Mixture of Salt VII; (C) N=0.554 Mixture of Salt VI.

Figure III-5.9 CV scan at 71°C for a mixture of 55.4% $AlCl_3$ and Salt VI neutralized with 100% excess NaCl and $SOCl_2$ added.

Figure III-5.10 CA scan at 71°C for a mixture of 55.4% $AlCl_3$ and Salt VI neutralized with 100% excess NaCl and $SOCl_2$ added.

Figure III-5.11 CV scan at 25°C for a mixture of 55% $AlCl_3$ and Salt VII neutralized with 100% excess NaCl and $SOCl_2$ added.

Figure III-6.1 CV scans at room temperature for 5 ILs with different LiCl:NaCl ratios.

Figure III-6.2 CA curve at room temperature for the 90% LiCl/10% NaCl IL.

Figure III-7.1 CV curves for neutralized N=0.55 BME IL with 5 mole % PCl_5 added.

Figure III-7.2 CA test results for neutralized N=0.55 BME IL with 5.8 mole % PCl5 added.

Figure II-7.3 Conductivity versus temperature for neutralized N=0.55 BME IL with 0, 0.66, 1 and 1.5 mole % 18-Crown-6 added.

Figure III-7.4 CV results for neutralized N=0.55 BME IL with 1.8 mole % 18-Crown-6.

Figure III-7.5 CV scan following the addition of dichloromethane to the N=0.55 BME IL.

Figure III-7.6 CV test results with carbon tetrachloride and chloroform-D added to a neutral N=0.55 BME IL.

Figure III-7.7 CV results 0 days, 2 weeks and 4 weeks after addition of chloroform-D to neutral N=0.55 BME IL.

Figure III-7.8 CV test results after addition of 0.34, 0.96 and 1.79 mole % chloroform-D.

Figure III-7.9 Results of chronoamperometry tests with 0.34, 0.96 and 1.79 mole % chloroform-D added.

Figure III-7.10 Conductivity versus mole % chloroform-D in a neutral IL.

List of Tables

Table III-7.2 Self-discharge test results for $CDCl_3$ and CCl_4 added to a neutralized N = 0.55 BME IL.

I. Introduction

I-1. Background

The need for low-cost, high-energy density, durable, secondary batteries continues to rise with the demands of the electronics and automobile industries. Sodium-based batteries have received attention as an alternative to the lithium-based batteries due to several factors. Formation of lithium dendrites during deposition has required the use of a separator that lowers the coulombic efficiency.[2,3] A wide separation between the electrodes results in high resistance and low current density. On the other hand, sodium electrodeposits evenly on the surface of electrodes. The low atomic weight of sodium could also lead to a system with a high-energy density. Furthermore, sodium is an abundant element in nature.

The "Zebra" Cell, a rechargeable sodium battery, has demonstrated encouraging results with a specific energy greater than 130 Wh/Kg.[4] This secondary cell operates at ~250ºC and uses a molten chloroaluminate inorganic salt, NaCl: aluminum chloride ($AlCl_3$), as the electrolyte. At this operating temperature, the Zebra cell contains molten sodium (melting point 98ºC) as the anode and a solid-state separator between liquid Na and the electrolyte. Under typical operating conditions an appreciable voltage drop (ca. 350 mV) results from the use of the separator.[5] However, direct contact between sodium and the electrolyte results in a chemical reaction (Equation I-1.1) that produces aluminum and NaCl.

$$3Na + NaAlCl_4 \rightarrow Al + 4\ NaCl \qquad \text{(I-1.1)}$$

The separator and high operating temperature are obstacles to making the "Zebra" cell practical. To overcome these obstacles, room temperature ionic liquids could potentially function as the electrolyte in place of $NaAlCl_4$ in the Zebra cell. Dialkylimidazolium chloride: aluminum chloride has widely been investigated for this purpose. The 1-methyl-3-ethylimidazolium chloride (MEIC) forms a liquid phase when mixed with aluminum chloride at ambient temperature over a wide range of compositions.[6] 1-methyl-3-proplyimidazolium chloride (MPIC) and methanesulfonyl chloride (MSC) have demonstrated encouraging results for sodium-based batteries.[7]

In this study, we are investigating ionic liquids based on quaternary ammonium salts. Previously several salts were mixed with aluminum chloride to form ionic liquids, including methyltriethylammonium chloride, methyltributylammonium chloride, and benzyltrimethylammonium chloride (BTMACl).[8] The properties of these liquids, in particular the electrochemical stability (available electrochemical window), are similar to the imidazolium salts. For the BTMACl: $AlCl_3$ ionic liquid a coulombic efficiency for the sodium couple of greater than 90% was achieved. However, the melting point for this liquid is 56°C leading to an operating temperature approximately 40°C above room temperature.

I-2. Motivation

The purpose of our study is to identify ionic liquids that give a low operating temperature, low viscosity, high stability (especially to reduction), and high battery performance. In this study, non-imidazolium ionic liquids are being investigated because

of their low cost and versatility. Quaternary ammonium salts (Quats) are less harmful and easier to make than alkylimidazolium chloride or MSC. Also, there are numerous ammonium salts that can be made by modifying alkyl branches.

Systematic modification of the alkyl branches can be useful in understanding a variety of the ionic liquid properties. The alkyl groups present determine the melting point of the ionic liquid. The stability and viscosity of the ionic liquid is impacted by the size and electron releasing nature of the pendant groups. These properties impact the stability of sodium in the melt and the rate at which sodium can be plated and removed.

To reversibly produce sodium in both imidazolium and Quat salts an additive is necessary, such as $SOCl_2$ or HCl.[9,10] Understanding the role these additives play in catalyzing the reduction of sodium could lead to new additives and modifications of the Quat that result in improved electrolyte performance.

Utilizing the Quat-based ionic liquids several electrode materials (gold, platinum, tungsten) are being investigated to determine the best electrode material. In order to study the stability of sodium in the melt, self-discharge tests are carried out for the materials that show reversible sodium deposition.

II. Technical approach

The half-cell reactions and overall cell reaction for sodium batteries are as follows.

Charge ⇆ Discharged

Anode: $2Na \leftrightarrows 2Na^{+} + 2e^{-}$ (II.1)

Cathode: $MCl_2 + 2e^{-} \leftrightarrows M + 2Cl^{-}$ (II.2)

Overall: $MCl_2 + 2Na \leftrightarrows 2NaCl + M$ (II.3)

Where M could be a transition metal, such as Cu,[11] Fe,[1,11] and Ni.[12] These cathodes gave cell potentials from 2.3 V to 3.3 V in a MEIC: $AlCl_3$ melt. It has been shown that the substrate for the anode reaction (Na/Na^{+}) can play an important role because the sodium must nucleate on the surface (desired reaction) and the melt can be electro-decomposed (undesired reaction). In this study, Pt and W have primarily been used as electrodes.

II-1. Measurements

Six methods are being used to evaluate the ionic liquids. These are melting point, viscosity, density, conductivity versus temperature, coulombic efficiency, and Na/Na^{+} (anode) self-discharge current. Ionic liquids with melting points below room temperature are desired due to the large range of possible battery operating temperatures. Both viscosity and temperature are measured at room temperature utilizing a calibrated viscosimeter and Gay-Lussac bottles, respectively. Conductivity is a function of temperature and inversely related to the viscosity of the melt. Coulombic efficiency of the Na/Na^{+} couple is measured by chronopotentiometry (CE). The coulombic efficiency is the ratio of oxidation charge to reduction charge. Therefore, the coulombic efficiency

shows the percentage of Na, which can be utilized after it has been electroplated on a substrate.

Coulombic efficiency of (Na/Na^+) = (oxidation charge / reduction charge) (II-1.1)

The self-discharge current is useful in quantifying the stability of plated sodium. An open circuit period between plating and stripping of Na is used to evaluate sodium in contact with the ionic liquid. The amount of charge recovered is measured as a function of open circuit time and expressed as an equivalent current density. Self-discharge current (A/cm^2) is obtained from the slope of the charge versus open circuit time curve.

II-2. Quaternary Ammonium Chloride Salts ($Quat^+Cl^-$)

Equations II-2.1 and II-2.2 show the acid-base reactions between the quaternary ammonium chloride salts and $AlCl_3$. The Lewis acid, $AlCl_3$, forms $AlCl_4^-$ (Lewis neutral) and $Al_2Cl_7^-$ (Lewis acid) when mixed with the Quat, as shown in Equation II-2.1 and II-2.2. Neutralization of the $Al_2Cl_7^-$ occurs by reacting $Al_2Cl_7^-$ with a Lewis base, Cl^- from NaCl or $Quat^+ Cl^-$, to produce neutral $AlCl_4^-$ ions (Equation II-2.3).[13]

$$Quat^+Cl^- + AlCl_3 \rightarrow Quat^+ + AlCl_4^- \quad \text{(II-2.1)}$$

$$AlCl_4^- + AlCl_3 \rightarrow Al_2Cl_7^- \quad \text{(II-2.2)}$$

Basic melts ⇆ Neutral melts ⇆ Acidic melts:

$$AlCl_4^- + Cl^- \leftrightarrows \quad AlCl_4^- \quad \leftrightarrows AlCl_4^- + Al_2Cl_7^- \quad \text{(II-2.3)}$$

The acidity of the melt is defined using the mole fraction of $AlCl_3$, N = $nAlCl_3/(nAlCl_3 + mQuat)$. For example, neutral melts containing equal moles of $AlCl_3$ and Quat (N = 0.5) contain only the $AlCl_4^-$ ions. Acidic melts contain an excess of $AlCl_3$, N > 0.5, and form $AlCl_4^-$ and $Al_2Cl_7^-$ anions. Melts containing a excess of Quat, N < 0.5, are basic and contain $AlCl_4^-$ and Cl^- anions.

Neutral melts have the widest electrochemical window (~ 4.5 V). The $Al_2Cl_7^-$ anion is easily reduced to Al in acidic melts, and Cl^- is easily oxidized to chlorine in basic melts. Alkali chlorides can be used to buffer acidic melts and provide neutral conditions.[13] Excess NaCl converts $Al_2Cl_7^-$ to $AlCl_4^-$ while also providing the sodium source for the battery. Excess NaCl buffers the melt be providing a source of chloride. $Quat^+$ is believed not to be involved in the electrochemical reaction. It does however limit the potential window by being reduced near the Na/Na^+ redox couple. The Quat has a crucial role in determining the melting point of ionic liquids. Its interaction with aluminum chloride anions ($AlCl_4^-$ or $Al_2Cl_7^-$) is the main ionic interaction that affects the melting point.

Many short-chain alkyl-chain salts do not have low operating temperatures. For long alkyl-chain Quats, where the number of carbons > 20, the Quats are liquids, but very viscous. Having a moderate operating condition will reduce the overall energy necessary to run the battery and therefore lead to higher overall system efficiencies. In this report, we discuss the properties and structures of Quats for room temperature operation.

Figure II-2.1 shows several Quats that have been investigated in this study. These Quats were selected because of their unique aliphatic alkyl chains. The physical properties of the melts formed using these Quats will direct the synthesis of new Quats.

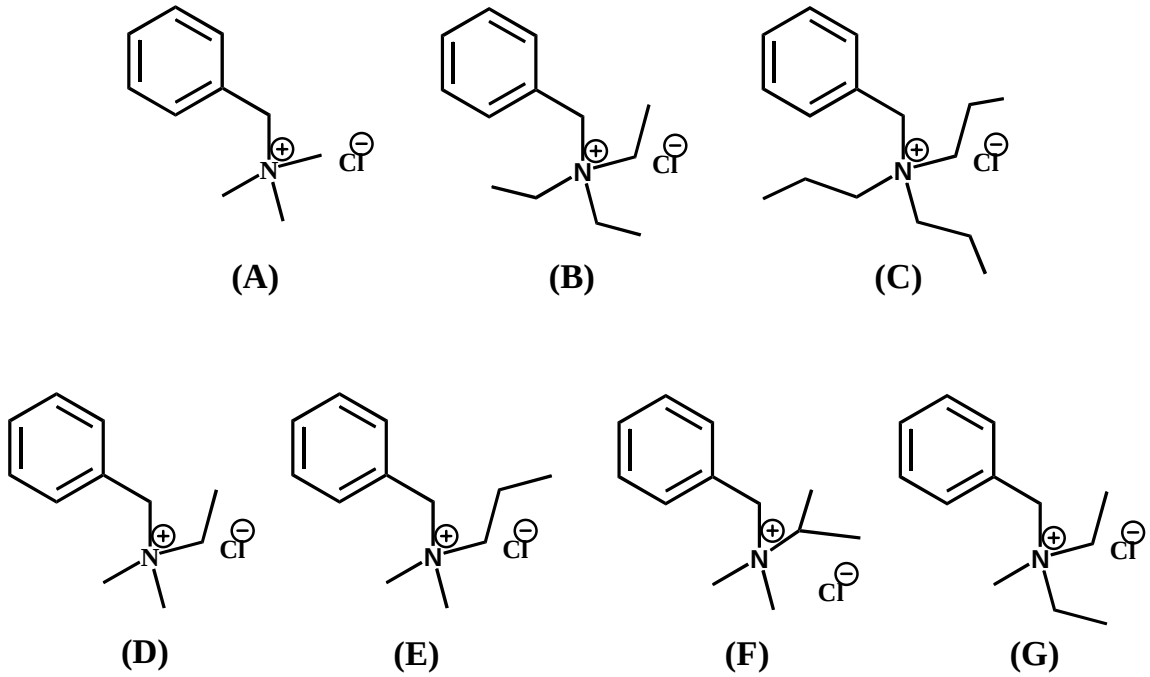

Figure II-2.1. Quaternary ammonium salts (Quats): (A) Benzyltrimethylammonium chloride (BTMACl); (B) Benzyltriethylammonium chloride (BTEACl); (C) Benzyltributylammonium chloride (BTBACl); (D) Benzylethyldimethylammonium chloride (BEDMACl); (E) Benzyldimethylpropylammonium chloride (BDMPACl); (F) Benzyldimethylisopropylammonium chloride (BDMIPACl); (G) Benzyldiethylmethylammonium chloride (BDEMACl).

Four of the Quats (BEDMACl, BDMPACl, BDMIPACl, and BDEMACl) desired for investigation could not be purchased. Therefore, they must be made in the lab by way of a substitution nucleophilic bimolecular (SN2). An example of this type of reaction can be seen below in Figure II-2.2 with the making of BEDMACl. In this reaction ethyldimethlyamine is reacted with benzylchloride dissolved in Acetonitrile.

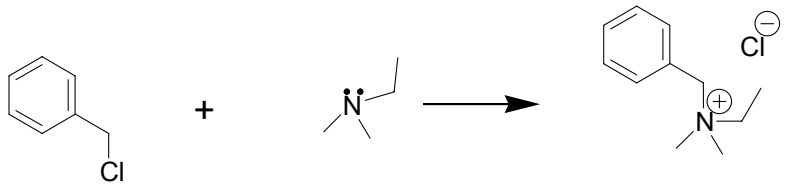

Figure II-2.2. Reaction of an amine and alkyl-chloride to make a Quat.

II-3. Additives

It is necessary to add HCl (g) or $SOCl_2$ to the neutral ionic liquid to activate the Na/Na^+ redox process.[9] Without an additive, Na^+ reduction has not been observed previously. Identifying the role of the additives is another important aspect in selecting and understanding the quaternary ammonium salts. In this study we propose the role that the additive plays in catalyzing the reduction of sodium metal in the Quat: $AlCl_3$ melts.

III. Results and Discussion

This work focused on (i) the development of room-temperature ionic liquids (IL) for use in electrochemical devices, including batteries, (ii) development and evaluation of secondary sodium batteries using room-temperature ILs, and (iii) advancing the fundamental understanding of the electrochemical processes involving ILs and battery technology. The following 7 chapters discuss in detail the results obtained throughout the course of this study.

III-1. ***Electrochemical Investigation of Novel Electrolytes for Ambient Temperature Sodium Batteries***

Chapter 1 shows the early work with melts formed using the commercially available Quats. The melts formed each had melting points higher than room temperature. The electrochemical properties of the melts as battery electrolytes are discussed. From this work, we identified how the Quat might be modified in order to lower the melting point of the resulting liquid.

Results

Figure III-1.1 shows the structure of the Quats used in this study. These Quats were selected because of their unique aliphatic alkyl chains (e.g. short chain, long chain, a benzyl (aromatic resonance)). Acidic melts were formed and later neutralized with NaCl to form the buffered, neutral melt. Acidic melts higher than N = 0.6 were difficult to buffer. It is not clear why melts with high acidity (N > 0.6) are more difficult to neutralize than those closer to N = 0.5. Thus, N = 0.55 was chosen as a moderate composition used as the starting composition for the melting point studies. The melting points of the ionic liquids formed from the Quats in Fig. III-1.1 and $AlCl_3$ are shown in Table III-1.1.

The positive charge on the ammonium ion is delocalized by alkyl substituents. Longer alkyl chains release more electron density to the positive center than shorter alkyl chains. However, the charge delocalizing ability of the benzyl group is greater than the alkyl branches. Thus, $BTMA^+$ has weaker ionic strength with chloride ions compared to the MTEACl and MTBACl in Table III-1.1. Even though the BTMACl:$AlCl_3$ melting point is above room temperature, the melting point of the BTMACl melt is lower than the melting point of Na (98°C) making it potentially interesting for battery usage. In an attempt to lower the melting point, longer alkyl chains were used on the Quat to increase the charge delocalization.

The melting point of benzyltriethylammonium chloride (BTEACl) was greater than benzyltributylammonium chloride (BTBACl). However, the melting point of the BTEACl melt is higher than that of the BTMACl melt due to charge delocalization. This result implies that there are other contributions to the melting point, such as, the

symmetry of the ions.[14] A higher degree of symmetry increases the melting points of salts because of the ease of crystallization. Also, when compared to the ethyl and butyl groups found in MTEACl and MTBACl, the benzyl group is more effective in disrupting symmetry.

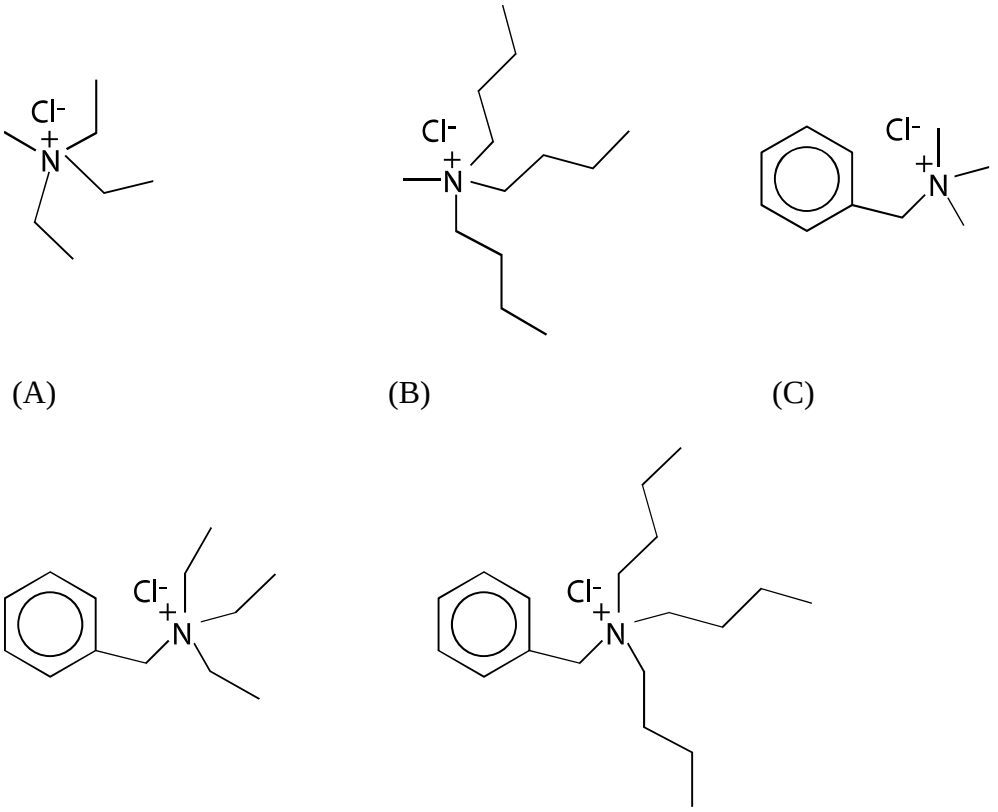

(A) (B) (C)

(D) (E)

Figure III-1.1 Quaternary ammonium salts (Quats): (A) methyltriethylammonium chloride, (MTEACl); (B) methyltributylammonium chloride, (MTBACl); (C) BTMACl; (D) BTEACl; (E) BTBACl.

	MTEACl	MTBACl	BTMACl	BTEACl	BTBACl
Melting Point (°C) of Acidic Melt	278.2	105.2	55.6	66.4	40.6
Melting Point (°C) of Neutralized Melt	--	--	65.3	66.0	42.7

Table III-1.1 Melting point of ionic liquids (55 mole % of $AlCl_3$ and 45 mole % Quat).

The addition of sodium chloride to neutralize the three acidic melts in Table III-1.1, does not greatly impact the melting points. In this case the chloride ions from NaCl convert $Al_2Cl_7^-$ to $AlCl_4^-$. The change in concentration by the amount of sodium chloride and change caused by it was not great enough to show an effect on the melting points. However, we are conducting further analysis and measurements about the nature of ions in ionic liquids.

Figure III-1.2 shows the temperature dependence of the conductivity for the BTMACl:$AlCl_3$ ionic liquid. For operating temperatures of 65°C to 82°C, the values range from 2.5 to 5 mS/cm, which is lower than that of 1-methyl-3-ethylimidazolium chloride (35 mS/cm at room temperature).[9] The conductivity increases with the acidity of the melts. As shown in Equation II-2.3, the fraction of $Al_2Cl_7^-$ ions also increases with the acidity of the melts. The higher conductivity is attributed to a reduction in the viscosity of the melt and the increased percentage of $Al_2Cl_7^-$ ions and possibly a lower degree of ion pairing between the $Al_2Cl_7^-$ and $Quat^+$ ions as compared to the $AlCl_4^-$ and $Quat^+$ ions. Melting points of 55.6 and 57.7°C were measured for the N= 0.55 and N= 0.53 melts, respectively. These results are consistent with previously reported findings.[6]

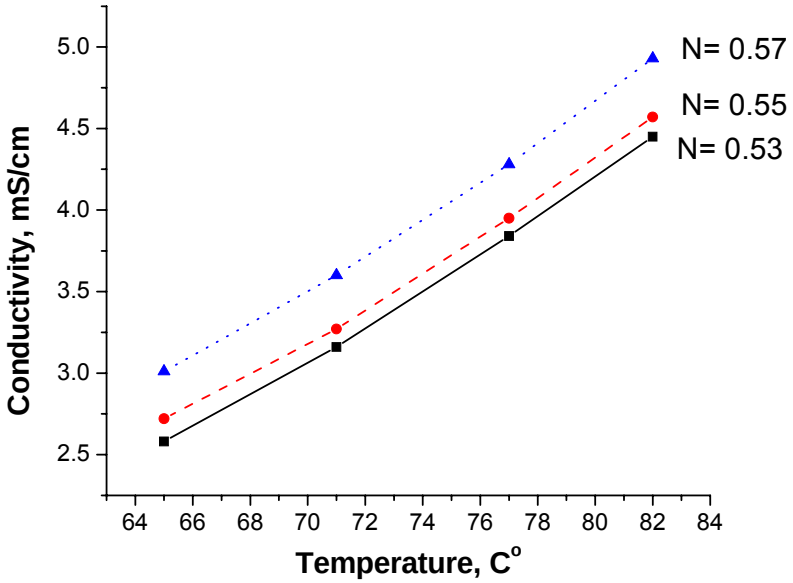

Figure III-1.2 Conductivity vs. temperature for three BTMACl:$AlCl_3$ melts.

Figure III-1.3 shows a cyclic voltammogram (CV) for BTMACl:$AlCl_3$ (N = 0.55) neutralized with excess NaCl and a trace amount of $SOCl_2$, at 71°C on a tungsten electrode. The coulombic efficiency of 86% will vary depending on the switching potentials and the measurement conditions. The shape of the reduction and oxidation peak are very sharp, indicating a rapid redox process. The sharp rise in the reduction current and hysteresis loop shows that the nucleation of the first layers of sodium requires a small overpotential related to the nucleation and crystallization of the sodium metal on a non-sodium surface. This current-voltage shape is typical of the sodium couple in dialkylimidazolium ionic liquids. Figure III-1.3 shows a wide potential window with low background current, which indicates the presence of few impurities. Therefore, further purification of the starting materials may not result in appreciable improvements in the coulombic efficiency.

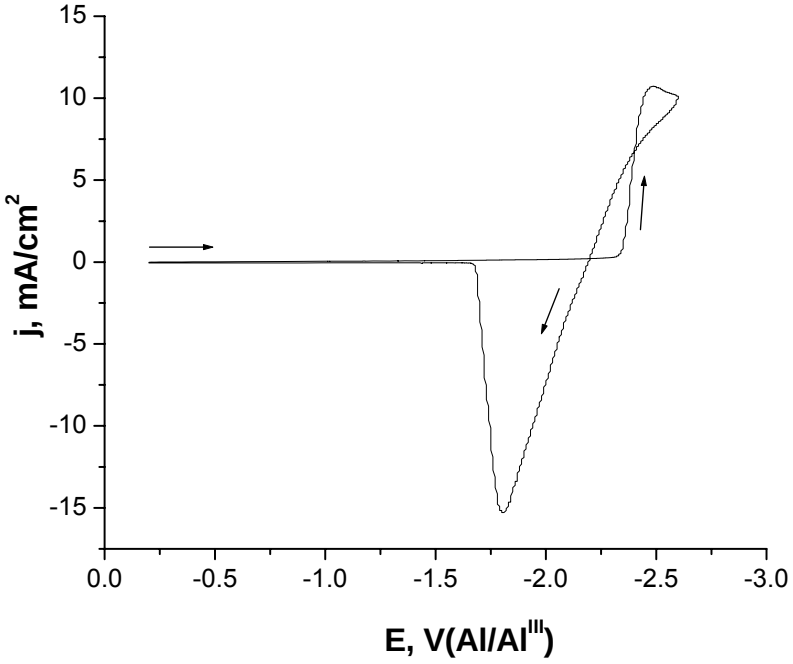

Figure III-1.3 CV of the BTMACl:$AlCl_3$ melt (N = 0.55) neutralized with excess NaCl and a trace of $SOCl_2$ at 71°C on a tungsten electrode.

The efficiency of reduction and re-oxidation can also be measured by utilizing chronoamperometry (CA). Using this technique the reduction of sodium is initiated by applying the appropriate voltage for a fixed period of time. The voltage is then switched to that corresponding to the re-oxidation of sodium for a set period of time. The efficiency can be found by comparing the areas under each of the curves (which corresponds to the total charge deposited and removed). In Figure III-1.4, the discharge time is 2 seconds longer than the charge time. The average current for the reduction process is higher than that for the re-oxidation process, indicating a slower oxidation rate (when compared to the reduction rate). By modifying the switching potential and the time, we can get different efficiencies. The efficiency for Figure III-1.4 is 87%.

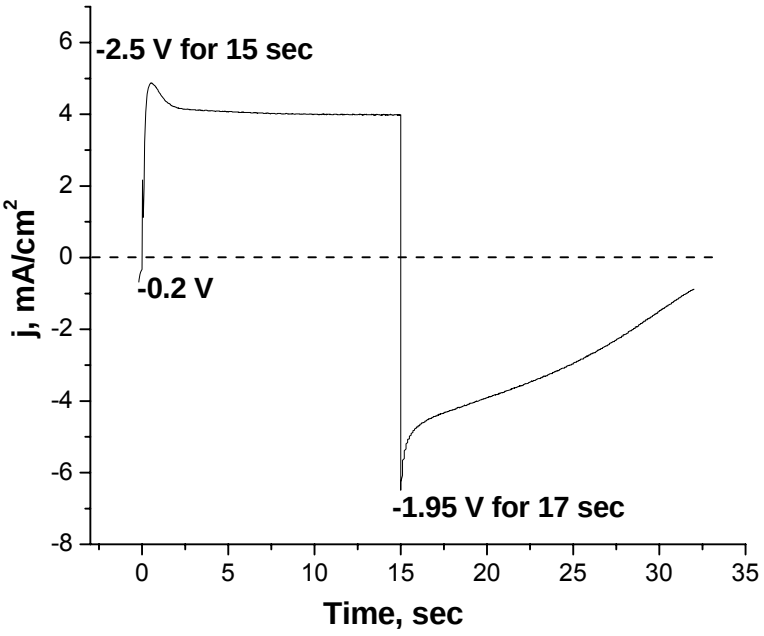

Figure III-1.4 Chronoamperometry of the BTMACl:$AlCl_3$ melt (N = 0.55) neutralized with excess NaCl on a W electrode at 65°C with $SOCl_2$ added.

A critical question in the study of ionic liquids is the optimum current for reduction and oxidation of sodium. This value is dependent on the melt composition, the electrode utilized and the operating temperature. Table III-1.2 summarizes the resulting coulombic efficiency when the current density (for a CE test) and reduction/re-oxidation time is varied. From this table it can be seen that the maximum efficiency can be achieved at currents of 5.7 to 6.3 mA/cm^2, with very low efficiencies when the current density approaches low (1.3 mA/cm^2) or high (10 mA/cm^2) values.

Current Density (mA/cm^2)	1.3	2.5	3.8	4.4	4.4	5.1	5.1	5.7	6.3	6.3	6.3	7.6	10
Charge/Discharge Time (sec)	10	10	60	50	60	30	60	60	60	80	100	60	10
Efficiency (%)	31	52	85	86	88	82	88	89	89	90	88	84	16

Table III-1.2 Coulombic efficiencies of a buffered BTMACl:$AlCl_3$ melt (N = 0.55) with trace $SOCl_2$ at a tungsten electrode at 71°C.

Figures III-1.5 and III-1.6 illustrate why low efficiencies were obtained with the high and low currents. Figures III-1.5A and III-1.5B are examples of low and high current densities, respectively. Fig. III-1.5 shows the reduction current with time for sodium plating. Though the background current is low, there are species present that can be reduced more easily than the Na^+ ions in the melt. In Panel A the current density (0.63 mA/cm^2) is low enough that it takes a significant amount of time (4 out of 10 seconds) and charge to reduce these species before the sodium ions can be reduced at approximately –2.4 V. In Panel B, the time prior to sodium deposition was negligible due to the high current density (10 mA/cm^2). However, the current density exceeds the maximum value for sodium ion reduction resulting in the reduction of some other species, probably $Quat^+$ (and a slight shift of the potential to more negative values) after ~3 seconds. The CE curves for the optimum case are shown in Figure III-1.6. In Panel A the current was high enough (6.3 mA/cm^2) that the voltage for the reduction of sodium ions rapidly reached –2.4 V, but still low enough that the voltage remained relatively constant for the entire deposition process. Following the reduction of sodium, the re-oxidation portion of the process is carried out at the same current (6.3 mA/cm^2) and is

shown in Panel B. During the re-oxidation, the potential remained fixed at –2.0 V until the rapid increase near 70 sec. The plateau at 2.3 V represents Cl_2 gas evolution. The efficiency for the process shown in Figure III-1.6 is 90%.

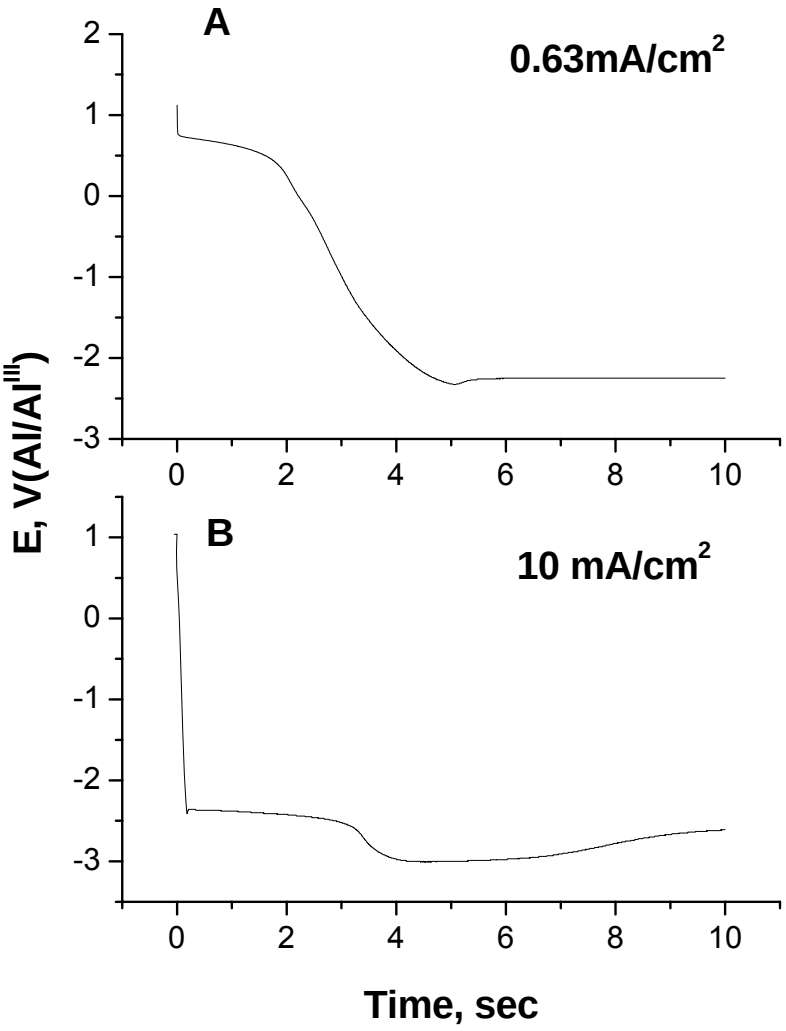

Figure III-1.5 Chronopotentiometry of a buffered BTMACl:$AlCl_3$ melt (N = 0.55) with trace $SOCl_2$ added on a W electrode at 71°C. The oxidation currents, not shown here, were applied after the reduction measurements.

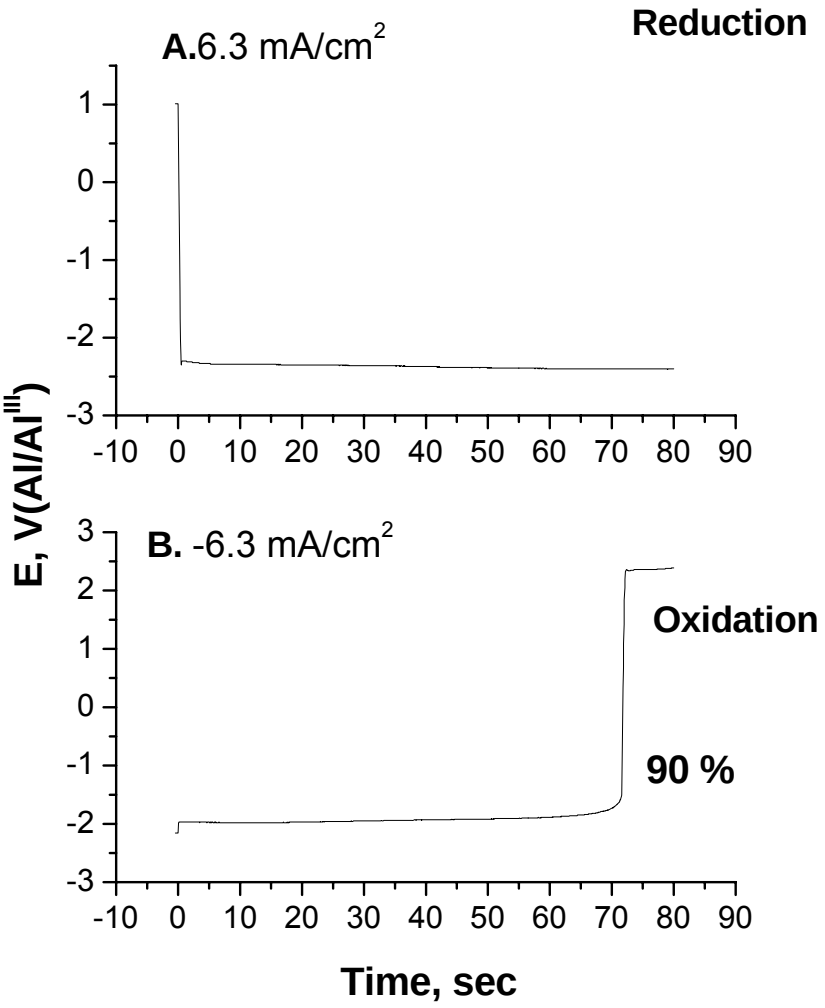

Figure III-1.6 Chronopotentiometry on a W electrode at 71°C. The buffered BTMACl:$AlCl_3$ melt (N = 0.55) has $SOCl_2$ added. The current density was 6.3 mA/cm^2.

To quantify the parasitic reactions on the plated sodium in the melt, the self-discharge current, $I_{self\text{-}discharge}$, was calculated by measuring the efficiency as a function of the open circuit time. Using CE the self-discharge current was measured at a tungsten electrode with reduction and oxidation current densities of 6.3 mA/cm^2 for 100 seconds and an operating temperature of 71°C. Under these conditions, with no open circuit time, the average efficiency was 88.8%. Figure III-1.7 shows the self-discharge current using a

linear-fit of the data points for the neutralized BTMACl:$AlCl_3$ (N = 0.55) melt with $SOCl_2$ added. The self-discharge current was 76.6 μA/cm^2, which is higher than that of the 1-methyl-3-propylimidazolium chloride melt (22 μA/cm^2).[10] It suggests that the parasitic reactions in the BTMACl melt are more active than those in the MPIC melt. The higher operating temperature of the BTMACl melt could account for the increase in the activity of the parasitic reactions.

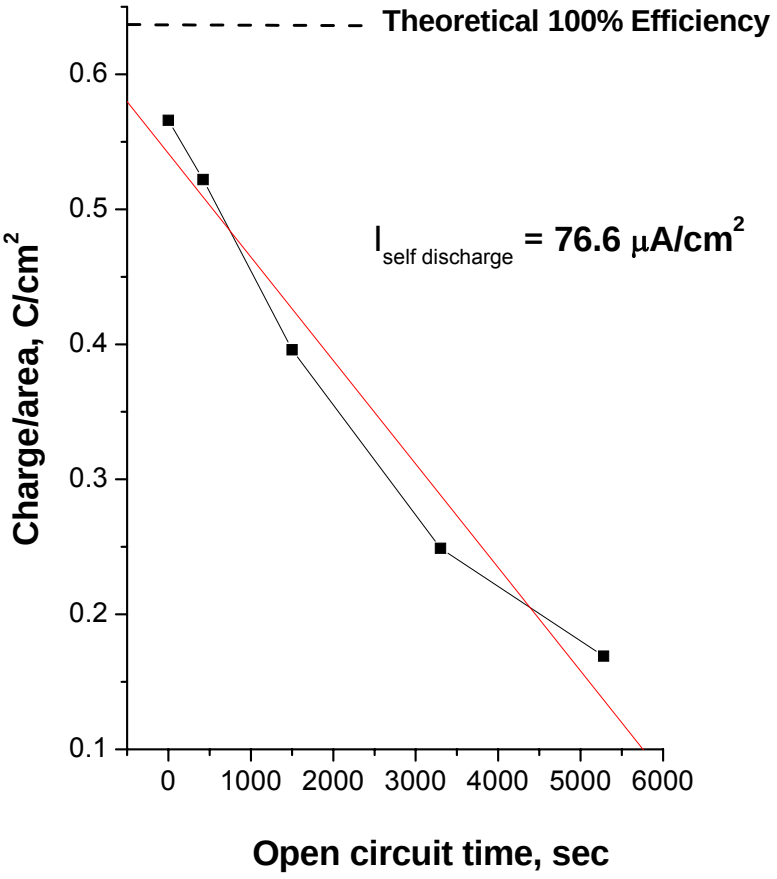

Figure III-1.7 Charge density vs. open circuit time on a W electrode at 71°C in a buffered BTMACl:$AlCl_3$ melt (N = 0.55) with $SOCl_2$ added.

The most likely candidate to scavenge electrons from the plated sodium is the $Quat^+$ ion. The reduction potential of the $Quat^+$ depends on the electron withdrawing (or releasing) nature of the constituents groups. As discussed earlier, the ionic strength is related to the ability of the constituent groups to delocalize the charge on the nitrogen. In this regard, the aromatic ring of MPIC has a higher level of positive ion delocalization than the benzyl and methyl groups in the BTMACl melt resulting in the lower self-discharge current for MPIC. The addition of more electron releasing groups on the cation should help in reducing the self-discharge current.

The self-discharge tests were performed using a buffered BTEACl:$AlCl_3$ (N = 0.55) melt. Utilizing the CE test procedure outlined previously, an average baseline efficiency of 91.0% was determined using a current density of 6.37 mA/cm^2 on a tungsten electrode at 82°C. Under these conditions the self-discharge current was 32.7 $\mu A/cm^2$, which is approximately half that measured for the BTMACl melt. Ethyl groups release more electron density on the positive center than methyl groups. This result is very encouraging since the operating temperature (82°C) for the BTEACl tests was higher than that used for the BTMACl tests (71°C), which should result in more active parasitic reactions for the BTEACl case.

To see if the thickness of the sodium deposit affects the self-discharge current, self-discharge tests were carried out using the same conditions for the BTEACl melt but a lower current density (2.55 mA/cm^2). With these conditions, the average baseline efficiency was 92.0% and the self-discharge current was 18.0 $\mu A/cm^2$. The decrease in the self-discharge current with a lower current density may be due to the deposit of a thinner film. We need further investigations to prove this issue.

While the results for the BTMACl melt and the BTEACl melt were encouraging, the plating of sodium in a BTBACl melt was poor. Both platinum and gold electrodes showed reduction/re-oxidation cycle efficiencies of less than ~20%. The efficiency on a tungsten electrode was the highest. Efficiencies for the CV tests ran at 100 mV/sec and 74°C varied from 38 to 59%. The maximum efficiency (75.3%) was achieved using chronopotentiometry by applying a current density of 2.55 mA/cm^2 at 74°C. Due to the low efficiency the self-discharge current was not measured. The long butyl chains increase the viscosity of the melt, which is believed to be, at least in part, responsible for the low efficiencies.

Discussion

In this paper, we discuss the properties and structures of non-imidazole based quaternary ammonium salts for ionic liquids. The ultimate goal of this work is to develop a room temperature ionic liquid for use in sodium batteries. Having a moderate operating condition will reduce the overall energy necessary to run the battery and therefore lead to higher overall system efficiencies. Due to the size of the benzyl group, when the Quat pairs with chloroaluminate, the viscosity is higher than desired. The extreme case is the BTBACl melt where the long alkyl chains lead to a liquid with a viscosity that is high enough to prevent the efficient reduction and re-oxidation of sodium. In contrast, both BTMACl and BTEACl form ionic liquids near room temperature (70 to 85°C) that support the efficient plating and stripping of sodium. The improved performance of the BTEACl melt when compared with the BTMACl melt is attributed to the increased electron releasing ability of the ethyl groups over the methyl groups.

In this study, we investigated the modification of the cation and its effect on melting points. However, modifying the anion can also impact the melting point of an ionic liquid. In other studies, larger, asymmetric anions have been shown to lower the melting points of ionic liquids.[15] In order to achieve a room temperature ionic liquid, the symmetry of both the cation and the anion must be reduced. Though effective in lowering the melting point, it may become necessary to substitute the benzyl group with alternative alkyl or aromatic groups to achieve our ultimate goals. Regardless, the data collected using the melts discussed in this report will be useful in determining the structures of the salts to be synthesized and examined in future studies.

Conclusion

Benzyl(trialkyl)ammonium chlorides were found to be good quaternary ammonium chlorides to make ionic liquids with chloroaluminate at slightly above room temperatures (70 to 85°C). The benzyl ring serves two functions: the aromatic resonance distributes the positive charge around the $Quat^+$, while also disrupting the symmetry of the $Quat^+$. These effects both contribute to the melting points of the melts. As compared with the BTMACl melt, the BTEACl melt had better reduction/re-oxidation efficiencies and a lower self-discharge current. The longer alkyl groups (ethyl groups) release more electron density toward the positive center than the shorter ones (methyl groups).

III-2. ***Properties of Benzyl-substituted Quaternary Ammonium Ionic Liquids***

Chapter 2 summarizes the synthesis of new room temperature ionic liquids. These ionic liquids show improved physical properties over those investigated in Chapter 1. The physical properties, density, conductivity, and viscosity, are presented.

Results and Discussion

Imidazolium ions are known to form ionic liquids (ILs) with chloroaluminate ions. They have been used as the electrolyte for electroplatings[15-18] and energy conversion devices.[9,19] Also, many fundamental studies have been performed with imimdazolium-based Ils.[6,20] The imidazolium ion is useful in forming ionic liquids because it has moderate size giving the IL adequate conductivity, modest viscosity, and high solubility for other species. Recently, a variety of quaternary ammonium based ILs have been reported.[14,21] Quaternary ammonium salts (Quats) are attractive for use in ILs because they are easy to synthesize, relatively safe, and can have very low molecular weights, possibly leading to lower viscosity and higher conductivity.

In this work, a new series of quaternary ammonium chloride salts are introduced as the cationic part of room temperature ILs. Figure III-2.1 shows a series of Quats investigated in this study. They are composed of a benzyl group, and three alkyl groups (methyl, ethyl, and/ or propyl groups). The melting point and conductivity were investigated as a function of the asymmetry of the cation. The Quats were mixed with $AlCl_3$ in the ratio of 55 mole % $AlCl_3$ and 45 mole % Quat, N=0.55. (N represents the mole fraction of acid in the melt.) The Lewis acid, $AlCl_3$, forms $AlCl_4^-$ (Lewis neutral) and $Al_2Cl_7^-$(Lewis acid) when mixed with the quaternary ammonium chloride, as shown in Equation III-2.1 and III-2.2. Neutralization of the $Al_2Cl_7^-$ occurs by reacting the

$Al_2Cl_7^-$ with a Lewis base (e.g. Cl^-, such as from NaCl[13]), to produce neutral $AlCl_4^-$ ions (Equation 3).

$$Quat^+Cl^- + AlCl_3 \rightarrow Quat^+ + AlCl_4^- \quad \text{(III-2.1)}$$

$$AlCl_4^- + AlCl_3 \rightarrow Al_2Cl_7^- \quad \text{(III-2.2)}$$

$$Al_2Cl_7^- + NaCl \rightarrow NaAlCl_4 + AlCl_4^- \quad \text{(III-2.3)}$$

Blomgren et al. reported that 67 mole % $AlCl_3$ (acidic melts) with Quats were usable for aluminum plating.[22]

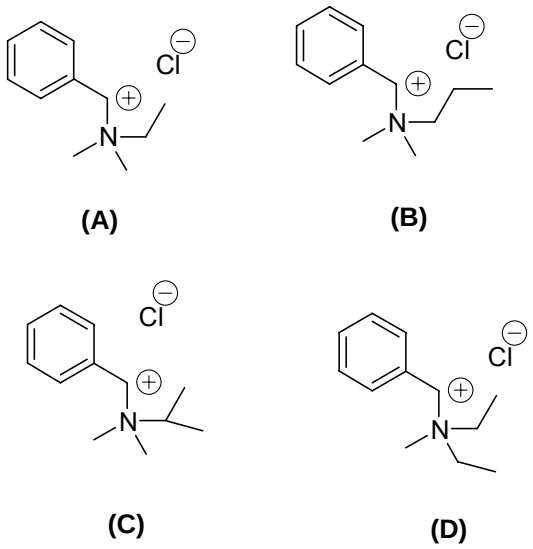

Figure III-2.1 Quats with a benzyl substituent. Quat A: BEDMACl; Quat B: BDMPACl; Quat C: BDMIPACl; Quat D: BDEMACl.

The conductivity (κ), density (ρ), melting point (MP), and viscosity (η) of the ILs at N=0.55 are shown in Table III-2.1 for acidic (55 mole % $AlCl_3$) melts. Three of the Quats shown in Fig.III-2.1 are structural isomers, and the molecular weight of the non-isomer (Fig III-2.1A) is close to the others. The density for each acidic IL is nearly the same. However, the viscosity and conductivity of the Quats are quite different. It appears that the packing density around the nitrogen is important. For example, the isopropyl substituent on Quat C is more compact than the n-propyl on Quat B leading to a higher viscosity for Quat C.

Quat	η (cP) at 27°C	ρ (g/ml) at 27°C	κ (mS/cm) at 27°C	$T_{g(°C)}$	m.p. (°C)
A	278	1.26	0.716	-67.9	13.4
B	364	1.25	0.570	-63.1	-
C	735	1.24	0.333	-57.9	-
D	771	1.25	0.343	-64.1	-

Table III-2.1 Property from acidic RTILs composed of 55 mole % $AlCl_3$ + 45 mole % Quat. Quat A: BDMEACl, Quat B: BDMPACl, Quat C: BDMIPACl, Quat D: BDEMACl.

Previously, we reported the MPs of several benzyltrialkylammonium chloroaluninates.[23] MPs of ILs with benzyltrimethylammonium chloride (BTMACl) and benzyltriethylammonium chloride (BTEACl) were 55.6°C and 66.4°C, respectively. Figure III-2.2 compares the structures of Quats and their MPs. The three Quats in Figure III-2.2 have similar structure and molecular weights. However, the asymmetric nature of benzyldimethylethylammoniuim chloride (BDMEACl) (mixture of the methyl and ethyl groups from the other two) has a dramatic effect on its melting point compared to BTMACl and BTEACl. It is believed that the higher symmetry of the Quat permits easier crystallization resulting in a higher MP. There are two phase transitions for the BDMEACl's IL. The transition at -67.9°C is the glass transition point and the secondary

transition at 13.4°C is the MP of the IL. Quats B, C, D in Figure III-2.1 do not have MPs but glass transition points. Figure III-2.3 shows the transitions for two of the ILs. The IL composed of Quat A with $AlCl_3$ has a glass transition and a melting point, however the Quat C melt has a glass transition only. Sun et. al. reported a similar DSC thermogram for an ionic liquid.[21]

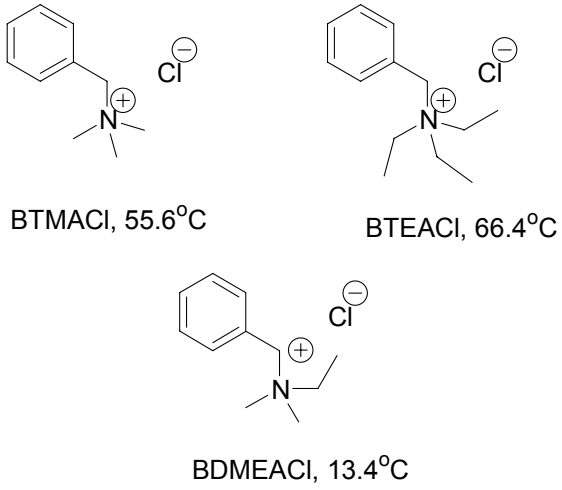

Figure III-2.2 Structural comparison of Quats and their MPs. Quats are: BTMACl, BTEACl and BDMEACl.

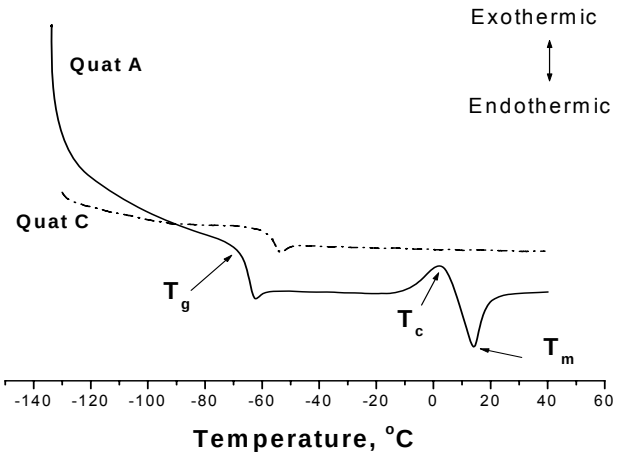

Figure III-2.3 DSC curves for two acidic melts. The curve shows glass transition (T_g), crystallization (T_c), and melting point (T_m).

The conductivity of the neutralized melts (excess NaCl added) is lower and the MPs are higher than those of acidic ILs. Acidic melts are composed of $QuatAlCl_4$, and $QuatAl_2Cl_7$. The neutralization reaction converts the melts into $QuatAlCl_4$ and $NaAlCl_4$. Due to the smaller radius and higher charge density of the sodium ion, the $NaAlCl_4$ in neutral ILs has higher ionic strength than the $QuatAl_2Cl_7$ and $QuatAlCl_4$ in the acidic melts. The higher ionic strength causes lower ionization (more ion paring) resulting in a higher MP and lower conductivity for the neutral ILs.[24]

Table III-2.2 shows the properties for the neutral melts (N=0.50). The neutral melts were formed by adding a NaCl to the N= 0.55 melts. A two-fold excess of NaCl was added to each melt to ensure neutrality. The viscosity was not measured because of the undissolved salt.[25] The glass transition point occurred at higher temperature compared to their acidic counterparts. Also, Quat B and C had MPs even though none were observed in the acidic melts. The second phase-transition points observed in the neutral melts with Quats B and D prohibit the electrochemical measurements at low temperature.

Quat	κ (mS/cm) at 27°C	T_g(°C)	m.p. (°C)
A	0.324	-56.1	-
B	0.216	-57.1	33.3
C	0.125	-45.9	-
D	0.160	-61.4	-9.57

Table III-2.2 Property from neutral RTILs. Acidic melts in Table 1 were neutralized with two fold excess of NaCl. Quat A: BDMEACl, Quat B: BDMPACl, Quat C: BDMIPACl, Quat D: BDEMACl.

Neutral melts formed with Quat A have a wide electrochemical potential window, in excess 4 V as shown in Figure III-2.4. The acidic melt has a relatively narrow potential window because the $Al_2Cl_7^-$ ion can be reduced near 0 V.[26] Figure III-2.4

shows current-potential scans at Pt, Au, and tungsten (W) electrodes in the neutral ILs. Chloride ion is oxidized at about 2.0 V.[26] We believe that the reduction current near –2.0 V is from the reduction of the $Quat^{+}$ ion. The current density at Pt is the highest, probably, due to its catalytic activity and lack of a native oxide. The electrochemical properties of the neutral melts are currently under investigation. The availability of low viscosity, stable, room temperature ILs could enable a variety of electrochemical energy conversion and storage devices.

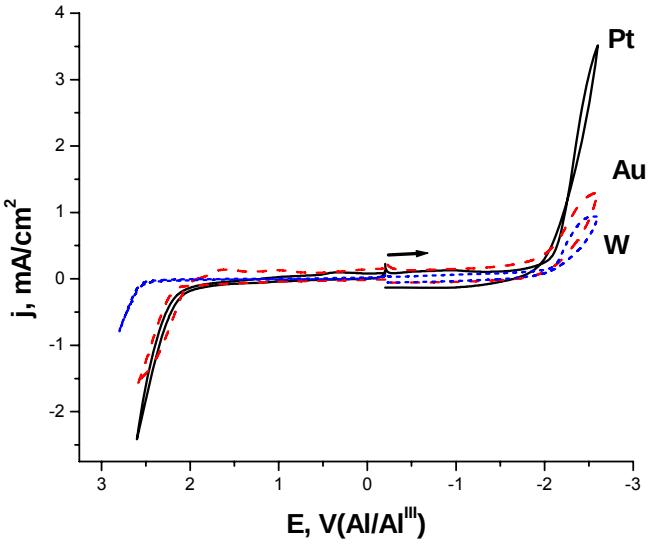

Figure III-2.4 Cyclic voltammetry of the neutral Quat A ionic liquid. Working electrodes are platinum, gold and tungsten electrodes, 1 mm diameter discs. The scan rate was 100 mV/sec.

III-3. ***Electrochemical Investigation of Benzyl-substituted Quaternary Ammonium Ionic Liquids***

Chapter 3 shows the electrochemical performance of the new ionic liquids demonstrated in Chapter 2. Coulombic efficiencies and self-discharge currents for the liquids are presented as a function of temperature and electrode materials.

Results and Discussion

Figure III-3.1 shows a series of Quats investigated in this study. They are composed of a benzyl group, and three alkyl groups (methyl, ethyl, and/ or propyl groups). Acidic melts (N = 0.55) with these Quats formed room temperature ionic liquids. Asymmetric structure of the Quats lowered the melting points of the melts. Properties of the melts were discussed elsewhere.[24] An acidic melt at a higher acidity (N=0.67) reported were applicable for aluminum plating.[22]

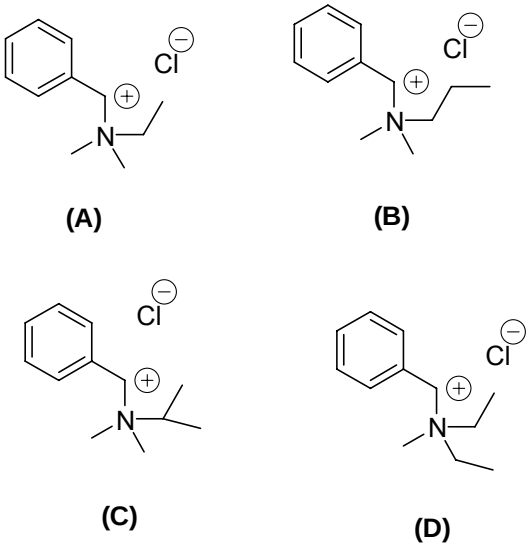

Figure III-3.1 Quats with a benzyl substituent. Quat A: BEDMACl; Quat B: BDMPACl; Quat C: BDMIPACl; Quat D: BDEMACl.

Figure III-3.2 shows the conductivity vs. temperature with the acidic melts (N = 0.55). Quats B, C, D are structural isomers. Quat A has lower molecular weight (1 CH_2 less) than others. The melts with Quat A has a clearly higher conductivity than the others because it is less viscous than the others. Melts with Quat C and D are much viscous than A and B, because the packing density around the nitrogen is denser for Quat C and D. Figure III-3.3 is the conductivity vs. temperature with neutral melt. Figure III-3.3 shows that the structural isomers behave similarly in conductivity as temperature increases. The conductivity difference between the melt of Quat and others increased as temperature increased. It means that the mobility/temperature is higher with smaller ions than the bigger ions.

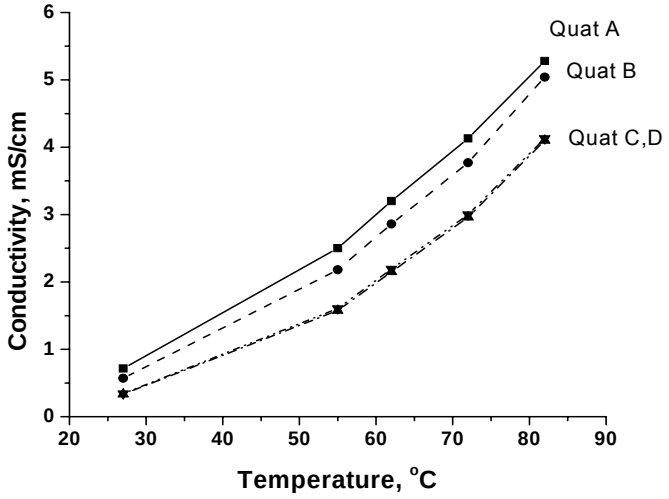

Figure III-3.2 Conductivity vs. temperature with the acidic melts (N= 0.55).

Electrochemical properties for the sodium battery were measured with the neutralized melt from the acidic melt (N = 0.55). The chronopotentiomety was performed for the coulombic efficiency and the self-discharge current measurements.

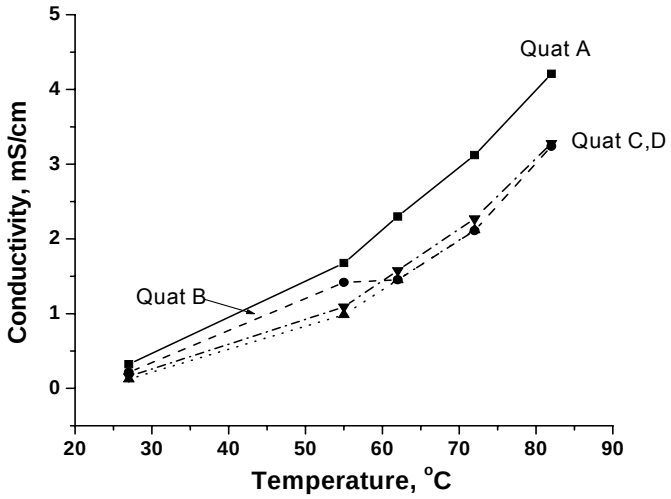

Figure III-3.3 Conductivity vs. temperature with the neutal melts.

Table III-3.1 is the comparison of the two electrodes in the same melt at the same temperatures. The current density was the optimum current density where the maximum efficiency was obtained under the given condition. Therefore, the current density for the measurements was not identical for the electrodes. At the same temperature, the efficiency and the self-discharge current for the two electrodes were also comparable. The thickness of the sodium deposit is thick enough to prohibit the two electrodes showing the nature of each metal substrate. Temperature rise gives higher efficiency, but worse self-discharge currents. The better mobility at the higher temperature caused higher efficiencies. However, the higher temperature also expedites unwanted reaction for the self-discharge current.

Temperature	Electrode	Current Density , mA/cm^2	Coulombic efficiency, %	Self-discharge current, $\mu A/cm^2$
25ºC	Pt	0.68	87.5	3.96
	W	1.02	88.5	5.25
50ºC	Pt	4.09	92.4	15.6
	W	5.09	92.0	15.6

Table III-3.1. Comparison between Pt and W electrodes for coulombic efficiency and self-discharge current. The measurements were performed by chronopotentiometry for 100 seconds. The melt is composed of 45 mole % BEDMACl and 55 mole % $AlCl_3$. It is neutralized with NaCl and $SOCl_2$ is added.

Table III-3.2 shows the comparison of electrochemical properties of sodium plating with melts. Quat B and C have higher viscosity that Quat A. Therefore, the melts of Quat B and C need higher than room temperature to compare their properties with the melt Quat A. Quat D was too viscous to obtain electrochemical data for any condition. It produced no electrochemical data but very high noise. The melt of Quat A shows better performance than the melt of Quat C in both the efficiency and the self-discharge current. The melt of Quat A has better efficiency only than the melt of Quat B. High viscosity of the Quat B melt might cause the low efficiency and the low self-discharge current. We could observe low efficiency and low self-discharge current at the high viscosity (low temperature, 25ºC) in Table III-3.1. The self-discharge current value from the IL composed of MPIC[10] gave 22 $\mu A/cm^2$. MSC[7] based IL showed 3 $\mu A/cm^2$. The IL of Quat A has comparable values of self-discharge currents at room temperature.

Temperature	Quat	Current Density, mA/cm^2	Coulombic efficiency, %	Self-discharge current, $\mu A/cm^2$
50ºC	A	4.09	92.4	15.6
	C	1.98	91.2	28.7
71ºC	A	4.09	91.5	52.0
	B	3.40	81.7	36.4

Table III-3.2 Self-discharge current vs. Quats. Chronopotentiometry measurements were performed for 100 sec with Quat A melts. The charge was matched for all melts by adjusting time, because each melt has different optimum current density.

Conclusion

Benzylethyldimethylammonium chloroaluminate has a coulombic efficiency and self-discharge current comparable to the MPIC and the MSC based sodium battery electrolytes. The substrate materials does not affect the efficiency and the self-discharge current as long as they are inert in the system.

III-4. ***The Role of Additives In the Electroreduction of Sodium Ions in Chloroaluminate-based Ionic Liquids***

In Chapter 4, we discuss how the additive catalyzes the plating of sodium metal in the melts. We approach the problem by measuring the conductivities of different acidity melts, and analyzing the ionic interaction with and without the additive.

Results

Acidic mixtures were prepared by mixing excess aluminum chloride with the Quat. Varying the mole fraction of $AlCl_3$ changed the acidity of the ionic liquid by altering the mole fraction of $Al_2Cl_7^-$ and $AlCl_4^-$. Table III-4.1 shows the density, viscosity, and conductivity for mixtures, N = 0.51, 0.53, 0.55 and 0.59. A significant increase in viscosity was observed as the melt approaches neutrality (N approaches 0.5).

Mole Fraction		Mole fraction*		Measurement at 27 ± 1ºC		
$AlCl_3$	BDMEACl	$AlCl_4^-$	$Al_2Cl_7^-$	Density (mmol/ml)	Viscosity (mm^2/s)	Conductivity (mS/cm)
0.51	0.49	0.479	0.021	7.40	370	0.512
0.53	0.47	0.436	0.064	-	-	0.617
0.55	0.45	0.389	0.111	6.95	222	0.715
0.59	0.41	0.279	0.221	6.59	123	1.010

Table III-4.1 Properties of acidic melts of BDMEACl: $AlCl_3$.
(* Due to the equilibrium constant[1], the fraction of Cl^- is of the order of 10^{-17}.)

The conductivity of a liquid is a function of the concentration (or density) of the ions and their interaction (mobility). For each of the acidic IL mixtures, the cation mole fraction, $BDMEA^+$, was kept constant, so that the relative contributions of the $Al_2Cl_7^-$ and $AlCl_4^-$ ions to the conductivity could be evaluated. A significant drop in conductivity is observed as the liquid approaches neutrality (N approaches 0.5) with the lowest conductivity, 0.512 mS/cm, observed for the N = 0.51 melt. The maximum number of anions possible in 1 ml was obtained from the density (mmol/ml) and the molecular weight. The maximum number of anions are 4.46×10^{21}, 4.18×10^{21}, and 3.96×10^{21} anions/ml for N = 0.51, 0.55 and 0.59 melts, respectively. As the acidity decreases (from N = 0.59 to N = 0.51) and the mole fraction of $Al_2Cl_7^-$ decreases, the

potential number of anions increases, however, the conductivity decreases. The potential number of ions increases because $Al_2Cl_7^-$ converts to two $AlCl_4^-$ species as the melt approaches the neutral point (N approaches 0.5). However, the increased number of $AlCl_4^-$ anions does not provide higher conductivity. These results indicate a higher individual contribution to the conductance for the $Al_2Cl_7^-$ ion than for the $AlCl_4^-$ ion. On a per mole basis, the equivalent conductance of $Al_2Cl_7^-$ is about 4.4 times that of $AlCl_4^-$. This value was obtained from the number of ions and the conductivity of the IL. The size of $Al_2Cl_7^-$ is larger than $AlCl_4^-$ ($Al_2Cl_7^-$ ion has a bridging chloride between two $AlCl_3$ units). Thus, the electrostatic interaction between $Al_2Cl_7^-$ and $Quat^+$ is weaker than between $AlCl_4^-$ and $Quat^+$ at this temperature. Although the mobility of an unassociated $AlCl_4^-$ ion would be higher than that of $Al_2Cl_7^-$ (because of its size), the degree of association between $AlCl_4^-$ and $Quat^+$ (i.e. ion pairing) is apparently responsible for the low contribution of $AlCl_4^-$ to the conductivity. Figure III-4.1 shows the decrease in conductivity as the mole fraction of $AlCl_4^-$ is increased. At higher temperatures, one would expect higher conductivity due to greater disassociation of the ion pairs and higher mobility (lower viscosity) of the IL.

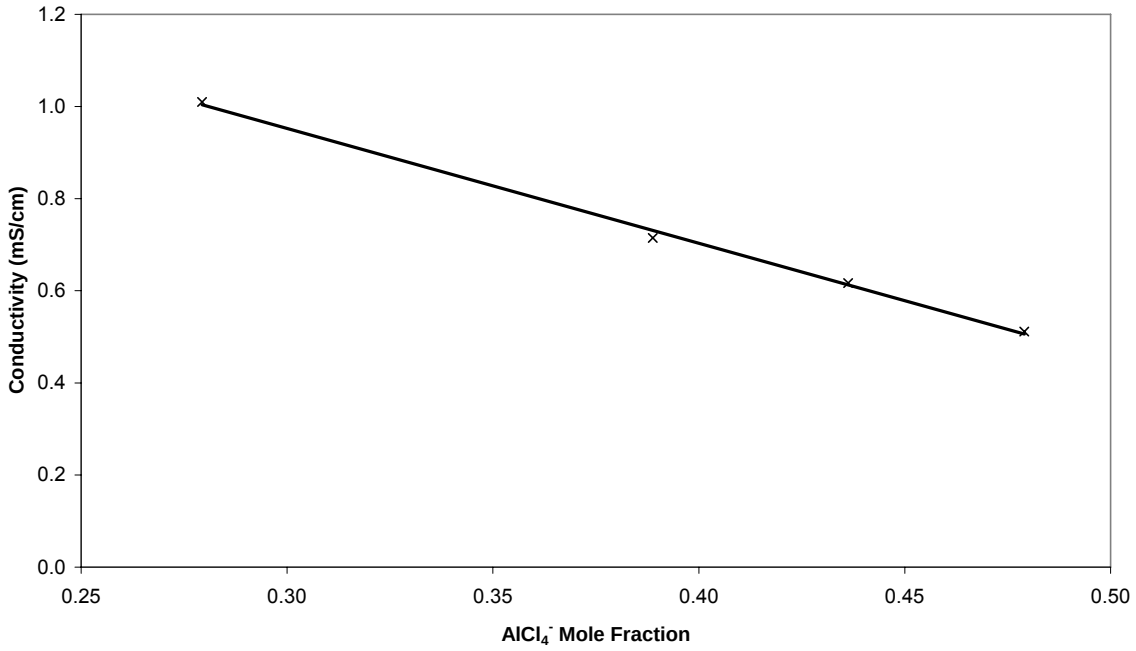

Figure III-4.1 Conductivity versus $AlCl_4^-$ mole fraction for a mixture of 55% $AlCl_3$ and 45% BDMEACl at 27ºC.

Neutralization of the N = 0.55 acidic melt with excess NaCl results in a mixture with 41% $Quat^+$, 9% Na^+, and 50% $AlCl_4^-$ ions on a molar basis. The conductivity dropped from 0.715 mS/cm to 0.324 mS/cm even though the total number of potential ions per volume increased. If the conductivity of the cations ($Quat^+$ and Na^+) were the same and the equivalent conductances of $AlCl_4^-$ and $Al_2Cl_7^-$ were the same as in the acidic melts then, the conductivity of the N = 0.5 melt could be estimated from extrapolation of Table III-4.1 to N = 0.5. The expected value would be 0.455 mS/cm. The actual value (0.324 mS/cm) is 0.130 mS/cm lower than the extrapolated value. This result indicates that the individual conductivity of Na^+ is actually lower than that of $Quat^+$. That is, there is little contribution from $Al_2Cl_7^-$ in the N = 0.51 melt and the most significant change caused by neutralization is the addition of Na^+ in place of $Quat^+$. If we

assume $NaAlCl_4$ has no contribution to conductivity, the $Quat^+$: $AlCl_4^-$ pair comprises roughly 82% of the mixture. The expected conductivity from $Quat^+$: $AlCl_4^-$ in N = 0.5 melt is 0.372 mS/cm, which is 0.05 mS/cm higher than the observed value. These results indicate that the addition of excess NaCl to the liquid is responsible for the 0.05 mS/cm short fall. That is, the NaCl has a negative impact on the solution conductivity.

In each case, the ion fractions were calculated assuming that the solubility of NaCl is sufficiently low so as not to affect the final mole fractions of the other ions. When excess NaCl is added, a solid powder is observed at the bottom of the liquid supporting this assumption. The salt that is dissolved could either stay as NaCl or disassociate into its respective ions, Na^+ and Cl^-. In both cases the salt will impact the solution conductivity. If the salt disassociates, the small Na^+ and Cl^- ions in the melt would be expected to increase the conductivity. Salt present as NaCl would hinder conductivity by introducing a neutral, nonconductive species to the liquid.

The relative contribution of Na^+ in comparison to $Quat^+$ was investigated by comparing the conductivity of the melts with the same acidity but different Na^+-to- $Quat^+$ ratios. An N = 0.55 melt was partially neutralized to N = 0.53 by the addition of NaCl and compared to a N = 0.53 melt with no NaCl. Also an N = 0.59 melt was converted to N = 0.51 with NaCl and compared to an N = 0.51 melt with no NaCl. The conductivity versus temperature for each of the aforementioned melts was measured and plotted in Figure III-4.2. At 27°C the sample partially neutralized to N = 0.51 (Fig. III-4.2D) formed a slurry comprised of liquid and very thick gel that prevented the measurement of its conductivity. The other mixtures each formed liquids that were a single homogeneous phase at 27°C. When the temperature was increased from 55°C to 82°C the conductivity

values for the N = 0.51 mixtures rose from 2.18 to 5.12 for the acidic case (Fig. III- 4.2C) and 1.647 to 4.65 mS/cm for the partially neutralized sample (Fig. III-4.2D). For the N = 0.53 mixture, the difference in conductivity between the acidic (Fig. III-4.2A) and partially neutralized (Fig. III-4.2B) samples increased with temperature from 0.092 mS/cm at 27°C to 0.58 mS/cm at 82°C. In each of the two acidities, at each temperature, the exchange of Na^+ for $Quat^+$ (as a result of partial neutralization) lowered the conductivity. Once again, this shows that the presence of Na^+ in the melts contributes little or nothing to the melt conductivity, and the Na^+ contribution is less than that of $Quat^+$ even though Na^+ is smaller.

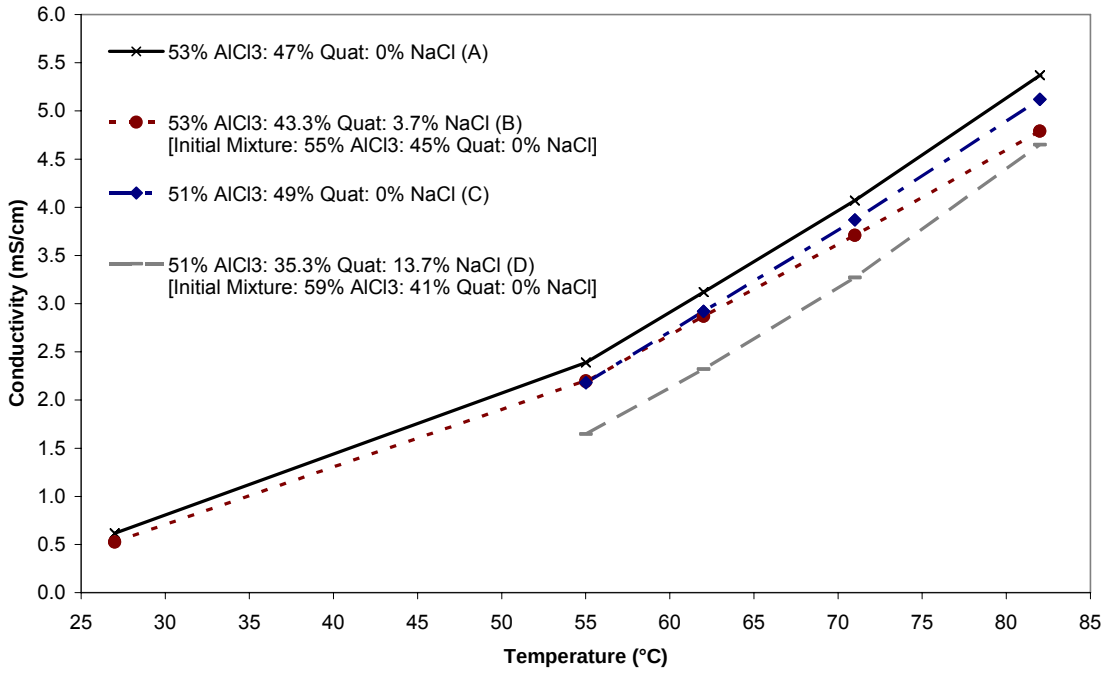

Figure III-4.2 Conductivity versus temperature for: (A) Mixture of 53% $AlCl_3$ and 47% BDMEACl; (B) Mixture of 53% $AlCl_3$, 43.3% BDMEACl, and 3.7% NaCl.; (C) Mixture of 51% $AlCl_3$ and 49% BDMEACl; (D) Mixture of 51% $AlCl_3$, 35.3% BDMEACl, and 13.7% NaCl.

The conductivity contribution of $NaAlCl_4$ can be evaluated by addition of $NaAlCl_4$ fine powder to the melt. If $NaAlCl_4$ is completely insoluble in the liquid, the addition will have no positive effect on the conductivity. An acidic melt (N = 0.53) with an initial conductivity of 0.618 mS/cm at 27°C was used as the starting liquid. An acidic mixture was chosen since the fraction of ions present ($Quat^+$, $AlCl_4^-$, and $Al_2Cl_7^-$) is known. The conductivity versus mole % $NaAlCl_4$ is shown in Figure III-4.3. Upon addition of 1.76 mole % $NaAlCl_4$, the conductivity decreased 12% to 0.544 mS/cm. No solid precipitate was observed after mixing for two days. After two days, $NaAlCl_4$ was again added bringing the $NaAlCl_4$ content of the liquid to its final value, 3.46 mole %. As a result of the addition, the conductivity dropped further to 0.485 mS/cm (an additional 9.5%). After the second addition, a solid precipitate was observed indicating that the liquid was saturated with $NaAlCl_4$. The results show a reduction in conductivity greater than can be accounted for just by a change in the fraction of ions (i.e. addition of an inert substance to an ionic liquid). The drop in conductivity indicates a decrease in the individual conductances of the ions present, as would occur with increased ion association.

Previously, it has been shown that sodium metal cannot be electrodeposited from a neutralized ionic liquid (e.g. imidazolium-based melts) even though sodium ions are in the melt.[9,10] A trace amount of an acidic additive activates the electrodeposition process producing sodium metal. These previous results are consistent with a lack of free sodium ions in the IL (ions available for deposition). To test this hypothesis, very small amounts of $SOCl_2$ were added to a NaCl-neutralized IL. An IL composed of BDMEACl and $AlCl_3$ (N = 0.55) was prepared and neutralized with two-fold excess NaCl. $SOCl_2$ was

added with a micropipette and the conductivity was measured after one hour of stirring for each addition of $SOCl_2$. Long mixing times were avoided because $SOCl_2$ could evaporate. The results of the conductivity tests after each addition are shown in Figure III-4.4. The addition of 1 weight % $SOCl_2$ results in nearly a 10% increase in the conductivity even though $SOCl_2$ itself is not expected to be ionized in the melt.

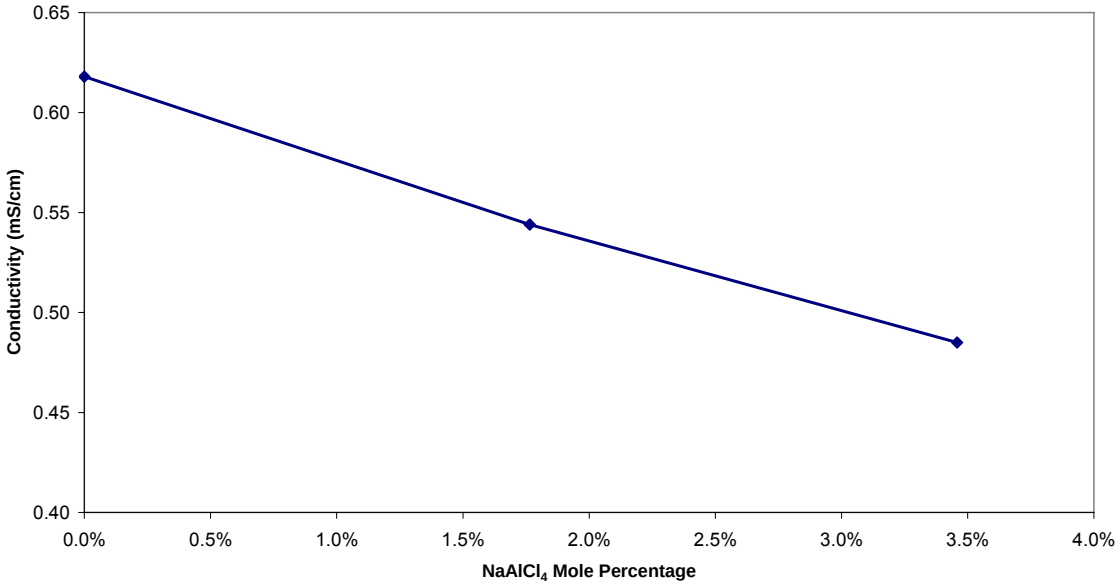

Figure III-4.3 Conductivity versus mole % $NaAlCl_4$ for an initial mixture of 53% $AlCl_3$ and 47% BDMEACl at 27°C.

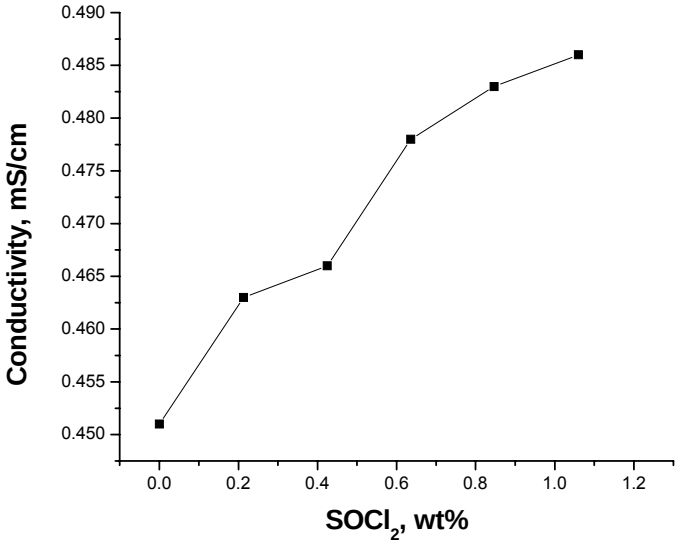

Figure III-4.4 Conductivity at 30°C versus weight % $SOCl_2$ for an initial mixture of 50% $AlCl_3$, 40.9% BDMEACl, and 9.1% NaCl.

The remarkable ability of $SOCl_2$ (and other additives) to facilitate the deposition of sodium can be shown electrochemically. A cyclic voltammogram (CV) of a Pt electrode in a neutralized BDMEACl: $AlCl_3$ melt (starting material N = 0.55) results in no electroreduction of sodium ions, only the irreversible reduction of the $BDMEA^+$. Similar results were obtained for mixtures tested with less than 0.025 mole % $SOCl_2$. However, the CV results for the same melt with 0.18 mole % $SOCl_2$ is shown in Figure III-4.5. The reduction and re-oxidation of sodium at ca. -2 V is observed. The reduction current is far in excess of the flux that could be provided by the $SOCl_2$. This result suggests that the $SOCl_2$ additive is working to increase the concentration of sodium ions, in a catalytic way and is not being consumed. As the concentration of sodium ions in the solution increases the reduction potential shifts to more positive potentials. Increasing the $SOCl_2$ level also led to higher current densities for the reduction and re-oxidation rather than changes in the potential at which reduction occurred.

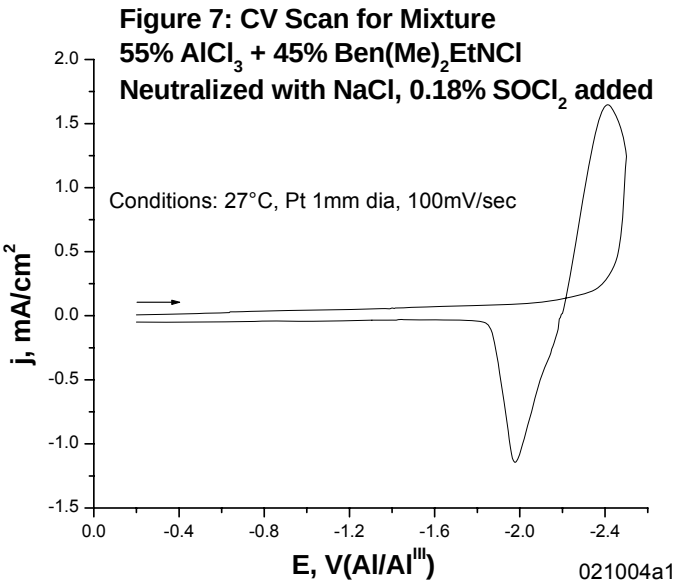

Figure III-4.5 CV scan at 27°C for a mixture of 55% AlCl3 and 45% BDMEACl neutralized with 100% excess NaCl and 0.18 mole % $SOCl_2$ added.

Discussion

The Zebra cell that operates at a high temperature does not require the addition of an additive because all components are molten and ionized. However, the low-temperature ionic liquid cell requires an additive to electrodeposit sodium even though the melt is liquid. The conductivity data showed that exchange of $Quat^+$ for Na^+ resulted in a drastic drop in conductivity to a level where it appears that the Na^+ is contributing nothing toward the overall melt conductivity. The addition of $NaAlCl_4$ also lowers the melt conductivity, even though it appears to dissolve. Finally, the addition of trace amounts of HCl (previous results) or $SOCl_2$ appear to activate the sodium ions in the melt so that they can be electrodeposited at rates far in excess of the flux of the additive. The increase in the melt conductivity (Fig. III-4.4) with $SOCl_2$ addition, shows that $SOCl_2$ dramatically increases the melt conductivity. This behavior is consistent with the concept

that the $SOCl_2$ serves to release Na^+ ions from ion-pairs enabling them to contribute to the conductivity and be reduced to sodium metal. Scheme III-4.1 shows the proposed interaction between the additives and sodium ions in the melt. As the acid is added to the melt the interaction between the additive and the chloride becomes stronger. This interaction weakens the interaction between Na^+ and $AlCl_4^-$ ions. Na^+ is thus available for conduction and electrodeposition. HCl acts in a similar way to provide more freedom to the Na^+ ion. Thus, $SOCl_2$ and HCl act as a Lewis acid[27-29] and compete with $AlCl_3$ for Cl^-.

(A)

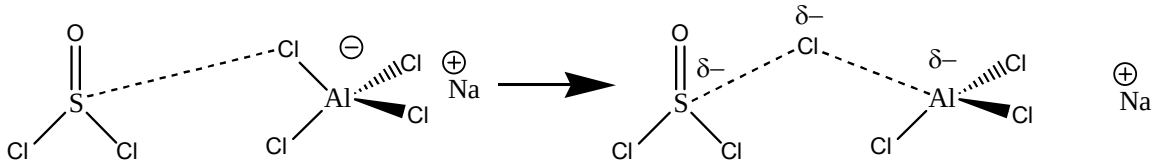

(B)

Scheme III-4.1 Interaction between additives and $NaAlCl_4$ ion.

III-5. ***Cation Electrochemical Stability in Chloroaluminate Ionic Liquids***

In Chapter 5, the electrochemical stability of ten organic cations is investigated. The structures of the salts are shown in Figure III-5.1. The stability of the ten cations was investigated as the solute in acetonitrile (ACN). Previously, similar cations were investigated in ACN by Gifford and Palmisano to investigate the impact of replacing the beta hydrogen in an imidazolium cation with a methyl group.[30] For salts III, VI and VII, the stability in the chloroaluminate IL was also evaluated. The reduction mechanism of salts III, VI, and VII, was studied using mass spectroscopy.

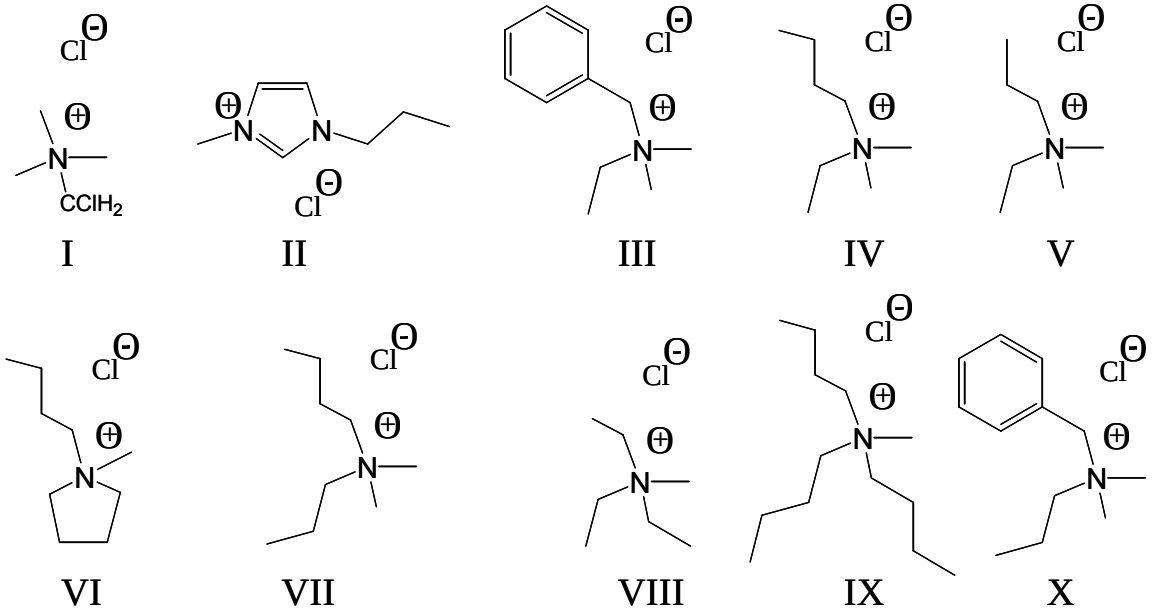

Figure III-5.1 I: $Me_3MeClNCl$; II: 1-methyl-3-propylimidazolium chloride; III: benzylethyldimethylammonium chloride; IV: butylethyldimethylammonium chloride; V: ethyldimethylpropylammonium chloride; VI: butylmethylpyrrolidinium chloride; VII: butyldimethylpropylammonium chloride; VIII triethylmethylammonium chloride; IX tributylmethylammonium chloride; X benzyldimethylpropylammonium chloride.

Results

Cyclic Voltammetry in Acetonitrile:

Room-temperature ILs can be formed by mixing an imidazolium or quaternary ammonium salt with aluminum trichloride. Upon formation of an IL, the reduction potential of the cation will determine the negative potential limit of the electrochemical window. In this work, the stability of the salts was evaluated by dissolving the organic chloride salts (compounds I to X shown in Fig. III-5.1) in acetonitrile to form 0.1M solutions. The chloride salts were used so that only the cation was changed between the samples. Cyclic voltammetry (CV) was performed scanning from the open circuit voltage toward the negative potential direction until a significant reduction current was observed. The reduction potentials reported in this text correspond to the potential at which the current exceeded 1 mA/cm^2 at a scan rate of 100 mV/s.

Figure III-5.2 shows a comparison of three salts: salt I (Me_3(MeCl)NCl), salt II (1-methyl-3-propylimidazolium chloride) and salt III (benzylethyldimethylammonium chloride). Sodium metal can be electrodeposited from salts II and III when they are used in chloroaluminate ILs.[7,24] Salt I is most easily reduced as shown in Figure III-5.2 where a reduction current of 1 mA/cm^2 was observed at –1.35 volts. The chloromethyl group is easily reduced due to the electron withdrawing nature of the halogen. The imidazolium, salt II, is more difficult to reduce than I, 1 mA/cm^2 at –1.53 volts, and salt III is the most difficult to reduce with 1 mA/cm^2 at –1.74 volts. Finkelstein et al. found that during reduction the leaving group is the benzyl radical.[31,32] The benzyl radical is the most likely product from the reduction of salt III. However, the hydrogen at the beta position of the imidazolium ring of salt II is more easily reduced resulting in the lower reduction potential (1.53 vs. 1.74 volts) for salt II compared to salt III.[30]

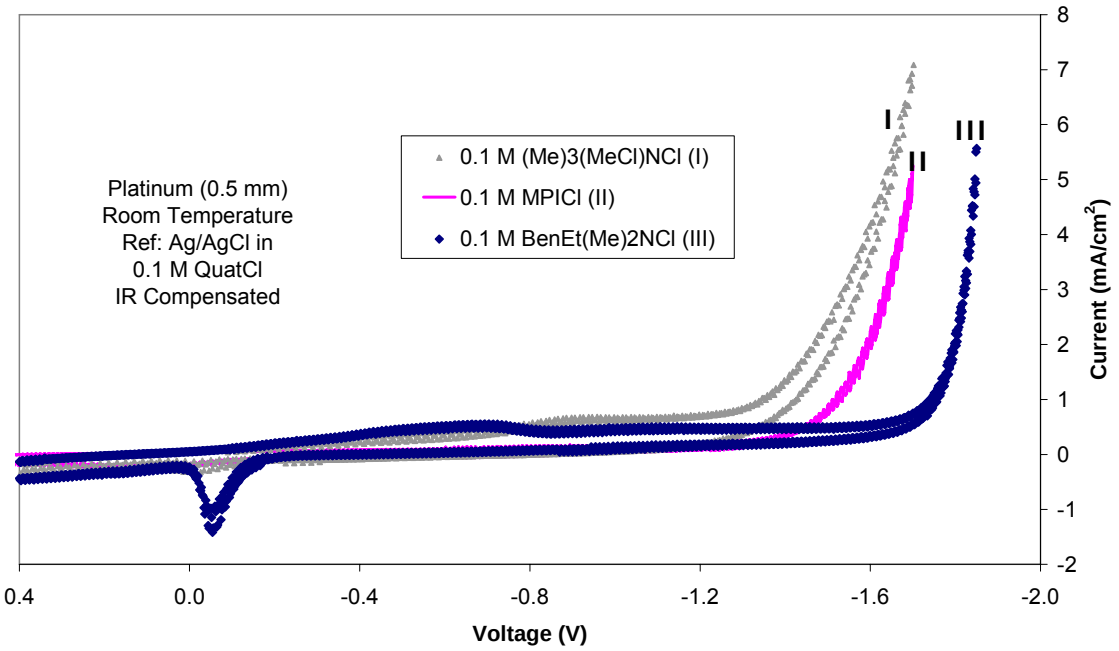

Figure II-5.2 CV scans for 0.1M solutions of salts I, II and III in acetonitrile.

Alkyl substituents on the quaternary ammonium cation are more difficult to reduce than benzyl groups because they form less stable radicals (i.e. poorer leaving groups). A comparison of two alkyl-substituted quaternary ammonium cations to the benzyl-substituted quaternary ammonium salt is shown in Figure III-5.3. The benzyl-substituted quaternary ammonium cation is the most easily reduced among the three, -1.74 V. The reduction potential of the cation becomes more negative (more difficult to reduce) when an alkyl group is used in place of the aromatic benzyl substituent. Further, the shorter the alkyl chain length, the more negative its reduction potential due to stability of the resulting product. The smallest cation, salt V, is the most difficult to reduce at -1.89 V, with salt IV at -1.87 volts. The difference between salts III and IV (benzyl to alkyl) is more significant than the difference between salts IV and V (both are alkyl substituted).

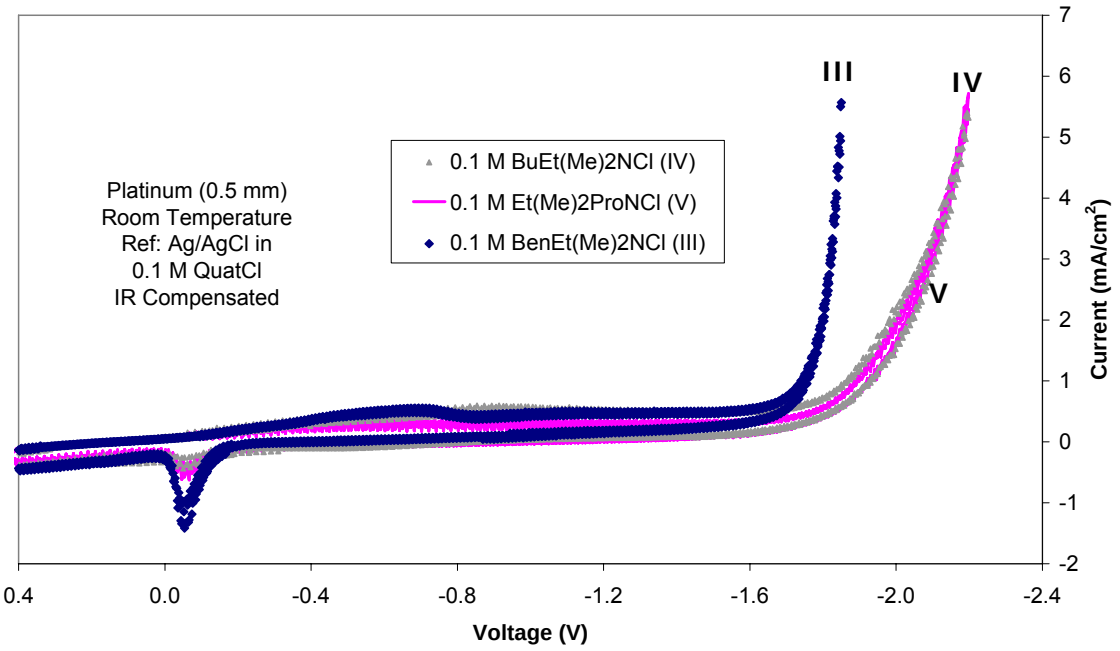

Figure III-5.3 CV scans for 0.1M solutions of salts III, IV and V in acetonitrile.

Figure III-5.4 shows the stability of the pyrrolidinium-substituted quaternary ammonium cation (VI), to the benzyl-substituted (III) and tetra alkyl-substituted cation in ACN. Salts VI and VII both have nine total carbons, however, salt VI, the pyrrolidinium cation, is different in that a heterocyclic ring is formed by four of the carbons. Salt VI is significantly more stable than salt III (1 mA/cm^2 at -2.09 V vs. -1.74 V) and more stable than salt VII (1 mA/cm^2 at –1.78 V). The heterocyclic ring structure of salt VI makes for a very poor leaving group. If this increased stability translates to a wider electrochemical window when the cation is used in an IL, this cation would be an attractive candidate at negative potentials (e.g. stable in the presence of sodium or lithium for metal anode batteries).

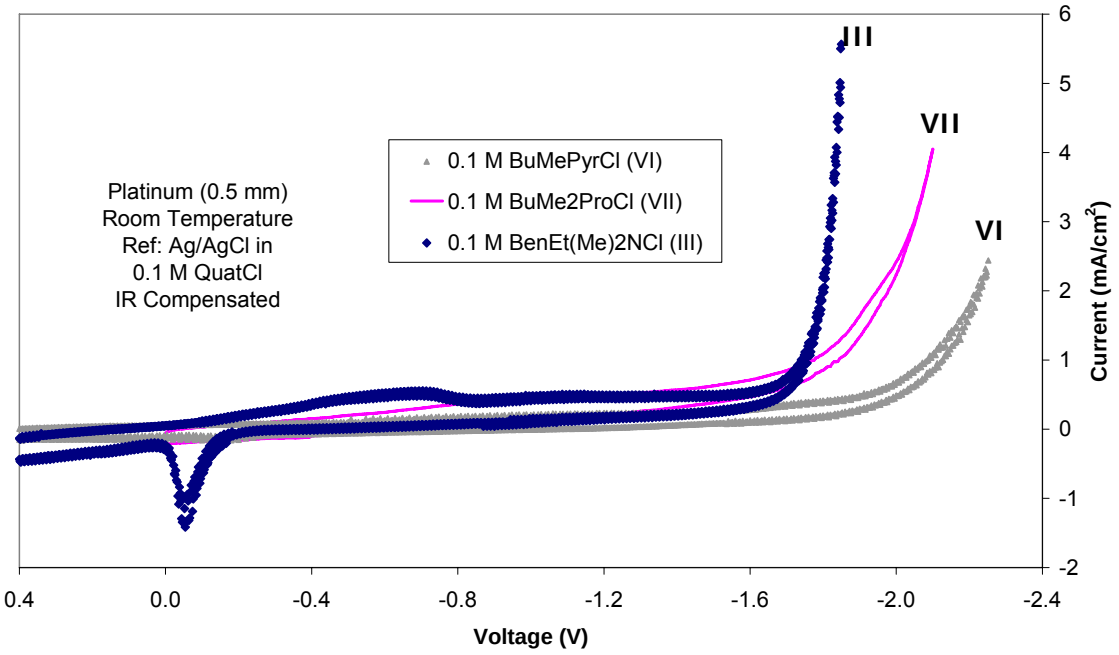

Figure III-5.4 CV scans for 0.1M solutions of salts III, V and VI in acetonitrile.

Along with the previous 7 salts, the reduction potential of three additional quaternary ammonium cations (VIII, IX and X) in acetonitrile were investigated. Table III-5.1 summarizes the reduction potentials measured utilizing CV tests for these three salts, as well as salts III, IV and V. The seven carbon salts, salts V and VIII, are structural isomers that both had a reduction potential of -1.89 volts. The best stability measured for a quaternary ammonium cation was for the salt with the largest molecular weight, salt IX, which reduced at –1.95 volts. The two salts with benzyl groups, salt III and X, reduced at similar potentials, -1.74 and –1.75 volts, respectively. The similarity in reduction potential indicates that the aromatic benzyl group is the primary substituent determining the stability of the cation.

Name	MW	Carbon #	Reduction Potential
	(g/mol)		(volts)
Et_3MeNCl (Salt VIII)	151.68	7	-1.89
$ProEtMe_2NCl$ (Salt V)	151.68	7	-1.89
$BuEtMe_2NCl$ (Salt IV)	165.71	8	-1.87
$BenEtMe_2NCl$ (Salt III)	199.73	11	-1.74
$BenProMe_2NCl$ (Salt X)	213.75	12	-1.75
Bu_3MeNCl (Salt IX)	235.84	13	-1.95

Table III-5.1 Reduction potentials of 0.1M salt solutions in acetonitrile.

For the structural isomers, the propyl group in salt V is a better leaving group than the ethyl groups of salt VIII. However, this effect appears to be offset by replacing a methyl group with the larger ethyl group. The presence of three ethyl groups is believed to stericly hinder reduction of the nitrogen. This would explain the increased stability when the three ethyl groups are replaced with butyl groups, going from salt VIII to IX. Though the butyl groups are better leaving groups, their size more effectively blocks the reduction of the nitrogen. The longer alkyl chains are also beneficial as they release more electron density to the positive nitrogen center.[23]

Mass Spectroscopy of Acetonitrile Solutions:

Mass spectroscopy was used to help identify the reaction products from electroreduction of the cations in ACN. A 0.1M solution of salt III in ACN was electrolyzed and the results are shown in Figure III-5.5. The mass spectrum of an electrolyzed solution, where charge corresponding to 12.5% of the cations being reducted, is compared to a control solution, which was not electrolyzed. The electrolysis was carried out at 0°C to slow the evaporation of acetonitrile and volatiles produced during the electrolysis period. The dominant peak observed for both the electrolyzed salt III solution and the control was mass 165, which corresponds to the mass of the salt III

cation alone. The intensity of the other masses was normalized to the 165 peak for comparative purposes. Both the control and the electrolyzed solution show mass peaks at 58.9, 100 and 363.2. The peak at 363.2 was produced in the spectrometer and corresponds to two cations bridged by a chloride anion. The electrolyzed solution shows new peaks at 42.1, 74.1, 114.9, 135.9, 141.9, 150.1, 273.1 and 335.2. The peak at 42.1 is most likely due to addition of a proton to acetonitrile.

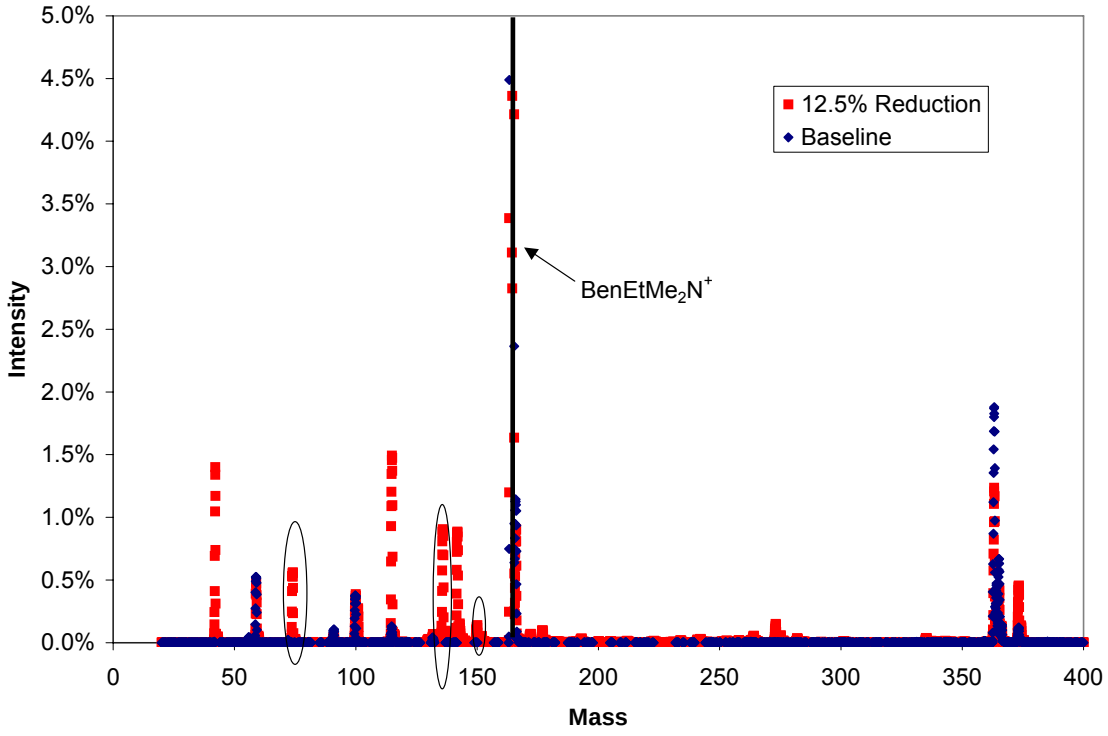

Figure III-5.5 Mass spectroscopy results for 0.1M acetonitrile solution of salt III before and after 12.5% reduction.

Several of the new peaks correspond to decomposition products from the cation. The peak at 74.1 corresponds to the loss of the benzene. Similarly, the peak at 114.9 could be the loss of benzene and the additional presence of acetonitrile. Loss of the ethyl group matches with the peak seen at 135.9. The loss of a methyl group corresponds to

the peak seen at 150.1. Finally, the loss of the benzene and the ethyl groups from the di-cation with bridging chloride are seen at masses 273.1 and 335.2, respectively.

The mass spectrometry results for the electrolysis of a 0.1M ACN solution (charge corresponding to 10% electrolysis of the cations present) of salt VI is shown in Figure III-5.6. The results from the electrolyzed solution are compared to a control sample. The spectra are normalized to the dominant peak at 142, which corresponds to the cation, $BuMPyr^{+}$. Both the electrolyzed and control solution show peaks at mass 58.9, 100, 116.9, and 319.2. No new significant peaks were observed from the electrolyzed solution. The peak at 319.2 appears to be due to two cations bridged by a chloride anion, similar to the results for salt III. There are two potential explanations for the absence of daughter peaks resulting from the reduction of butyl methyl pyrrolidinium cation. First, the loss of a butyl group results in a small molecule that evaporates prior to mass analysis, however, no quaternary ammonium fragment was found. Second, and more likely, is that the reduction of the salt VI cation resulted in breaking the carbon-nitrogen bond within the heterocyclic ring. If this were the case, the reduced form would result in one fragment with the same mass as the parent cation. That is, reduction of the non-cyclic alkyl results in an alkyl leaving group, but the cyclic structure does not because it remains bonded to the nitrogen.

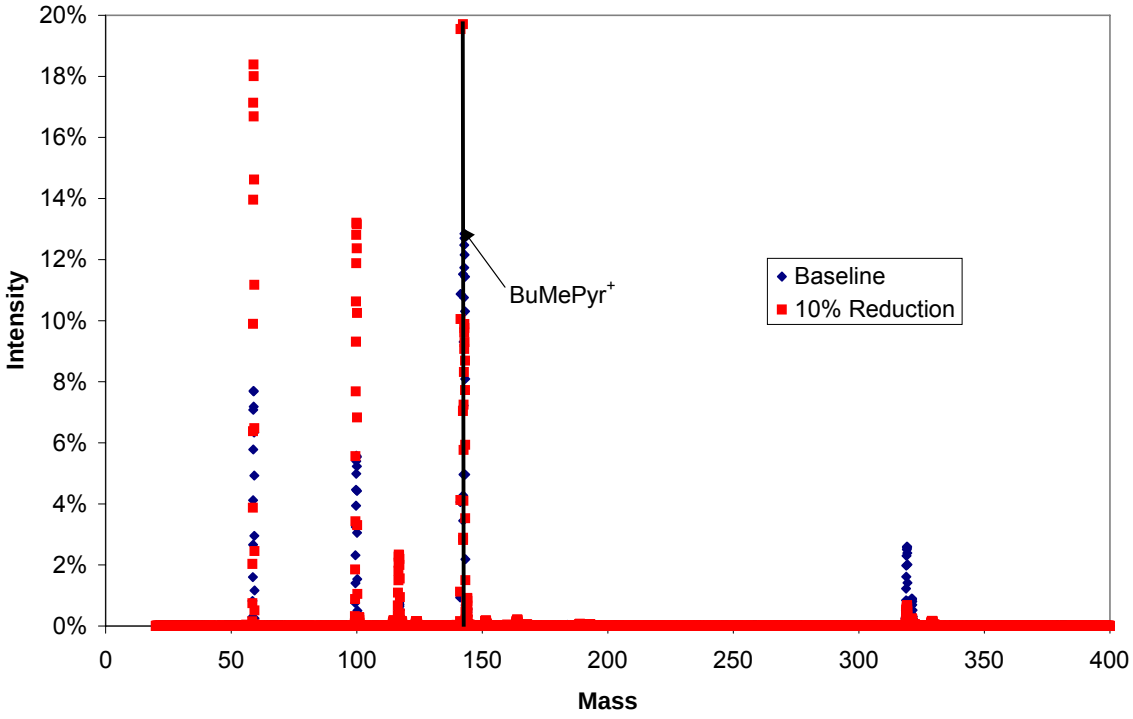

Figure III-5.6 Mass spectroscopy results for 0.1M acetonitrile solution of salt VI before and after 10% reduction.

Figure III-5.7 shows the spectrometry results before and after a 20% reduction for a 0.1M acetonitrile solution of salt VII. Salt VII has the same number of carbons as salt VI, however, the four carbon, one nitrogen heterocyclic ring has not been formed between the propyl and methyl substituents. The dominant peak in both electrolyzed and control sample is mass 144, which corresponds to the cation, $BuMe_2ProN^+$. Both solutions showed peaks at 129.9, 158, 323.2, and 333.3. The peak at 323.2 corresponds to two cations bridged by a chloride anion. New peaks due to electrolysis of the solution are seen at mass 59, 75.9, 100, 116.8, 123.9, 164.1 and 375.3. The peak at 129.9 corresponds to the loss of a single methyl group, while the peak at 116.8 corresponds to the loss of two methyl groups. The absence of additional daughter peaks is believed to be

due to the formation of a lower molecular weight, more volatile species, such as when butyl and/or propyl are the leaving groups.

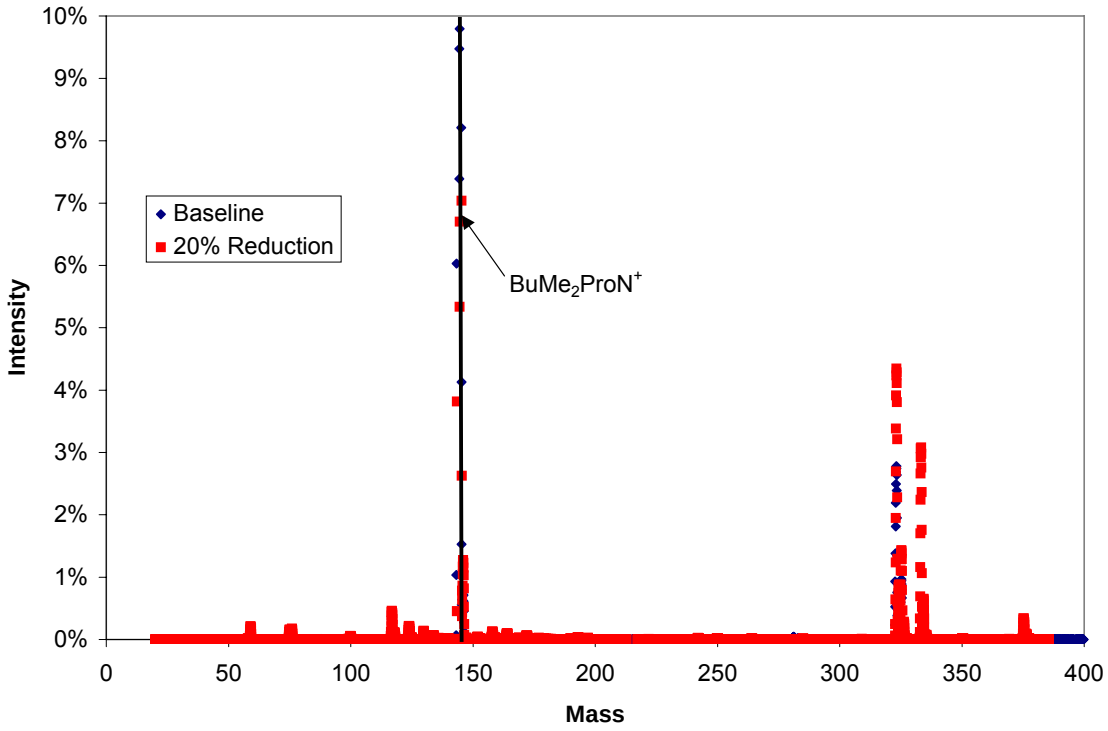

Figure III-5.7 Mass spectroscopy results for 0.1M acetonitrile solution of salt VII before and after 20% reduction.

Ionic Liquid Properties:

Ionic liquids, mixtures that contain only ions and are liquids at or near room temperature (T < 100°C), were formed from the salts III, VI and VII by mixing them with aluminum chloride. While we previously reported on the IL formed with salt III[24], this is the first report of ILs formed by mixing salts VI or VII with $AlCl_3$. MacFarlane et al. reported the formation of a room-temperature IL when salt VI was mixed with the bis-(trifluoromethane sulfonyl) imide ion.[33] ILs of salt VI and its isomer, salt VII, were studied due to the increased stability in ACN. Salt III was chosen as a reference based on its ability to form a room temperature IL and support the reduction/reoxidation of

sodium.[24] When mixed with $AlCl_3$, salts I, VIII and IX did not form room temperature ILs. Though salt X formed an IL it was not studied due to its increased viscosity, relative to the salt III IL. ILs formed utilizing salt II have been widely investigated in the literature, for example by Gray et al.[10]

Acidic, N=0.55, mixtures were first prepared followed by neutralization with 100 mole% excess of NaCl. Previously, we showed that the acidic and neutral mixtures formed from salt III were liquid at temperatures slightly below room temperature.[24] For mixtures formed with salt VII, melting points of 0.3°C and 3.7°C for the acidic and neutral mixtures, respectively, were measured. The acidic mixture with salt VI was also fluid at room temperature. However, the DSC analysis showed two endothermic phase transitions. The first was a sharp, repeatable peak at -49.2°C. The other was a broad peak, with a base at 50°C to 55°C. Upon neutralization the mixture was not liquid at room temperature and a melting point of 43.2°C was measured. It is believed that the -49.2°C phase transition for the acidic melt could be due to the presence of the larger $Al_2Cl_7^-$ anion. Upon addition of NaCl, $Al_2Cl_7^-$ was converted to the smaller, more symmetric $AlCl_4^-$ anion, resulting in the higher melting point, 43.2°C.

For the acidic melt of salt VII the conductivity and viscosity were measured to be 2.86 mS/cm and 61 mm^2/s, respectively. This conductivity is almost four times greater than that measured for the acidic melt of salt III. This kinematic viscosity is nearly one-quarter of that measured for the IL of salt III, 222 mm^2/s.[24] The higher conductivity and lower kinematic viscosity is a result of the smaller size of salt VII versus salt III.

The electrochemical window for the neutralized ILs of salt III, VI and VII are shown in Figure III-5.8. The reference electrode was an N = 0.60 mixture of the

corresponding salt and $AlCl_3$. Due to the higher melting point, tests with the salt VI IL were performed at 71°C, versus 25°C for the ILs of salts III and VII. The reduction for the IL from salt III starts at -2 V with a peak at –2.65 V. The current was irreversible with no oxidation current observed upon scan reversal. This is typical of Lewis neutral ILs containing sodium ions and no 'additive' where the IL itself is reduced in favor of sodium metal deposition.[34] For the IL of salt VII, Fig. III-5.8b, the reduction begins at –2.2 V with a peak at -2.6 V. Again the cathodic current was irreversible with no oxidation current, as from sodium metal or other species, upon scan reversal. For the IL of salt VI the initial reduction peak is observed at –1.73 V with a maximum at –2.14 V, Fig. III-5.8c. A precipitous drop in current was observed after the initial cathodic peak. On repeat scans, the sharp decline in the current at –2.36 V also occurred, but at slightly different potentials. A black deposit was observed on the electrode surface after the reduction process. The drop in current and presence of a black film are consistent with the formation of a passivating film during reduction. The peak current was directly proportional to the square root of the scan rate, indicating diffusion-limited behavior during the reduction process. A second reduction peak was observed at –2.82 V, as shown in Fig. III-5.8c. Repetitive scans between 0 V and -3 V for the IL of salt VI showed a progressive decrease in the reduction current. The black deposit remained on the surface when the voltage was restricted to the 0 to -3 V range. The black deposit was removed when the voltage was scanned to +2 V where the $AlCl_4^-$ was oxidized to Cl_2.

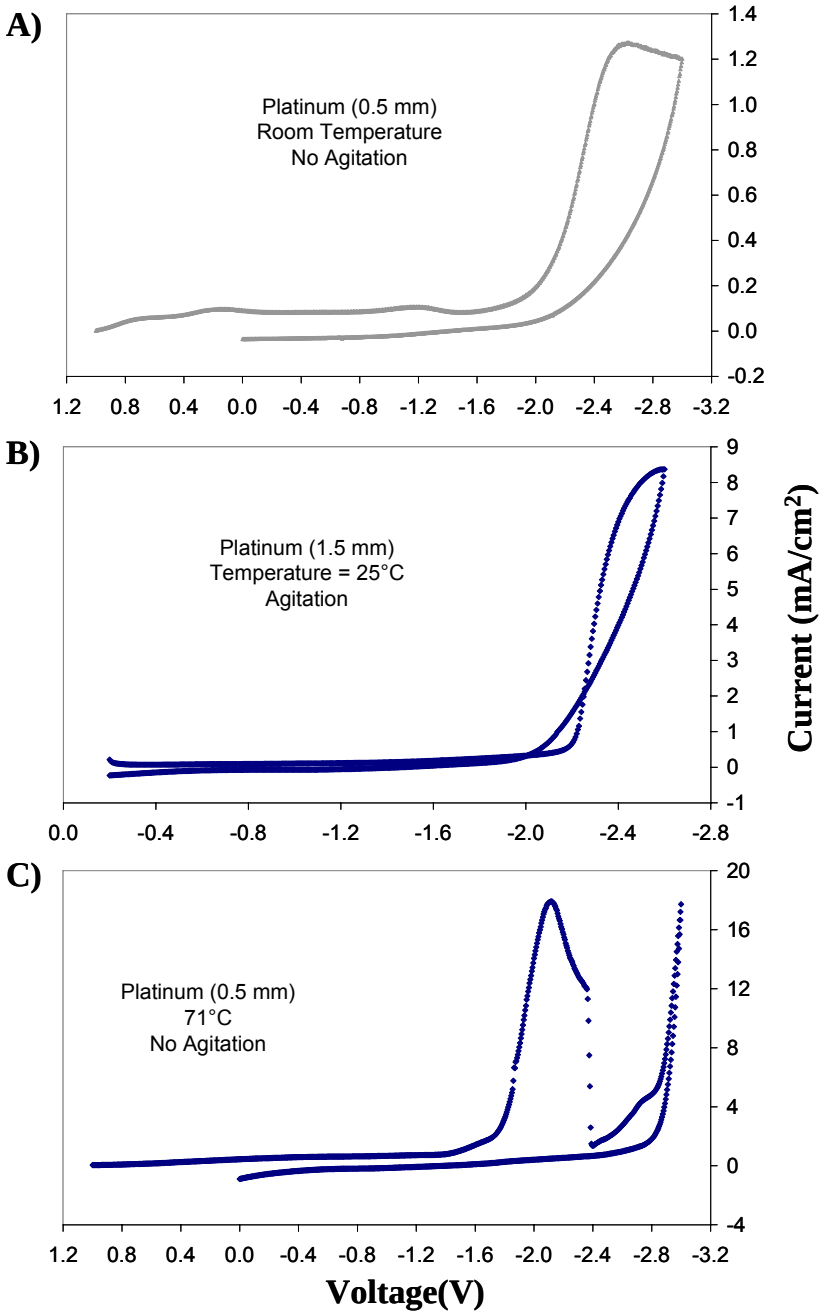

Figure III-5.8 CV scans with 100% excess sodium and: (A) N=0.55 Mixture of Salt III; (B) N=0.55 Mixture of Salt VII; (C) N=0.554 Mixture of Salt VI.

The presence of an insoluble reduction product is consistent with the mass spectrometry data presented previously in this paper. Reduction of the heterocyclic cation, salt VI, does not lead to low molecular weight products whereas reduction of salts

III or VII do produce low molecular weight products which apparently do not precipitate on the electrode surface.

The addition of a small amount of an acidic 'additive', such as $SOCl_2$ to a sodium-containing neutral IL facilitates the electrodeposition of sodium metal. The electrodeposition and reoxidation of sodium from the neutralized IL of salt VI $SOCl_2$ is shown in Figure III-5.9. The reduction of sodium ions on the initial scan to negative potentials occurs at –2.3 V with a peak current of 33.2 mA/cm^2 at –2.4 V. However, a precipitous drop in current occurred at more negative potentials, just as in the previous figure, Fig. III-5.8c, when no $SOCl_2$ was present. On scan reversal, an oxidation current corresponding to sodium oxidation was observed. The oxidation peak current was 30.6 mA/cm^2 and occurred at –1.96 V. The columbic efficiency for reduction and reoxidation of sodium (charge due to oxidation divided by the charge due to reduction) was 79.2%. Thus, about 21% of the reduction current did not result in recoverable sodium deposition. The precipitous drop in current, indicating reduction of the IL is consistent with the non-sodium related current.

If the reduction current were restricted to the less negative potentials during the reduction of sodium metal, the coulombic efficiency for reduction of sodium improved. The reduction potential was stepped to -2.3 V and held, chronoamperometry (CA), and then stepped to -1.8 V to oxidize the deposited sodium, as shown in Figure III-5.10. The resulting coulombic efficiency for the neutral IL of salt VI was 87.2%. No precipitous drop in current was observed at -2.3 V showing that the reduction of the salt VI cation was less a factor at these potentials.

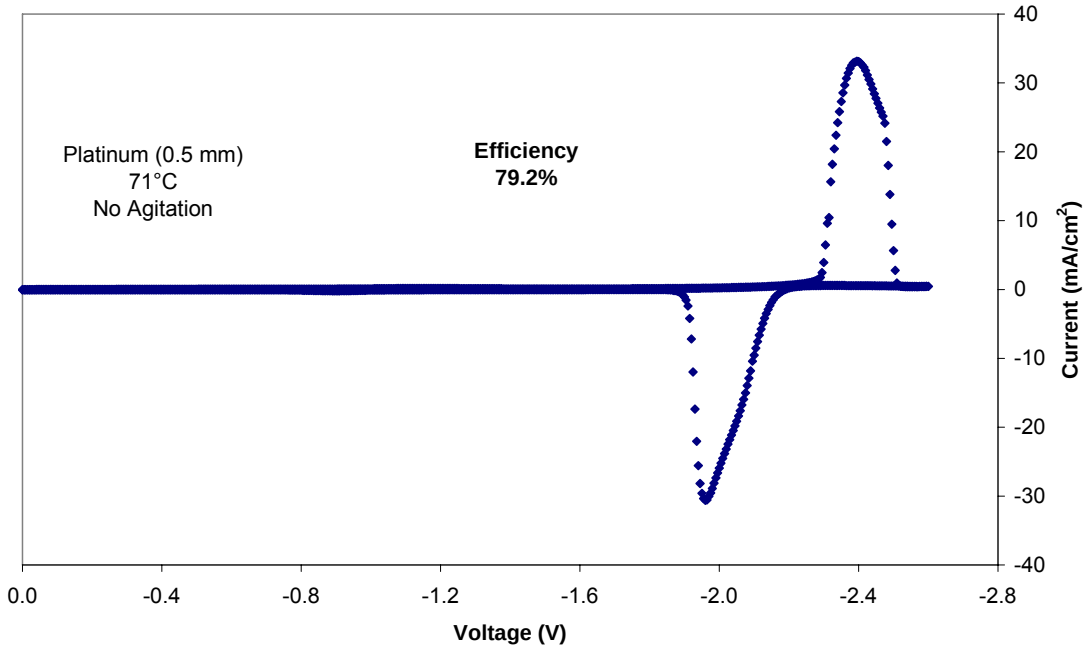

Figure III-5.9 CV scan at 71°C for a mixture of 55.4% $AlCl_3$ and Salt VI neutralized with 100% excess NaCl and $SOCl_2$ added.

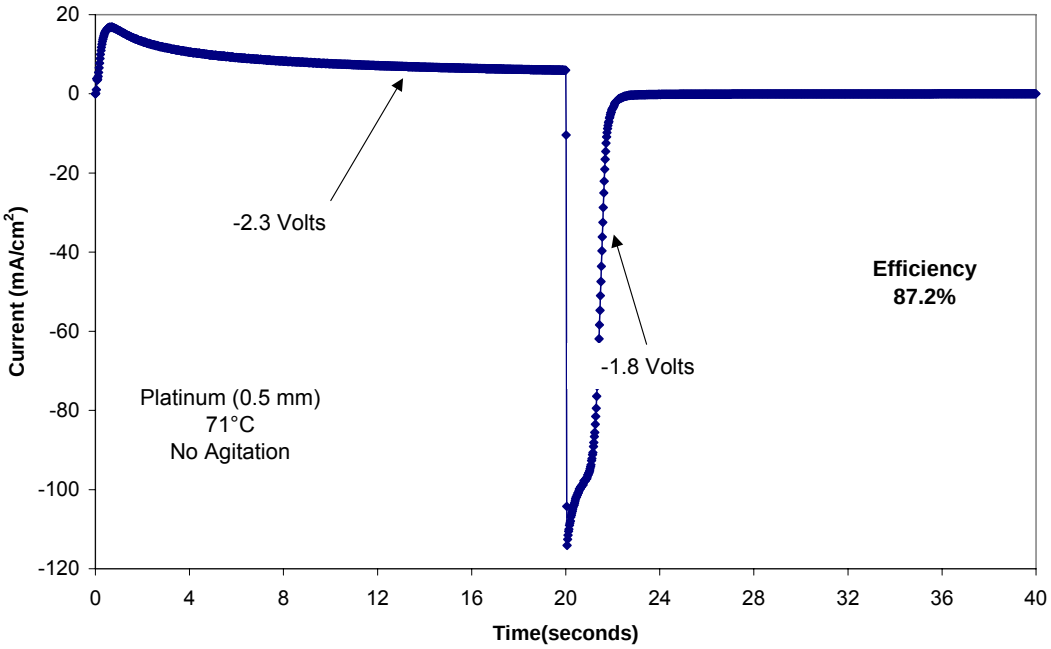

Figure III-5.10 CA scan at 71°C for a mixture of 55.4% $AlCl_3$ and Salt VI neutralized with 100% excess NaCl and $SOCl_2$ added.

The long-term stability of sodium in the IL formed from salt VI was measured by use of chronopotentiometry (CE). Sodium was electrodeposited at a current of 3.82 mA/cm^2 for 100 sec. An open circuit delay was inserted prior to applying an oxidation current. The average coulombic efficiency for 23 CE tests with open circuit times of 7-9 seconds was 80.3%. The loss in recoverable sodium was converted to a self-discharge rate. The effective self-discharge current over a one-hour open circuit time was 57.9 $\mu A/cm^2$ using a platinum electrode. On tungsten, the average coulombic efficiency from CE experiments was 79.3% and the effective self-discharge current was 86.9 $\mu A/cm^2$.

The voltammogram for the neutralized IL of salt VII with $SOCl_2$ is shown in Fig. III-5.11. Although salt VII is a quaternary ammonium cation with the same number of carbon atoms as VI, the absence of the heterocyclic ring yields lower molecular weight reductive products, as discussed previously. The voltammogram in Fig. III-5.11 shows a reduction current without the presence of a passivating film. The reduction of Na^+ ions was observed starting at –2.35 V. Oxidation of the sodium occurred after scan reversal with a maximum current of 6.29 mA/cm^2 at –1.74 V. The columbic efficiency for the reduction and reoxidation process in Fig. III-5.11 was 76.2%. A higher coulombic efficiency, 90.8%, was observed in a CE experiment. The cathodic current was 1.13 mA/cm^2 for 200 seconds at a platinum electrode. On tungsten, a slightly higher efficiency (CE experiment) was observed, 91.3%, where the cathodic current was held at 1.53 mA/cm^2 for 200 seconds. The self-discharge current was 8.5 and 9.8 $\mu A/cm^2$ for tests at the platinum and tungsten conditions, respectively.

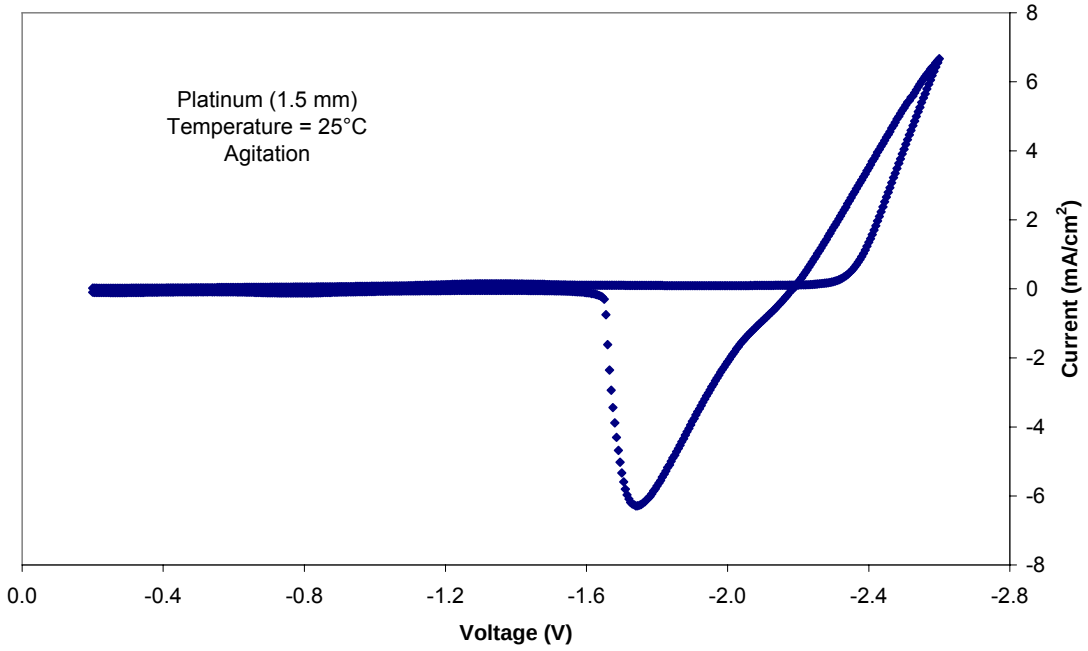

Figure III-5.11 CV scan at 25°C for a mixture of 55% $AlCl_3$ and Salt VII neutralized with 100% excess NaCl and $SOCl_2$ added.

In each of these previous tests with the salt VII melt no agitation of the sample was performed. When a CE test was performed while stirring the sample, the current using a tungsten electrode increased to 3.56 mA/cm^2. Though the baseline efficiency also increased, from 91.3 to 94.1%, the self-discharge current increased by a factor of 10 to 101 μA/cm^2. This indicates a greater increase in parasitic reaction rate.

The self-discharge values for the ILs of salts VI and VII can be compared with the previously reported results for the salt III IL. At 25°C, the self-discharge rate for salt VII is double the rate for salt III, 3.96 μA/cm^2. The discharge rate for salt VI though is similar to the value, 52.0 μA/cm^2, observed for a salt III IL at 71°C.[24] The increased self-discharge rate for salt VII is attributed to the reduced IL viscosity relative to the IL of salt III.

Summary

The electrochemical stability of ten organic cations as solutes in ACN was investigated. For salts III, VI and VII the stability in ACN was compared to that measured in the chloroaluminate IL, with the performance of the chloroaluminate ILs of salts VI and VII presented for the first time. Both salts were liquid at elevated temperatures, but only the IL for salt VII was a liquid at room temperature. In both medium, the benzyl substituted cation (salt III) was less stable than the alkyl substituted cation (salt VII), due to the benzyl group being a better leaving group than the smaller butyl chain. Mass spectroscopy measurements before and after electrolysis on the salt III samples, confirmed that reduction involves the loss of the various alkyl groups. In ACN, salt VI was the most stable molecule due to its cyclic structure. However, in the IL form, salt VI was the most easily reduced, resulting in an insoluble black deposit. This is consistent with the mass spectrometry data, which did not show formation of low molecular weight products, as in the reduction of salts III and VII. The ILs of salts III and VII demonstrate a greater ability to support the efficient reduction and reoxidation of sodium than the IL of salt VI. The formation of insoluble products through the reduction of the salt VI cation, leads to the inferior performance compared to salts III and VII, even though the I-V behavior in ACN is better.

III-6. ***Electrochemical Deposition of Li-Na Alloys from an Ionic Liquid Electrolyte***

In this chapter, we investigate a lithium metal anode for use in a secondary battery. However, anodes using lithium metal are prone to forming dendrites when recharged leading to capacity fading and electrode shorting. The formation of dendrites also occurs with other metals, such as in the electrodeposition of tin, silver, and zinc.[35-37] Electronic-system failures have been attributed to short circuits caused by metallic dendrites. The silver and tin whiskers observed in electronic components grow slowly over time when the circuit elements are maintained at different potentials. In general, dendrite suppression has been achieved by alloying the metal with a small amount of a second metal, ca. >1%. For example tin-lead and zinc-nickel are reliable metal systems for solderability and corrosion resistance.[38,39] The deposition potential and melting point of the alloy are often lower due to the alloy effect.

In this chapter, the lithium-alloy has been investigated as a means to producing a dendrite-free anode for lithium batteries. Sodium has been chosen as the alloying metal, although other elements can also be considered, such as potassium. The formation of dendrites for lithium, sodium, and their alloys were investigated in an IL electrolyte. The deposition potential, coulombic efficiency for the re-oxidation of the deposited metal, and composition of the deposit are reported.

Results

The IL was formed by mixing 45 mole % benzylethyldimethylammonium (BME) and 55 mole % aluminum chloride. NaCl and/or LiCl were then used to neutralize the IL

with excess salt added to maintain neutrality. The conductivity of the neutral IL containing sodium and/or lithium is of interest because of the degree of ion pairing that occurs between the alkali cation and $AlCl_4^-$. The conductivity of the ILs was measured as a function of the concentration of the dissolved lithium and sodium cations at 25°C. The mole fraction of BME^+, $AlCl_4^-$, and $SOCl_2$ was held constant in all the experiments. The conductivity values for five, neutral ILs with and without $SOCl_2$ are shown in Table III-6.1. The mole fraction of the alkali cation in the liquid phase was 9 mol% in each IL. The conductivity of the IL increased as the lithium-to-sodium ion ratio increased. The lithium-only ion IL had a conductivity of 549 μS/cm while the sodium-only IL had a conductivity of 321 μS/cm. Previously, it was shown that replacement of the organic cations with sodium ions results in a lower conductivity melt due to ion-pairing of Na^+ with $AlCl_4^-$. The improvement in conductivity by replacement of lithium ions for sodium ions may be due to the smaller size of the lithium ion. A smaller ion could result in a higher packing density along with a greater mobility resulting in an increase in conductivity. The conductivity of the LiCl neutralized melt may also be higher then that of the NaCl melt due to a higher molar saturation for Li^+ then Na^+ (i.e. some of the excess LiCl could dissolve). To ensure neutrality of the melt, excess LiCl and/or NaCl was added (depending on the desired melt composition). If a higher percentage of the excess LiCl was dissolved, relative to that of the NaCl, a higher conductivity would be observed due to the greater ion density of the melt.

Additives also affect the conductivity of the melts. Thionyl chloride ($SOCl_2$) has been shown to increase the conductivity by increasing the degree of dissociation of the Li^+ and Na^+ from their counter-ions allowing electrodeposition to occur.[34] The ~10%

increase in the conductivity of the Na-only melt (and little change in the Li-only melt) implies that the $SOCl_2$ increases the free Na^+ concentration more than for Li^+. The mixed melts show a small increase in conductivity after $SOCl_2$ was added. Since the $SOCl_2$ is neutral and its molar fraction is small, it itself has little influence on the overall conductivity.[34]

	Before Adding $SOCl_2$	After Adding $SOCl_2$
	Conductivity (μS/cm)	Conductivity (μS/cm)
100% LiCl	549	542
90% LiCl-10% NaCl	466	469
50% LiCl-50% NaCl	428	466
10% LiCl-90% NaCl	364	371
100% NaCl	321	363

Table III-6.1 IL conductivity at room temperature at various LiCl:NaCl ratios before and after adding $SOCl_2$.

Cyclic voltammetry (CV) was used to characterize the electrodeposition reoxidation of sodium and lithium. Figure III-6.1 shows CVs for five ILs with different sodium-to-lithium ratios. In each case, the IL had an acidity of N = 0.55 before neutralization.

The reduction potential of the IL neutralized with only NaCl has previously been reported to be -2.3 V.[23] The sodium-containing IL reduction potential is more negative than that of the IL neutralized with LiCl, which begins to reduce at -1.8 V. In each case, a hysteresis was observed where an overpotential for nucleation of the metal was present on the first scan to negative potentials. The 90% Li^+/10% Na^+ IL has a similar I-V behavior to that of the lithium-only IL, and the 10% Li^+/90% Na^+ IL is similar to the sodium-only IL. In each case, the metal was electrodeposited without the formation of

dendrites. The current and sweep rate was varied across a wide range and the deposits were examined for the presence of dendrites. Lithium dendrites have been recorded at currents as low as 0.5 mA/cm^2 forming in as little as one minute.[40] No dendrites were found in any of the ILs here. The cause of the suppression is thought to be due to the formation of Li-Na alloys and the effect of the IL itself on the deposition of lithium. These causes will be discussed in the next section. A more systematic survey of currents and times will be presented in a subsequent report.

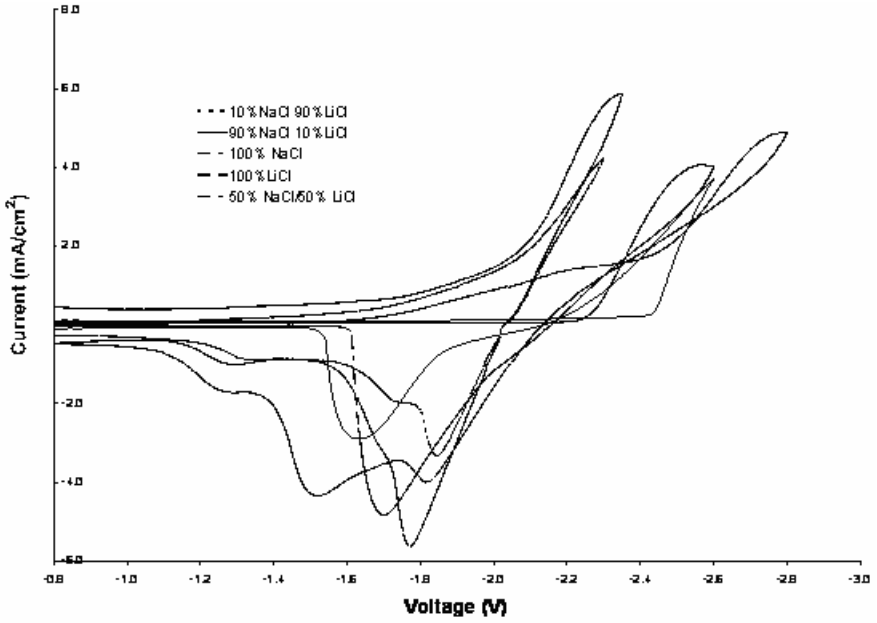

Figure III-6.1 CV scans at room temperature for 5 ILs with different LiCl:NaCl ratios.

The reoxidation of the metal is different for each mixture in Figure III-6.1. The pure sodium and pure lithium ILs have one large oxidation peak while the mixed sodium-lithium deposits have two or three oxidation peaks. This is possibly due to the presence of different Li-Na alloys (different ratios of metal), or the selective oxidation of one metal from the alloy at a more negative potential than the other metal. For example, the oxidation potential of pure sodium is different from pure lithium metal. It is important to

note that a less negative oxidation potential will prevent any reaction between the metal and the organic cation (BME^+) that is reduced at -2.8 V.

The CV curve for the 50% Li^+/50% Na^+ is shown in Figure III-6.1. The slope of the I-V curve is more gradual than the other melts indicating possible kinetic effects. The re-oxidation of the metal shows the most distinct double oxidation peaks of all the alloys studied here. A significant oxidation current is observed at potentials negative of the initial reduction values indicating that both lithium and sodium are reduced, with lithium at a more positive potential. The sodium is expected to be oxidized first (having a more negative reduction potential) from the alloy.

The coulombic efficiencies for the deposition-stripping of the metal was obtained from the CV curves by integrating the total charge on reduction and oxidation, as reported in Table III-6.2. The coulombic efficiency is the total oxidation charge divided by the reduction charge. The first column of results in Table III-6.2 shows the coulombic efficiencies from the CV experiments when a -2.6 V switching potential was used. The 90% LiCl/10% NaCl IL had the highest efficiency, 84%, and the 50% LiCl/50% NaCl melt had an efficiency of 83%. This is consistent with the previous observation that alloy deposition occurs at more positive potentials, where there is a lower probability of IL reduction. A survey of conditions was performed to find the highest coulombic efficiency in each IL. In these experiments, the scan rate was held constant at 100 mV/sec, while the switching potential was varied. The second column of Table III-6.2 shows the highest efficiency obtained from the survey experiments along with its corresponding switching potential. The 90% LiCl/10% NaCl melt had the highest efficiency at 88% (switching potential of –2.3 V). The pure lithium IL had an efficiency

of 74% (switching potential -2.4 V) while the pure sodium melt had an efficiency of 78% (switching potential -2.6 V). This is consistent with the observation that lithium is deposited at more positive potentials than sodium. The optimal switching potential for the 90% LiCl/10% NaCl melt is similar to that of the 100% LiCl melt. This is consistent with the data in Figure III-6.1, which shows a similar I-V behavior for the two ILs.

	Cyclic Voltametry		Chronoamperometry		Chronopotentiometry	
	Efficiency (%) at Switching Potential of -2.6 V	Max Efficiency (%) (Switching Potential, V)	Efficiency (%) at Voltage Steps of -2.5 V & -1.2 V	Max Efficiency (%) (Potential Steps, V)	Efficiency (%) at Current Steps of 0.51 mA/cm^2 & -0.51 mA/cm^2	Max Efficiency (%) (Current Steps, mA/cm^2)
100% LiCl	72	74 (-2.4)	N/A	62 (-2.35/-1.2)	50	75 (1.02:-1.02)
90% LiCl-10% NaCl	84	88 (-2.3)	31	91 (-2.3 /-1.3)	40	80 (1.02:-1.02)
50% LiCl-50% NaCl	83	87 (-2.4)	46	68 (-2.4/-1.3)	62	65 (0.41:-0.41)
10% LiCl-90% NaCl	74	74 (-2.6)	63	72 (-2.45/-1.3)	65	65 (0.51:-0.51)
100% NaCl	78	78 (-2.6)	71	71 (-2.5/-1.8)	85	85 (0.51:-0.51)

*Both current and voltage steps were performed with 100 second intervals

Table III-6.2 Coulombic efficiencies at room temperature for 5 ILs with different LiCl:NaCl ratios.

Chronoamperometry (CA) was also used to measure the coulombic efficiency, as shown in Table III-6.2. When the efficiency is measured by CV, the potential varies throughout the experiment. The current corresponding to metal deposition vs. that corresponding to IL reduction is a function of potential, especially at the extremes of the potential scans. In CA, potential steps are used which correspond more closely to that of a battery's operation. The reduction and oxidation potential steps used in the experiments were varied to find the optimal setting for deposition in each of the ILs. The 90% LiCl/10% NaCl melt had the highest efficiency, 91%, with potential steps of -2.3 V followed by -1.3 V (each step was for 100 seconds). The 90% LiCl/10% NaCl melt also gave the highest efficiency from CV measurements. The CA curve for the 90% LiCl/10% NaCl melt can be seen in Figure III-6.2.

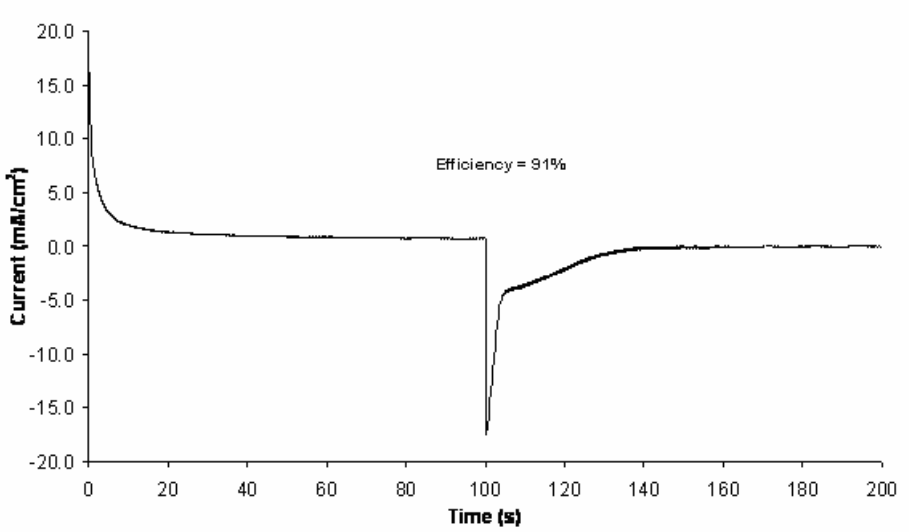

Figure III-6.2 CA curve at room temperature for the 90% LiCl/10% NaCl IL.

Constant potential steps and step times were applied to each melt to compare the melt efficiencies directly. The efficiency should increase as the amount of metal plated was increased. This was previously shown to be true in other IL's and was attributed to an initial parasitic current due to the reduction of impurities.[26] Potential steps of -2.5 V and -1.2 V (100 seconds per run) were applied to each melt. The efficiency values of each IL subjected to the same potential steps (-2.5 V/-1.2 V) can be seen in Table III-6.2 in the first chronoamperometry efficiency column. The 100% LiCl IL efficiency is not reported because the potential step to -2.5 V is beyond the stable range of the mixture. The general trend in the maximum efficiencies follows a trend similar to the CV data.

Chronopotentiometry (CE) was also used to measure the coulombic efficiency. The maximum efficiency was measured by optimizing conditions to maximize the efficiency for each IL. These results are shown in Table III-6.2. The values of efficiency are similar to those observed by the other techniques. The 90% LiCl/10% NaCl, which gave the highest efficiency values with CV and CA, had a coulombic efficiency of 80%

when the current steps were 1.0 mA/cm^2 for 100 seconds. It should also be noted that the current steps for maximum efficiency were higher in the ILs with high lithium concentration. This can be seen in the CVs in Figure III-6.1 during deposition where at lower overpotentials there is less competition from reduction of the IL. The current steps required for maximum efficiency for a CE measurement, depending on the melt, ranged from 0.41 mA/cm^2 to 1.22 mA/cm^2 as seen in Table III-6.2. Each melt was then directly compared by subjecting each IL to current steps of 0.51 mA/cm^2 for 100 seconds per step. These results are seen in Table III-6.2 and show that at a relatively low current, like 0.51 mA/cm^2, ILs with higher sodium concentrations have a higher efficiency.

Elemental analysis was performed on the metal deposits for each of the melts in order to determine if both lithium and sodium were present. Atomic absorption spectroscopy and a qualitative flame-test were used to determine the presence of lithium and sodium in the deposits. The metal from the electrochemical depositions was initially dissolved in deionized water. A platinum wire was immersed in the metal-containing solution and then placed into a blue flame. Sodium and lithium ions produce yellow and red flames, respectively. The pure sodium IL produced a deposit that resulted in a yellow flame and the lithium IL produced a deposit that resulted in a red flame. When the Li^+/Na^+ alloy deposits were tested, the flame color was clearly a mixed yellow and red flame. This qualitative analysis confirmed the presence of lithium and sodium deposit from the mixed Li^+/Na^+ IL. Atomic absorption was used to quantify the alloy ratio deposited from the 90% Li/10% Na IL. Standard solutions of LiCl and NaCl were prepared and used to calibrate the atomic absorption spectrometer. The electrodeposited metal was dissolved in DI water and the concentration of the two ions was measured.

The Na-to-Li ratio obtained by atomic absorption was compared to that in the melt. A Na:Li molar ratio of 50:1 was found from metal deposited from the BME IL. This ratio is not consistent with the composition of the melt. The indicates that the deposit was sodium rich, however, quantitative dissolution of the metal deposit may not have occurred. This result clearly shows that Li/Na alloys are present during deposition resulting in the changes of the electrochemical properties discussed earlier.

Discussion

The goal of this work is to deposit a Li-Na alloy that would in turn depress any formation of dendrites that occur during lithium deposition. Shifts in reduction potentials along with distinct double and triple oxidation peaks are consistent with alloy deposition. A reduction potential shift occurred during deposition for all the mixed Na^+/Li^+ ILs indicating alloy deposition. Studies have shown that the deposition of two or more metals (in this case, lithium and sodium) is possible as long as the reduction potentials are similar.[37] Figure III-6.1 shows that the pure lithium and pure sodium I-V curves are similar in shape and potential from -2.15 V to -2.32 V. The 90% Li/10% Na IL clearly exhibits reduction in this potential range. This would indicate the occurrence of codeposition of lithium and sodium.

The overpotential exhibited during oxidation of the 90% LiCl and 10% NaCl melt deposit further confirms the existence of alloys. Oxidation begins to occur at -2.0 V, which is 0.2 V more negative than the point of initial reduction (-1.8 V). This would imply the presence of multiple alloys or selective oxidation of one metal from the alloy at a more negative potential. Other studies have shown that two-phase alloys can codeposit

on a polarized electrode surface even if a system is capable of forming a continuous solid deposit.[37] Multi-phase alloys can produce the multiple oxidation peaks as seen in our results.

Like lithium, both silver and tin form dendrites in the presence of a potential gradient. Dendrite growth with silver and tin is suppressed by alloy formation. Dendrite formation was not observed here, even when a pure lithium melt was used. Currents were varied from 0.1 mA/cm^2 to 1.0 mA/cm^2 for anywhere between 1 minute to an hour with no occurrence of dendrites.[40] According to other studies, dendrites have been seen in a 2MeTHF-EC/$LiAsF_6$ electrolyte with a deposition current of 0.5mA/cm^2 in as little as 1 minute.[40] It is believed that the IL electrolyte itself has an effect on dendrite formation. However, regardless of the effect the IL has on dendrite formation, dendrites did not form when lithium and sodium were codeposited. This leaves the door open for the possibility that the alloying effect that occurs would still cause dendrite suppression. The elimination of dendrites will allow for much smaller anode and cathode separations eliminating high resistance and low current densities. Further studies into various ILs being used as electrolytes are currently being performed.

Lithium anodes are thermodynamically unstable and require the use of passivating films on the electrode surfaces to allow the system to function as a practical battery.[41] A rechargeable Li-ion battery consists of a lithium anode and a metal oxide cathode such as lithium cobalt oxide.[41] If a Li-Na alloy is going to be deposited, then trace amounts (ca.. 1%) of sodium will need to be present in the anode. The electrolyte will need to hold the entire Na^+ content when the battery is discharged because the cathode works on the Lithium-only cycle.

In summary, the IL also provides ambient temperature operating conditions. It was found that the 90% Li/10% Na IL had the highest coulombic efficiency.

III-7. ***Catalytic Additives for the Reversible Reduction of Sodium in Chloroaluminate Ionic Liquids***

In this chapter we investigate the ability of several compounds to catalytically facilitate the electrodeposition of sodium. Our initial work focused on determining the effect of Lewis acids (e.g. PCl_5) and Na^+ complexing species (e.g. 18-Crown-6, 18C6). However, it was discovered that small amounts of low molecular weight chlorocarbons produce the same catalytic effect.

Results

Effect of Lewis Acid Addition

The Lewis acid $SOCl_2$ has been demonstrated to be effective in promoting the reduction and reoxidation of sodium. In both imidazolium and quaternary ammonium chloroaluminate ILs, coulombic efficiencies of greater than 90% have been repeatedly measured.[23,24,42] It was proposed that Na^+ ions coordinate with $AlCl_4^-$ in the ILs and the $SOCl_2$ serves to weaken this coordination, freeing Na^+ ions for reduction to the metal.[34] In this work, PCl_5, a weaker Lewis acid than aluminum chloride, was added to a neutralized N = 0.55 BME IL. Initially, the liquid was stirred at room temperature for a day prior to performing CV tests and only the irreversible reduction of the cation was observed, similar to when no additive was present. However, the deposition and reoxidation of sodium were observed after the sample was stirred for a second day at 45-

50°C, as shown in Figure III-7.1. The scan shown in Fig. III-7.1 is at a tungsten electrode, but similar results were obtained with a platinum electrode. The reduction and oxidation peaks are both steep with a reduction overpotential due to nucleation and crystallization of the metallic sodium on a nonsodium surface.[23] The reduction peak at 0.4 V was only observed when PCl_5 was added to the IL and is believed to be due to the reduction of P(V). Fuller et al. observed a similar reduction peak after the addition of $SOCl_2$ and attributed it to the irreversible reduction of $SOCl_2$.[42] Fig. III-7.1 shows a CV scan at 45-46°C, but the reoxidation of sodium was also observed when a CV was performed at room temperature. This indicates that at room temperature PCl_5 is sufficiently soluble in the IL to catalytically promote sodium reduction, but the conversion to PCl_6^- is very slow. By increasing the temperature, the time to reach equilibrium in the IL is shortened.

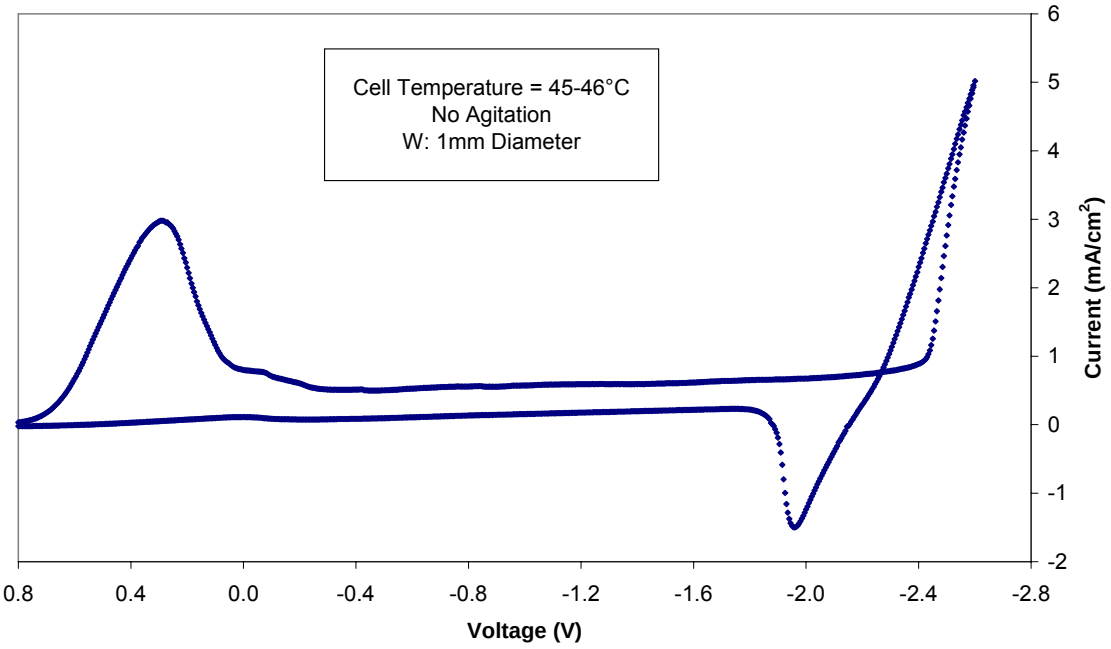

Figure III-7.1 CV curves for neutralized N=0.55 BME IL with 5 mole % PCl_5 added.

The maximum columbic efficiency measured for a CV test was 21%. Chronoamperometry (CA) experiments produced efficiencies greater than 60% for the reoxidation of sodium metal. Figure III-7.2 shows the highest efficiency CA experiment where the reduction was carried out at –2.6 V. Holding the potential minimized the time spent at potentials that were less efficient for depositing sodium metal. At more negative potentials, the IL is reduced and at more positive potentials the reduction of impurities can account for a majority of the current. The dissolution of PCl_5 in the IL as PCl_6^- produces sodium ions that are reducible at the working electrode. The lower charge density of PCl_6^-, compared to $AlCl_4^-$, lowers the degree of ion pairing between the Na^+ and the counter anion, enabling the deposition of sodium metal.

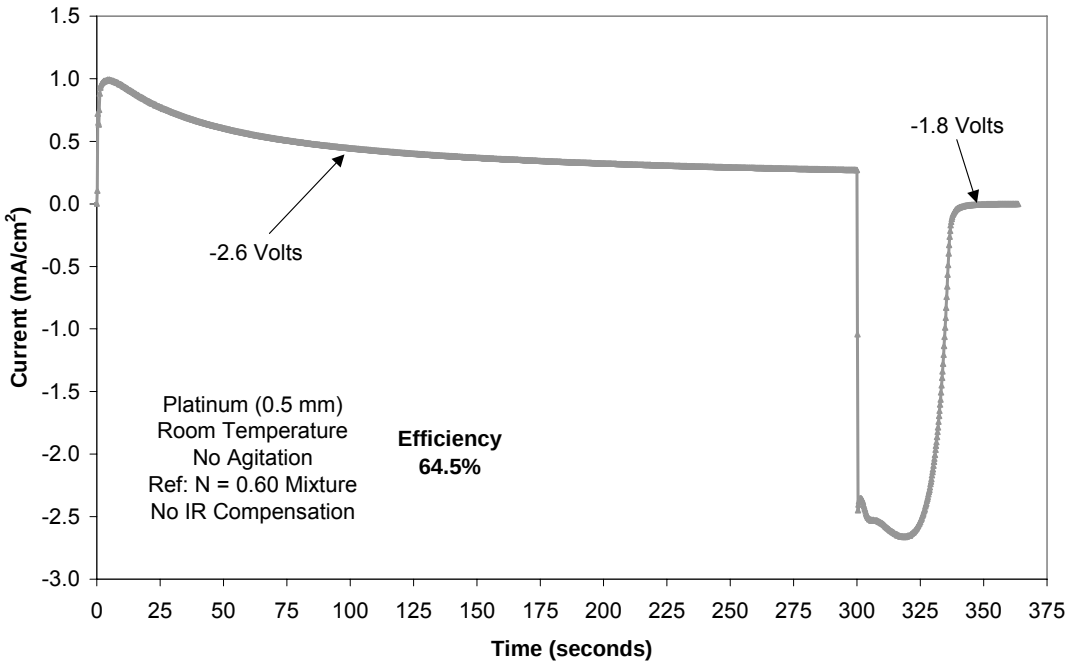

Figure III-7.2 CA test results for neutralized N=0.55 BME IL with 5.8 mole % PCl5 added.

Based on the results with PCl_6^- and $AlCl_4^-$, halogenated anions with a higher charge density than $AlCl_4^-$ are not expected to provide sodium ions with sufficient freedom to be electrodeposited due to ion pairing. This was tested by using BF_4^- as an additive in the chloroaluminate IL. The IL was made by adding 1-butyl-3-methylimidazolium tetrafluoroborate (BMIF), which is a liquid at room temperature, to a neutral IL. CV tests were performed after stirring the sample for 3 hours and more than 20 hours. However, all the CV tests performed with the BF_4^- additive showed no Na deposition/recovery whereas the larger anion, PCl_6^-, was effective in enabling the deposition of sodium. The smaller BF_4^- anion pairs more strongly with Na^+ than $AlCl_4^-$ resulting in an IL with no reducible sodium ions.

Effect of Na^+ Complexing Species

Based on the need for weak sodium ion complexes, 18-Crown-6 (18C6) was tested as an additive because of its ability to capture Na^+. A higher mixing temperature was used to increase the solubility and dissolution rate of 18C6 in the IL. Figure III-7.3 shows IL conductivity as a function of temperature and mole fraction of 18C6 in the IL. The conductivity decreased upon addition of the initial aliquot of 0.66 mole % 18C6. Additional aliquots of crown ether had no effect on the conductivity. The solubility limit of 18C6 in the IL was low (less than 0.66 mole %) and additional crown ether remained undissolved. Figure III-7.4 shows the voltammogram of the IL containing 1.8 mole % of 18C6. The crown ether provided a solvent shell for the sodium ions so that they were reducible. The reduction and reoxidation peaks in Fig. III-7.4 were very sharp. The reduction process showed a slight overpotential due to nucleation of the metal in the

foreign surface. In the coordinated state, the Na^+ ion is held within the cyclic ring of the crown ether. The additive specifically targets the cation, Na^+, disrupting the ion pair between the sodium ion and $AlCl_4^-$.

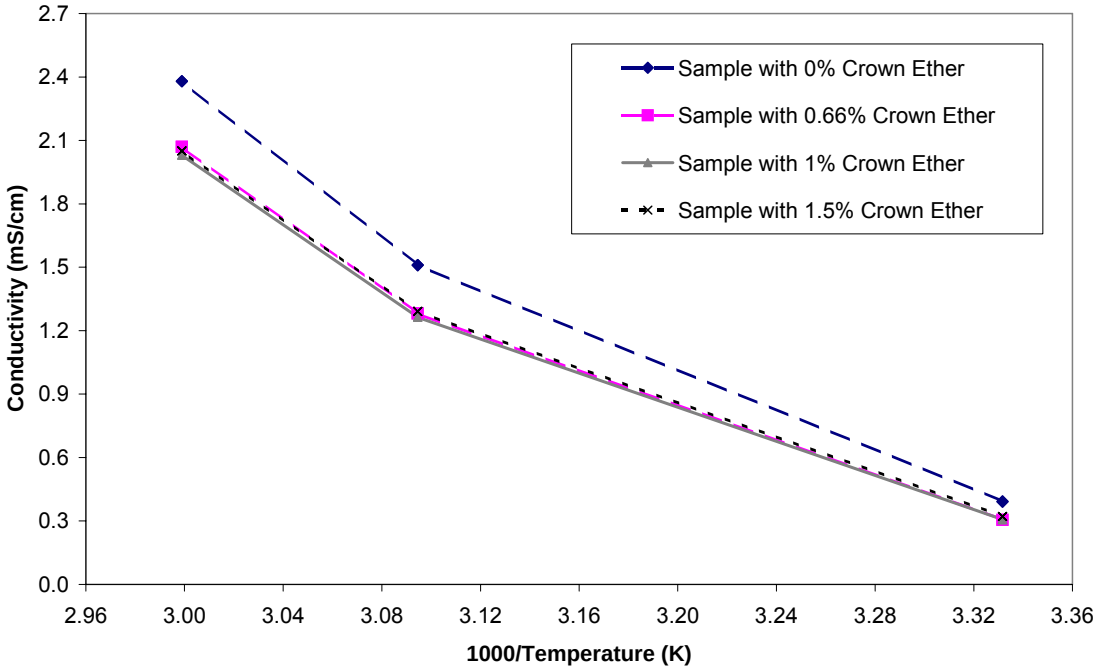

Figure II-7.3 Conductivity versus temperature for neutralized N=0.55 BME IL with 0, 0.66, 1 and 1.5 mole % 18-Crown-6 added.

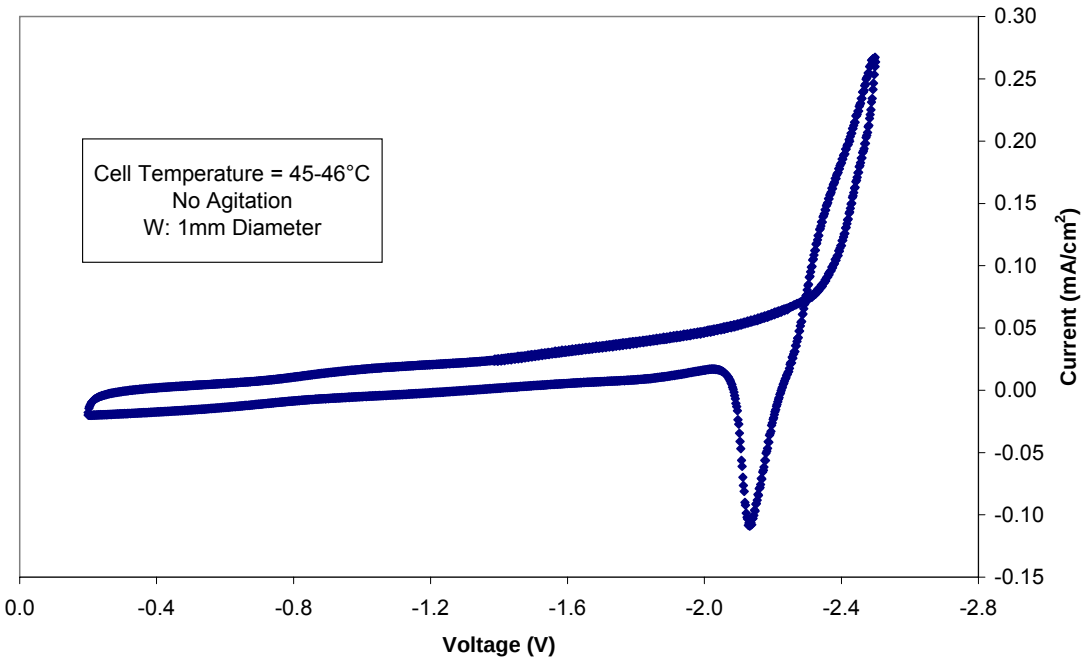

Figure III-7.4 CV results for neutralized N=0.55 BME IL with 1.8 mole % 18-Crown-6.

Effect of Chlorocarbons

Solvation of the sodium ions disrupts the anion-sodium ion pair so that the sodium ions can be reduced to the metal, as in the case of 18C6. The use of low molecular weight chlorocarbons was investigated as a solvating species for the sodium ions. It is desirable to have an additive more soluble than 18C6 and more difficult to reduce than PCl_6^-. The effect of dichloromethane on the deposition of sodium was investigated using a neutralized N = 0.55 BME IL. The reduction of sodium ions to the metal was observed after the addition of 4 mole % dichloromethane, as shown in the voltammogram, Figure III-7.5. The coulombic efficiency was improved by adjusting the temperature, switching potential in the potential scan, and other conditions. The reduction and reoxidation peaks for sodium are very steep, indicating a rapid redox process, similar to the results obtained for $SOCl_2$.[23] Dichloromethane can orient such that

the negative dipole of the chloride atoms are in close proximity to the Na^+ cations. The attraction between the partial negative charge on the chloride and the sodium cation weakens the interaction between the sodium cation and $AlCl_4^-$ anion.[34]

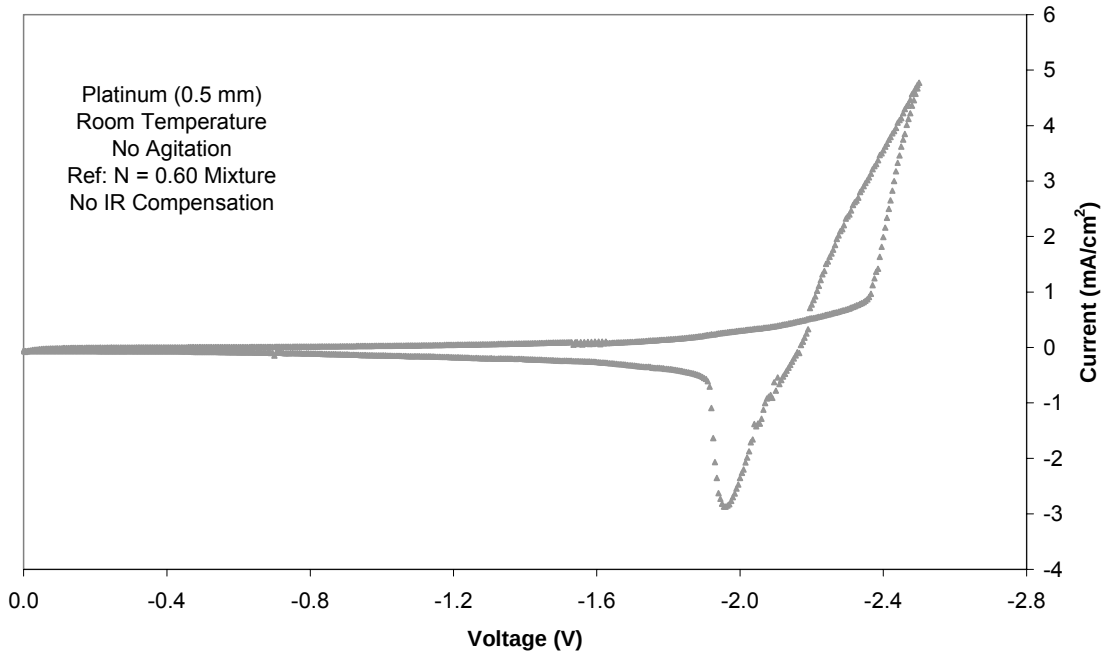

Figure III-7.5 CV scan following the addition of dichloromethane to the N=0.55 BME IL.

The coulombic efficiency for the reduction and reoxidation of sodium was measured using chronopotentiometry (CE) at a tungsten electrode at room temperature following the addition of dichloromethane. The initial experiments produced a coulombic efficiency of 63% for a 50 sec reduction current 0.64 mA/cm^2, followed by a 25 sec oxidation current at 1.27 mA/cm^2. After letting the sample sit for six days in an open vessel in the dry box, the same test resulted in a columbic efficiency of 52%. After an additional five days, it was not possible to obtain 0.64 mA/cm^2 without the voltage going to very negative potentials. However, at a reduction current of 0.32 mA/cm^2 for 50 seconds, followed by an oxidation current of 1.27 mA/cm^2 for 12.5 seconds, the

measured efficiency was 47%. An additional aliquot of dichloromethane, about 4 mole %, then improved the efficiency to 79% using 0.64 and 1.27 mA/cm^2 for the reduction and oxidation currents, respectively. The average coulombic efficiency was 77% (average of seven repetitions) when reduction and oxidation currents of 0.64 mA/cm^2 were applied for 50 sec.

The decrease in efficiency over time is consistent with the evaporation of the dichloromethane from the IL. The lower dichloromethane concentration results in fewer solvated sodium ions available for reduction. The coulombic efficiencies were less than when $SOCl_2$ was used as an additive under similar conditions (coulombic efficiency of 88.5%).[24]

To investigate the general nature of chlorocarbons as additives, chloroform-D and carbon tetrachloride were tested as additives in fresh, neutral ILs. Carbon tetrachloride provides an interesting comparison to dichloromethane and chloroform because of its symmetry (lack of dipole) and absence of a C-H bond. The first CV scans with $CDCl_3$ (6.5 mole %) and CCl_4 (6.1 mole %) from open circuit voltage to –2.6 volts are shown in Figure III-7.6. Both chloroform and carbontetrachloride are effective in providing reducible sodium ions. While the reduction and oxidation currents observed with each of the two additives are very steep, the reduction and reoxidation current for $CDCl_3$ are nearly double that for CCl_4. The higher oxidation current coincides with greater coulombic efficiency for chloroform-D (79.3%) versus carbon tetrachloride (55.2%).

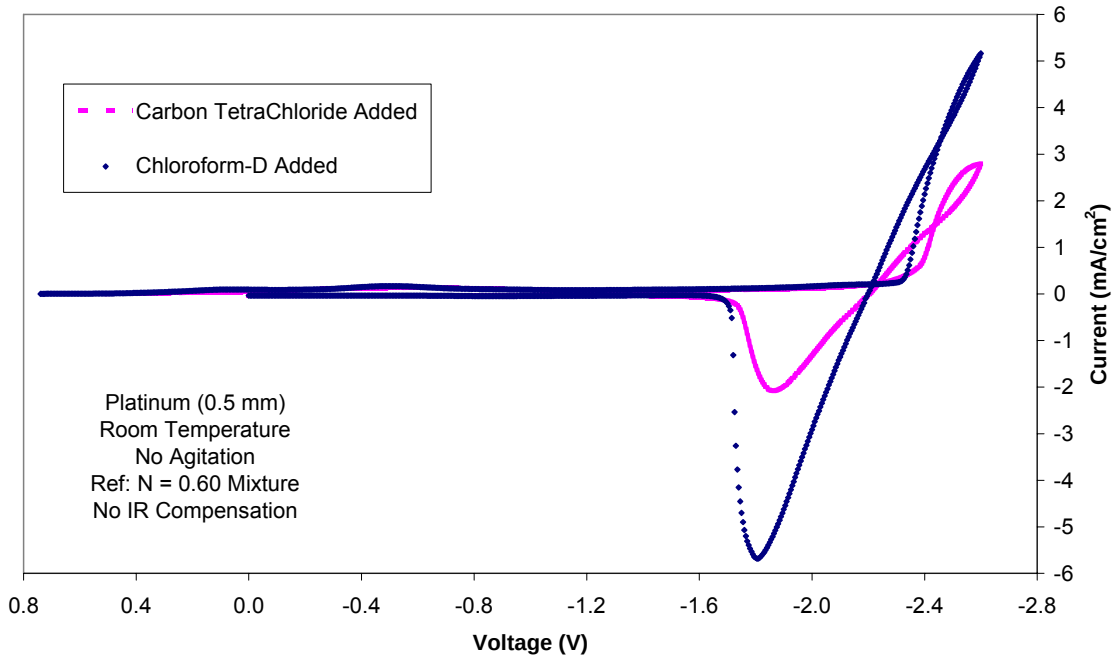

Figure III-7.6 CV test results with carbon tetrachloride and chloroform-D added to a neutral N=0.55 BME IL.

CA tests were performed to quantify the efficiency of the sodium reduction/reoxidation process with chloroform-D and carbon tetrachloride. The conditions at which the highest efficiencies were obtained are summarized in Table III-7.1. The maximum efficiency for the two additives is essentially the same: 90.5% for $CDCl_3$ and 88.2% for CCl_4.

	CA Test Results			
Additive	Reduction Voltage	Oxidation Voltage	Step Time (s)	Coulombic Efficiency
$CDCl_3$	-2.35	-1.96	300	90.5
CCl_4	-3.15*	-2.7*	300	88.2

Unless noted all tests performed at room temperature using 0.5 mm diameter Pt working electrode and N=0.6 acidic reference.
* Pt reference, estimated potential vs acidic reference: 700 mV.

Table III-7.1 CA test results for $CDCl_3$ and CCl_4 added to a neutral N = 0.55 BME IL.

CE tests were used to measure the long-term stability of sodium in the IL with each additive. Sodium was first deposited at a constant current followed by an open-circuit delay before reoxidation at the same current. The loss of recoverable sodium was then converted to a self-discharge rate.[10] The test conditions and results are summarized in Table III-7.2. The self-discharge rates, 5.62 and 5.47 $\mu A/cm^2$, for chloroform-D and carbon tetrachloride respectively, are within 3% of one another. These values are comparable to the self-discharge rate measured using $SOCl_2$ as the additive, 3.96 $\mu A/cm^2$.[24]

Additive	Reduction/Oxidation Current (mA/cm^2)	Step Time (s)	Open-Circuit Time (s)	Self-Discharge Rate ($\mu A/cm^2$)
$CDCl_3$	1.02	50	3600	5.62
CCl_4	0.76	50	3600	5.47

Unless noted all tests performed using 0.5 mm diameter Pt working electrode and N=0.6 acidic reference.

Table III-7.2 Self-discharge test results for $CDCl_3$ and CCl_4 added to a neutralized N = 0.55 BME IL.

Following the initial series of tests, the ILs were allowed to sit exposed to the dry box atmosphere. Figure III-7.7 shows the results of CV tests performed on the day chloroform-D was added, 2 weeks later, and finally 4 weeks later. The results after 2 weeks show a substantial decrease in both the reduction and oxidation currents. After 4 weeks, no sodium deposition was observed. Similarly, when carbon tetrachloride was used as the additive, no sodium reduction was observed after 3 weeks. These results are consistent with those obtained using dichloromethane where the evaporation of the solvent resulted in a decrease in the reducible sodium ions.

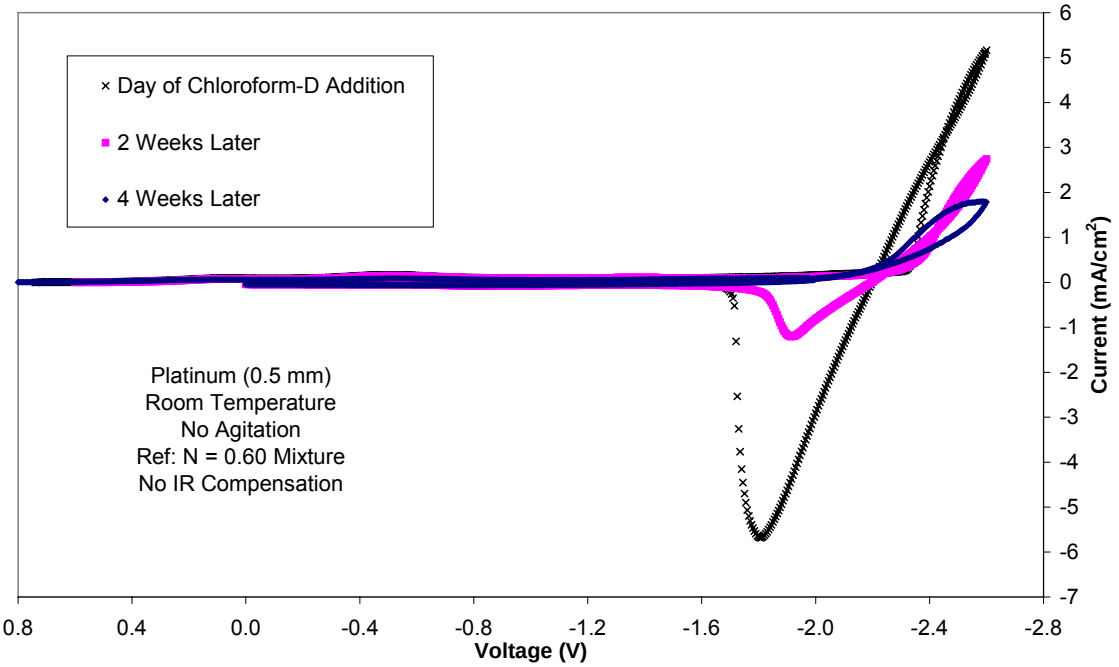

Figure III-7.7 CV results 0 days, 2 weeks and 4 weeks after addition of chloroform-D to neutral N=0.55 BME IL.

The minimum chloroform-D concentration was experimentally determined, as shown in Figure III-7.8. The addition of 0.34 mole % was adequate to provide a low level of reducible sodium ions. The sodium reduction and reoxidation currents were similar for the addition of 0.96 and 1.79 mole % chloroform-D. The addition of 0.34 mole % corresponds to 26 Na ions for each $CDCl_3$ molecule, however, the efficiency is only 25.1%. When the concentration of $CDCl_3$ was increased to 0.96 mole % (9 Na^+ per chloroform-D molecule), both the reduction and oxidation currents increased and the reduction current became much steeper. The coulombic efficiency increased to 60.8% with the higher additive concentration (0.96 mole %). Increasing the concentration to 1.79 mole % (5 Na^+ per chloroform-D) did not produce significant improvements and resulted in a coulombic efficiency of 66%.

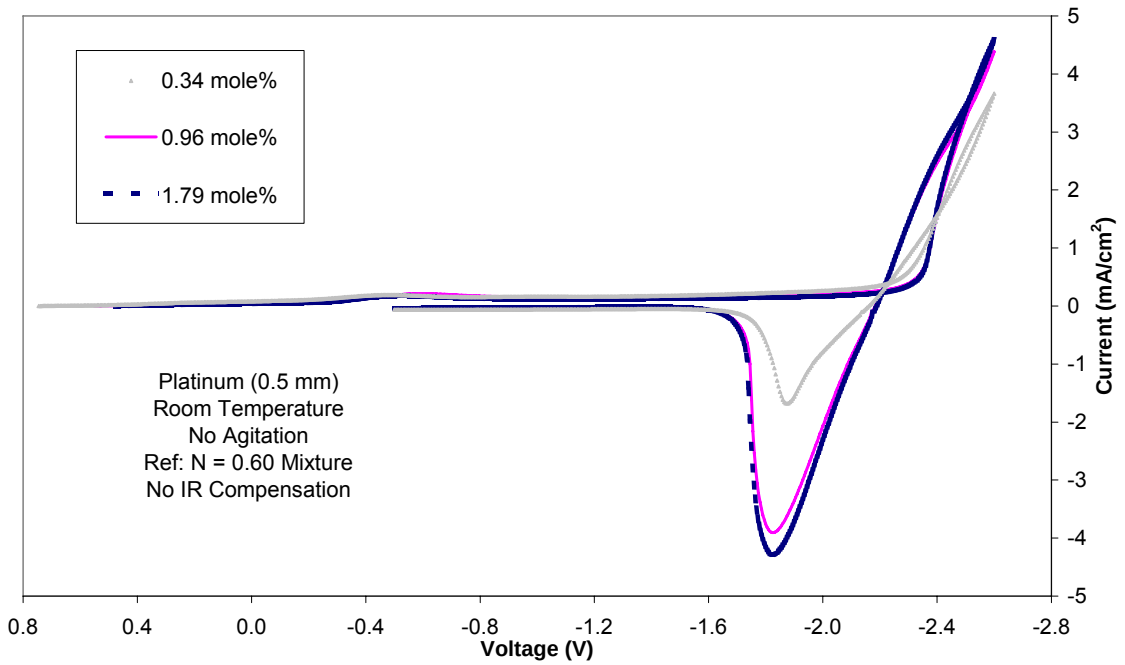

Figure III-7.8 CV test results after addition of 0.34, 0.96 and 1.79 mole % chloroform-D.

CA tests were performed at three additive concentrations (Figure III-7.9) where the potential was set at –2.4 V for 100 sec, followed by a potential step to –1.95 V for 100 sec. The efficiency was lowest (39.2%) at 0.34 mole % chloroform-D and highest (78.8%) at 1.79 mole % $CDCl_3$, which is in line with the CV tests. For the two higher concentrations, the peak current and overall behavior were similar to each other showing that additional additive, above a critical level, does not result in additional benefits. In all three cases, the current at longer times (> 40 sec) was the same indicating that it is independent of the chloroform-D concentration. The higher peak oxidation current at higher additive concentrations is due to a higher concentration of reducible sodium ions.

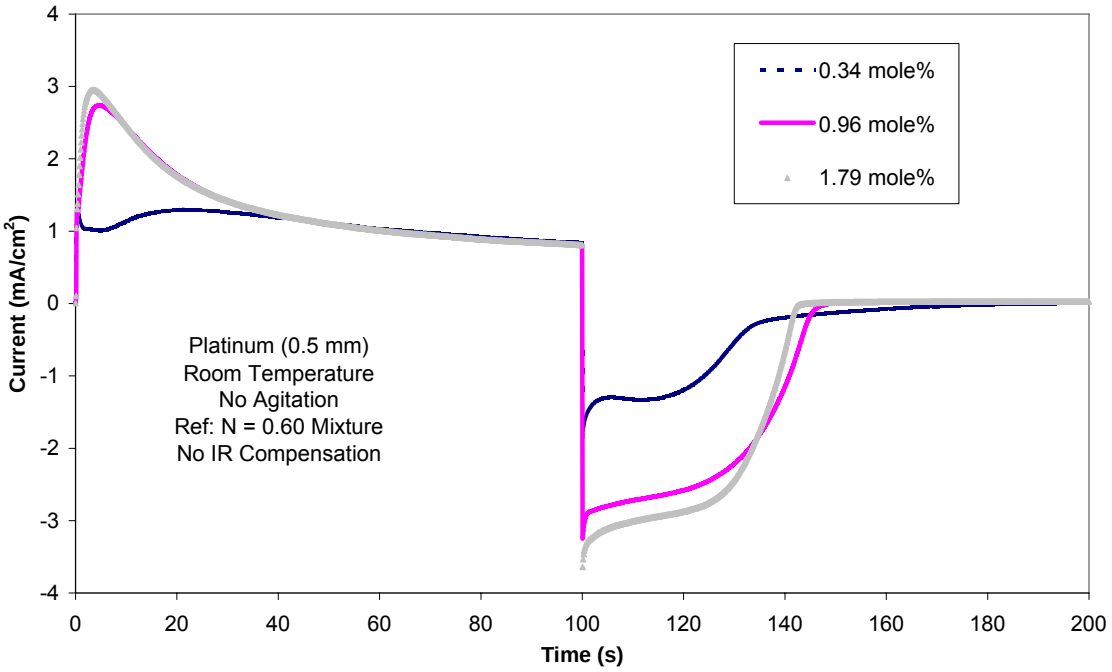

Figure III-7.9 Results of chronoamperometry tests with 0.34, 0.96 and 1.79 mole % chloroform-D added.

A similar test was carried out to determine the effect of chloroform-D concentration on conductivity, Figure III-7.10. There was little change in the conductivity when the additive was 0 to 0.5 mole %. There was a sharp increase in the conductivity when the additive concentration was increased above 1 mole %. The conductivity with 3.1 mole % $CDCl_3$ is nearly 35% greater than the IL without the $CDCl_3$ additive. The samples with greater than 1 mole % chloroform-D were less viscous than the initial sample. The increase in conductivity is due to two effects: less ion pairing of the sodium ions and lower viscosity. As with $SOCl_2$[34], chloroform-D is a neutral molecule that does not directly contribute to the conductivity. The CV and CA test results confirm that the concentration of free sodium ions is greater, as shown by the reduction current. The lower viscosity of the IL is because the hydrocarbon acts as a

solvent, similar to that demonstrated by Liao et al. in the plating of aluminum from a chloroaluminate IL with benzene added.[43]

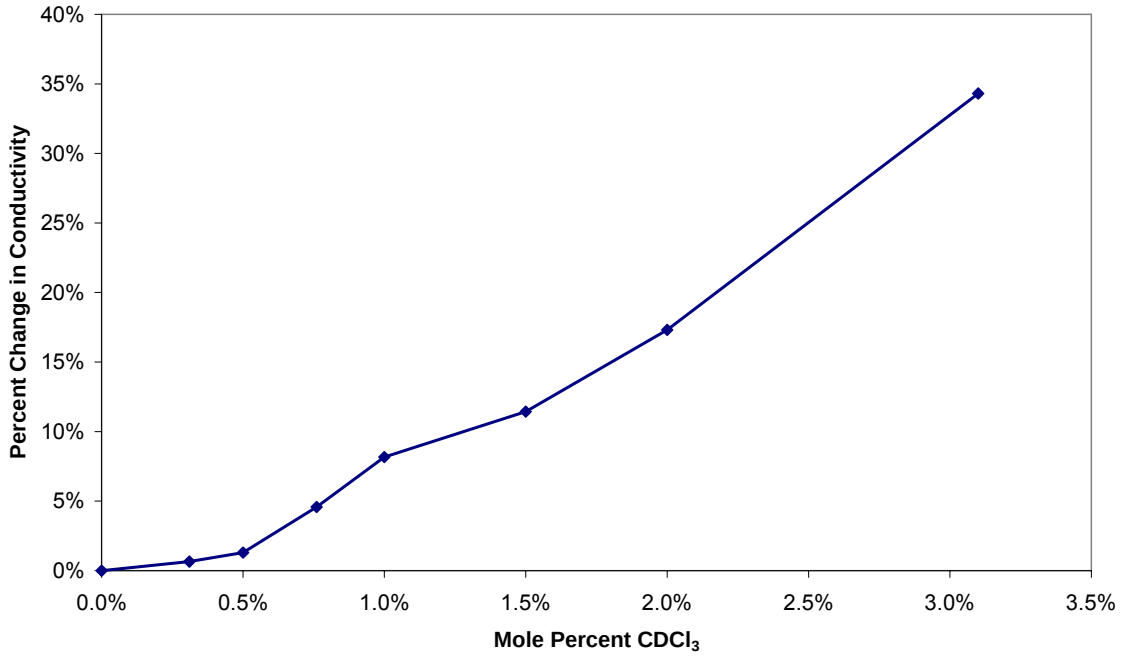

Figure III-7.10 Conductivity versus mole % chloroform-D in a neutral IL.

Summary

The ability of five different compounds to facilitate reduction of sodium from a chloroaluminate IL was investigated. PCl_6^- and 18-Crown-6 act to disrupt the Na^+ and $AlCl_4^-$ ion pairs producing reducible sodium ions. The addition of the small chlorinated compounds, CH_2Cl_2, $CDCl_3$ or CCl_4, resulted in the efficient reduction and reoxidation of sodium. It is believed that the electronegative chlorine atoms are oriented near the positive sodium cation, weakening its attraction to $AlCl_4^-$.

IV. Experimental

All experiments were carried out in a Vacuum Atmosphere glove box under dry nitrogen due to the sensitivity of the ILs to moisture. The glove box was maintained at oxygen and moisture levels below 10 ppm. Experiments above room temperature were performed in an oil-jacketed cell connected to a Fisher Scientific IsoTemp 3016 for temperature control. Salts I, II, VI, VIII, and IX (Fig. III-5.1) were obtained from Sachem, Inc. (Austin, TX) and purified before use. Methyl propyl imidazolium chloride (MPICl) was synthesized and purified following previously published procedures.[9] Aluminum trichloride, $AlCl_3$ (99.99%), anhydrous carbon tetrachloride (99.5+%), thionyl chloride, and $SOCl_2$ (99+%) were obtained from Aldrich and used as received. Benzyltrimethylammonium chloride (97%), benzyltriethylammonium chloride (98%) and benzyltributylammonium chloride (98%) were obtained from Alfa Aesar. Chloroform-D (99.9atom%) was purchased from Aldrich and stirred over fresh sodium metal in the dry box to remove any traces of water. 18-Crown-6 (99.95%) was obtained from Aldrich melted, dried under vacuum and re-crystallized. To dry dichloromethane, dry P_2O_5 was added and spun while performing vapor distillation under vacuum.

Four Quats were prepared by N-alkylation of 1:1 ratio of amines and alkylchlorides. Amines and alkylchlorides for each Quat are: N, N-dimethylethylamine and benzylchloride for benzylethyldimethylammonium chloride; N, N-dimethylbenzylamine and propylchloride for benzyldimethylpropylammonium chloride; N, N-dimethylisopropylamine and benzylchloride for benzyldimethylisopropylammonium chloride; N, N-diethylmethylamine and benzylchloride for benzyldiethylmethylammonium chloride. The salts were filtered and

re-crystallized in acetonitrile. The Quats, 1-butyl-3-methylimidazolium tetrafluoroborate (>97.0%, Fluka), LiCl (99.999%, Alfa Aesar), and NaCl (99.999%, Alfa Aesar) were dried under vacuum for 48 hrs at 70^{o}C before use in the glove box.

Conductivity measurements were performed using a custom-built probe and ThermoOrion conductivity meter.[34] Two platinum plates were set a fixed distance apart and the corners were sealed in glass to prevent bending or movement of the plates. Platinum leads were connected to each plate. Calibration was performed using a standard (Orion) NaCl solution before use in the glove box. After each use the probe was cleaned with nitric acid, rinsed with de-ionized water and dried.

An EG&G model 273 potentiostat was used for the electrochemical measurements. Pt (99.999%) and W (99.95%) wires were obtained from Alfa Aesar and fabricated into working electrodes by sealing them inside glass tubes. The electrodes were cleaned in hot HNO_3 prior to use. They were polished using 0.3 μm alumina powder and thoroughly rinsed with de-ionized water prior to use. The counter electrode was a twisted Pt wire or platinum foil sealed in glass on the corners. For the IL tests, the reference electrode was formed by immersing an aluminum wire (99.9995%) in an acidic melt (N = 0.6) in a glass tube separated from the electrolyte by a fine glass frit. The half reaction for the reference electrode is as follows.

$$4\ Al_2Cl_7^- + 3e^- \leftrightarrow Al + 7\ AlCl_4^- \quad E = 0.0\ V \qquad \text{(V-1.1)}$$

The reference electrode for the acetonitrile tests was formed by immersing a silver wire coated with AgCl in the 0.1 M acetonitrile solution in a glass tube separated from the

electrolyte by a fine glass frit. In all measurements, the three electrodes were positioned as close as possible to one another. IR compensation was not performed for the IL tests, but was performed for the measurements in acetonitrile solutions.

The melting points were determined using a Seiko Instruments S II 220C differential scanning calorimeter (DSC). The ramp rate of the cooling cycle was 1-2°C/min and the heating cycle was 5°C/min. In the electrochemical experiments involving the electrodeposition and reoxidation of sodium, the chemical reactivity of the sodium metal with the melt was quantified by measuring the self-discharge current. An open-circuit period was inserted between the plating and stripping of the sodium. The amount of charge recovered upon electrochemical stripping of the sodium was measured as a function of open-circuit time and expressed as an equivalent current density.[10]

§ Results of ^{1}H-NMR(400 MHz $CDCl_3$): butylethyldimethylammonium chloride: δ 0.98 (t, CH_3), 1.38 (m, CH_2 + CH_3), 1.68 (m, CH_2), 3.41(s, 2N-CH_3), 3.49 (t, N-CH_2), 3.72(q, N-CH_2); salt V: 0.99 (t, CH_3), 1.35(t, CH_3), 1.74(m, CH_2), 3.35(s, 2N-CH_3), 3.43 (t, 2N-CH_2), 3.68(q, 2N-CH_2); salt VII: 0.76 (m, 2CH_3), 1.18 (m, CH_2), 1.46 (m, CH_2), 1.55(m, CH_2), 3.14(s, 2N-CH_3), 3.30 (m, 2N-CH_2).

V. References

(1) Yu, C.; Winnick, J.; Kohl, P. *Journal of the Electrochemical Society* **1991**, *138*, 339.

(2) Besenhard, J. O. *Handbook of battery materials*; Wiley-VCH: Weinheim; New York, 1999.

(3) Yoshimatsu, I.; Hirai, T.; Yamaki, J. *Journal of the Electrochemical Society* **1988**, *135*, 2422.

(4) Bones, R.; Coetzer, J.; Galloway, R.; Teagle, D. *Journal of the Electrochemical Society* **1987**, *134*, 2379.

(5) Moseley, P. T.; Bones, R. J.; Teagle, D. A.; Bellamy, B. A.; Hawes, R. W. M. *Journal of the Electrochemical Society* **1989**, *136*, 1361.

(6) Fannin, A.; Floreani, D.; King, L.; Landers, J.; Piersma, B.; Stech, D.; Vaughn, R.; Wilkes, J.; Williams, J. *Journal of Physical Chemistry* **1984**, *88*, 2614.

(7) Park, S.; Winnick, J.; Kohl, P. *Journal of the Electrochemical Society* **2001**, *148*, A346.

(8) Kim, K.; Lang, C.; Kohl, P.; Winnick, J. "Annual Progress Report 1 (DE-FG02-02ER15328)," 2003.

(9) Gray, G.; Winnick, J.; Kohl, P. *Journal of the Electrochemical Society* **1996**, *143*, 2262.

(10) Gray, G.; Winnick, J.; Kohl, P. *Journal of the Electrochemical Society* **1996**, *143*, 3820.

(11) Park, S.; Moore, C.; Kohl, P.; Winnick, J. *Journal of the Electrochemical Society* **2001**, *148*, A1346.

(12) Pye, S.; Winnick, J.; Kohl, P. *Journal of the Electrochemical Society* **1997**, *144*, 1933.

(13) Melton, T.; Joyce, J.; Maloy, J.; Boon, J.; Wilkes, J. *Journal of the Electrochemical Society* **1990**, *137*, 3865.

(14) Matsumoto, H.; Kageyama, H.; Miyazaki, Y. *Chemical Communications (Cambridge, United Kingdom)* **2002**, 1726.

(15) Moffat, T. *Journal of the Electrochemical Society* **1994**, *141*, 3059.

(16) Chen, P.; Lin, Y.; Sun, I. *Journal of the Electrochemical Society* **1999**, *146*, 3290.

(17) Lin, Y.; Sun, I. *Journal of the Electrochemical Society* **1999**, *146*, 1054.

(18) Mitchell, J.; Pitner, W.; Hussey, C.; Stafford, G. *Journal of the Electrochemical Society* **1996**, *143*, 3448.

(19) Riechel, T.; Wilkes, J. *Journal of the Electrochemical Society* **1992**, *139*, 977.

(20) Karpinski, Z.; Osteryoung, R. *Inorganic Chemistry* **1985**, *24*, 2259.

(21) Sun, J.; Forsyth, M.; MacFarlane, D. *Journal of Physical Chemistry B* **1998**, *102*, 8858.

(22) Jones, S.; Blomgren, G. *Journal of the Electrochemical Society* **1989**, *136*, 424.

(23) Kim, K.; Lang, C.; Moulton, R.; Kohl, P. *Journal of the Electrochemical Society* **2004**, *151*, A1168.

(24) Kim, K.; Lang, C.; Kohl, P. *Journal of the Electrochemical Society* **2005**, *152*, E56.

(25) Koronaios, P.; Osteryoung, R. *Journal of the Electrochemical Society* **2000**, *147*, 3414.

(26) Gray, G.; Kohl, P.; Winnick, J. *Journal of the Electrochemical Society* **1995**, *142*, 3636.

(27) Bachrach, S.; Hayes, J.; Check, C.; Sunderlin, L. *Journal of Physical Chemistry A* **2001**, *105*, 9595.

(28) Chandler, W.; Johnson, K.; Fahlman, B.; Campbell, J. *Inorganic Chemistry* **1997**, *36*, 776.

(29) Smith, G.; Dworkin, A.; Pagni, R.; Zingg, S. *Journal Of The American Chemical Society* **1989**, *111*, 525.

(30) Gifford, P.; Palmisano, J. *Journal of the Electrochemical Society* **1987**, *134*, 610.

(31) Ross, S.; Finkelstein, M.; Petersen, R. *Journal of the American Chemical Society* **1960**, *82*, 1582.

(32) Finkelstein, M.; Petersen, R.; Ross, S. *Journal of the American Chemical Society* **1959**, *81*, 2361.

(33) MacFarlane, D.; Meakin, P.; Sun, J.; Amini, N.; Forsyth, M. *Journal of Physical Chemistry B* **1999**, *103*, 4164.

(34) Kim, K.; Lang, C.; Kohl, P. *Journal of the Electrochemical Society* **2005**, *152*, E9.

(35) Diggle, J.; Despic, A.; Bockris, J. *Journal of the Electrochemical Society* **1968**, *115*, C228.

(36) Rohnke, M.; Best, T.; Janek, J. *Journal of Solid State Electrochemistry* **2005**, *9*, 239.

(37) Zhang, Y.; Abys, A. *Modern Electroplating, Fourth Edition*; John Wiley & Sons, Inc.: New York, 2000.

(38) Kamitani, M.; Koga, T.; Tsuji, H. *Plating and Surface Finishing* **1985**, *72*, 31.

(39) Tench, D.; Anderson, D. *Plating and Surface Finishing* **1990**, *77*, 44.

(40) Yamaki, J.; Tobishima, S.; Hayashi, K.; Saito, K.; Nemoto, Y.; Arakawa, M. *Journal of Power Sources* **1998**, *74*, 219.

(41) Kim, Y.; Kim, H.; Kim, B.; Ahn, D.; Lee, J.; Kim, T.; Son, D.; Cho, J.; Kim, Y.; Park, B. *Chemistry of Materials* **2003**, *15*, 1505.

(42) Fuller, J.; Osteryoung, R.; Carlin, R. *Journal of the Electrochemical Society* **1995**, *142*, 3632.

(43) Liao, Q.; Pitner, W.; Stewart, G.; Hussey, C.; Stafford, G. *Journal of the Electrochemical Society* **1997**, *144*, 936.